Theoretical and Observational Viability of Modified Gravity

Melinda M. Andrews

A DISSERTATION

in

Physics and Astronomy

Presented to the Faculties of the University of Pennsylvania in Partial Fulfillment of the Requirements for the Degree of Doctor of Philosophy

2014

Mark Trodden, Fay R. and Eugene L. Langberg Professor of Physics
Supervisor of Dissertation

Randall Kamien, Vicki and William Abrams Professor in the Natural Sciences
Graduate Group Chairperson

Dissertation Committee:
Justin Khoury, Associate Professor of Physics
Adam Lidz, Assistant Professor of Physics
Masao Sako, Associate Professor of Physics
Evelyn Thomson, Associate Professor of Physics

Acknowledgments

This work would not have been possible without the support and encouragement of others. I would like to thank my parents, Lawrence and Patricia Gildner, for instilling in me an interest in science and providing the education necessary to pursue this research. My every success is a testament to your love, support, and general awesomeness. I am also grateful to my husband Sam for always being interested in my research, for encouraging me, and for being patient with long nights spent shut in the office. Your faith in me has been an indispensable pillar of support.

I would like to thank my advisor Mark Trodden for guidance, knowledge, and pushing me to improve not only in physics but as a professional as well. I have also learned a great deal from working with my collaborators Justin Khoury, Kurt Hinterbichler, Yi-Zen Chu, Daniel Wesley, Garrett Goon, James Stokes, and Matt Lewandowski.

I am grateful to my officemates Alexander Borisov, Joseph Clampitt, Alan Meert, and David Moore for creating a fun and helpful working environment. I

have been encouraged by the continued interest and support from my extended family, my church family at East Falls Presbyterian Church, and my sister Laura Ikeda. Thank you all for the part you've played in my life and work while completing this dissertation; I could not have done it without you.

ABSTRACT

Theoretical and Observational Viability of Modified Gravity

Melinda M. Andrews

Mark Trodden

The origin of the late-time cosmic acceleration is one of the most intriguing problems of modern physics; the standard theoretical explanation requires extreme fine-tuning to match observations. Resolution of this puzzle may require modifications to either the assumption that all matter has positive pressure or to the theory of gravity itself on cosmological distance scales. In this dissertation we explore the viability of several promising modifications to gravity unified by the presence of a Vainshtein-type screening mechanism suppressing the modifications within the solar system. In order to remain theoretically and observationally viable, a theory of modified gravity must:

1. be free of unphysical degrees of freedom that lead to instabilities,

2. produce a stable phase of cosmic acceleration,

3. allow stable field configurations around astrophysical objects, and

4. be consistent with measured limits on the strength of fifth forces in various environments.

We study three models: that of a scalar called the galileon that mediates a gravitational-strength fifth force, a braneworld-inspired theory of multiple galileons, and the theory of a massive graviton coupled to a galileon. We show that the massive graviton – galileon theory satisfies the first condition for viability but fails the second and that the multi-galileon theory fails the third condition. The theory of a single galileon satisfies the first three conditions; the last is known to be satisfied in the case of an isolated object. We develop a formalism to make more precise predictions regarding the galileon forces in multi-body systems. Finally, we consider the topological defect solutions of more general scalar theories with noncanonical kinetic terms and show that domain walls can mimic the field profile and energy density of a canonical domain wall, though the two are distinguishable by their fluctuation spectra.

Contents

List of Tables

List of Figures

Chapter 1

Introduction

Since ancient times, the origin, current state, and eventual fate of the universe have intrigued scientists and philosophers. It is only in recent times that we have begun to obtain observational evidence with which to answer these questions. The current state of the field of cosmology is a playground for theorists: guided by excellent and ever-growing data, we attempt to resolve the numerous theoretical puzzles posed by the observed behavior of the universe on the largest scales.

In this thesis, we will investigate the theoretical and observational viability of a class of theories modifying the infrared behavior of gravity, motivated by the hope of explaining the late-time cosmic acceleration. In Section 1.1 we will introduce the evidence for the cosmic acceleration; in Section 1.2 we will discuss the observationally-favored cosmological constant and the problems with its theoretical interpretation, and in Section 1.3 introduce dark energy and modified gravity as

possible alternatives to a cosmological constant.

1.1 The accelerating universe

Given that the action of gravity on all known forms of matter is attractive, it is reasonable within the context of a big bang universe to assume that the expansion of the universe would decelerate. However, as we will review here the observational evidence conclusively indicates that instead the expansion of the universe is accelerating.

The evidence for this relies on measurements of the distance to astrophysical objects as a function of the redshift experienced by photons due to the expansion of the spacetime they travel through. It is consistent with current observations to assume that the universe on large scales is homogeneous and isotropic, with no curvature [7, 191, 168, 169] and thus the cosmic expansion is characterized solely by the scale factor $a(t)$, or equivalently by the Hubble expansion rate $H(t) \equiv \frac{1}{a}\frac{da}{dt}$.

Rather than using time, it is observationally more convenient to use the redshift experienced by light emitted at a given time: for a monotonic $a(t)$ as in the standard big bang cosmology this is a one-to-one equivalence. Light emitted at a wavelength λ_e will be redshifted by the expansion of spacetime such that the observed wavelength is $\lambda_o = \frac{a(t_o)}{a(t_e)}\lambda_e$; the standard parameter used in place of time is

$$z \equiv \frac{\lambda_o - \lambda_e}{\lambda_e} = \frac{a(t_o)}{a(t_e)} - 1 \tag{1.1.1}$$

and thus $z = 0$ for nearby objects whose light was emitted recently and $z = \infty$ corresponds to the big bang singularity.

There are two different methods typically used to measure distance to astrophysical objects: the luminosity distance d_L and the angular diameter distance d_A. The luminosity distance is defined such that the apparent luminosity of an object with intrinsic luminosity L at a distance d_L from the observer is $L_{app} = \frac{L}{4\pi d_L^2}$. Similarly, the angular diameter distance is defined such that the observed angular size θ of an object is related to its absolute size x by $x = d_A\theta$. Taking into account the effects on light traveling over cosmological distances, these distances are related to the expansion history via

$$\begin{aligned} d_L &= (1+z)\int_0^z \frac{dz'}{H(z')} \\ d_A &= \frac{1}{1+z}\int_0^z \frac{dz'}{H(z')} \end{aligned} \tag{1.1.2}$$

and thus integral constraints on the expansion history can be obtained given that we are able to observe the redshift of light emitted by systems with either a known intrinsic luminosity ("standard candles") or size ("standard rulers").

The first evidence for late-time cosmic acceleration [189, 184] came from the observation of type 1a supernovae (SN1a), which serve as standard candles due to a known relationship between their peak intrinsic luminosity and the time scale over which the luminosity evolves after peak. Current SN1a results are included in the SNLS3 [195] and Union2.1 [196] compilations.

There are two types of standard ruler used to constrain the expansion history,

both originating in the physics of the early universe. The first is the sound horizon scale imprinted into the cosmic microwave background radiation (CMB) indicating the distance traveled by sound waves in the time from the big bang to the time when photons decouple from baryons. This distance scale survives in the distribution of structures in the later universe, known as the baryon acoustic oscillation (BAO) scale. Recent BAO data includes the 6dFGS [42], SDSS-II [182], BOSS [11], and WiggleZ [43] surveys.

These three observables rule out the possibility of a non-accelerating universe. The combined constraints on the fraction of the total energy density which drives acceleration Ω_Λ versus the fraction of the total energy density composed of clustering matter Ω_m in the context of the standard ΛCDM model of cosmology is plotted in Figure 1.1.

1.2 The cosmological constant problem

The current standard model of cosmology, ΛCDM, includes contributions to the energy density of the universe from radiation, baryonic matter, cold dark matter, and a cosmological constant (CC) Λ which has equation of state $p = -\rho$ and thus drives cosmic acceleration and does not evolve as the universe expands. This model is observationally very successful; however, the measured value of the CC is theoretically very challenging to explain.

The zero-point energy density of quantum fields is independent of the expansion

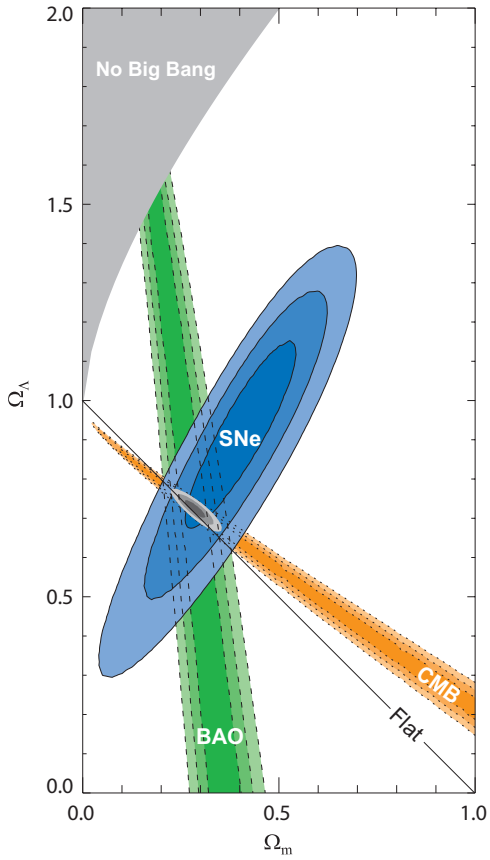

Figure 1.1: Constraints on the energy content of the late-time ΛCDM universe [41]. $\Omega_\Lambda \neq 0$ to high significance, indicating an accelerating universe.

of spacetime, and thus contributes to the value of the CC. Naïvely, this includes a contribution

$$E_{vacuum} = \sum_i g_i s_i \int_0^\infty \frac{d^3k}{(2\pi)^3} \sqrt{k^2 + m_i^2} \tag{1.2.1}$$

from a collection of species with masses m_i, degeneracy factors g_i, and $s_i = +1$ for bosons and -1 for fermions, which yields an infinite CC. Supposing that some new physics enters at an energy scale Λ_{UV} and that contributions to the vacuum energy from energies about Λ_{UV} are zero yields a contribution of order Λ_{UV}^4 to the

CC. The observed CC is of order $(\text{meV})^4$, an energy scale at which new physics is ruled out by experiment. Thus the "bare" value of the CC must be fine-tuned to at least one part in 10^{60} (for new physics at the TeV energy scale probed by the Large Hadron Collider) such that the value "dressed" by the large quantum zero-point contributions matches the observed value.

This problem is often split into the "old" cosmological constant problem of why the CC is very close to zero and the "new" cosmological constant problem of why the CC is not equal to zero. There are several proposed resolutions to the "old" cosmological constant problem (see [177] for a review). One such is the proposition of a symmetry mechanism, analogous to the $U(1)$ gauge symmetry that forbids the existence of a photon mass, forbidding the existence of a cosmological constant term. For example, as seen in Equation 1.2.1, unbroken supersymmetry causes each contribution with $s_i = +1$ to be canceled by a contribution with $s_i = -1$ and thus $E_{vacuum} = 0$; however, the nondetection of supersymmetric partners of the standard model particles up to TeV-scale energies indicates supersymmetry is broken at too high an energy scale to solve the old cosmological constant problem. Another suggestion is to assert that the zero-point energy is not any more "real" in gravity than it is in other fields of physics. The Casimir effect and the vacuum polarization contribution to the Lamb shift are often cited as cases where the vacuum energy has an observable consequence, but as discussed in [149] these effects can be formulated without reference to vacuum fluctuations and thus it is debatable whether

they provide evidence that the zero-point energy should be taken as "real" (having observational consequences).

We will assume in ensuing chapters that there exists such a resolution which sets the CC to zero and proceed to study a class of theories which address the "new" cosmological constant problem. We note here that there is a proposed resolution to both "old" and "new" CC problems in the form of an anthropic argument in the context of a multiverse theory [205]. Supposing that the universe is described by a theory with many different possible vacua, and that the actual solution in reality samples all such vacua, even if a very small CC is rare it is nevertheless likely that observers living in collapsed structures will measure a small CC due to the tendency of a large CC to prevent the formation of such observers. This resolution to the CC problem suffers from difficulty with interpreting probabilities in such a multiverse (the "measure problem") [208, 9] and from limited ability to predict the results of new experiments.

1.3 Alternatives to a cosmological constant

Despite the observational success of the ΛCDM model, due to the theoretical challenge of explaining the value of the CC it is worthwhile to explore alternative explanations for the origin of the cosmic acceleration. Such alternative models, even if eventually falsified, lead to the development of new observational tests with which to confront the standard paradigm. There are two broad classes of alternatives

to the CC: one may consider a new dynamical matter component, dubbed "dark energy", that behaves approximately as a cosmological constant at late times; or one may consider a modification to general relativity (GR) on large distance scales that mimics the effect of a cosmological constant.

The distinction between the two classes is somewhat fuzzy - many modified gravity theories are in fact equivalent to a theory of dark energy [206]. This is easy to see through the equations of motion: unmodified GR satisfies

$$G_{\mu\nu} = 8\pi G\, T_{\mu\nu}^{\text{matter}} \tag{1.3.1}$$

with gravitational degrees of freedom on the left and matter content on the right. One may modify gravity by adding a term $f(g_{\mu\nu})$ dependent on the spacetime metric $g_{\mu\nu}$ to the left hand side, but this is equivalent to adding the term $8\pi G\, T_{\mu\nu}^{\text{dark energy}}$ to the right hand side for $T_{\mu\nu}^{\text{dark energy}} = -\frac{1}{8\pi G} f(g_{\mu\nu})$. The dark energy component so defined is conserved due to the Bianchi identity $\nabla^\mu G_{\mu\nu} = 0$ and the conservation of matter $\nabla^\mu T_{\mu\nu} = 0$. Observationally, it is standard to classify models with no anisotropic stress (for which the stress-energy tensor $T_{\mu\nu}^{\text{dark energy}}$ is invariant under spatial rotations) as dark energy and those with anisotropic stress as modified gravity.

Typically, dark energy as first presented in [188, 58] (also called "quintessence") is taken to be a scalar field ϕ with potential $V(\phi)$, which has the equation of state $w \equiv p/\rho$ given by

$$w = \frac{\frac{1}{2}\dot{\phi}^2 - V(\phi)}{\frac{1}{2}\dot{\phi}^2 + V(\phi)}\,. \tag{1.3.2}$$

This scalar field behaves like a cosmological constant $w \approx -1$ when $\frac{1}{2}\dot{\phi}^2 \ll |V(\phi)|$. Depending on the choice of potential, one may obtain an attractor solution for which the late-time behavior of the dark energy is approximately a cosmological constant for a broad range of initial conditions. Additionally, motivated by the "coincidence problem" that the dark energy density and matter density are of the same order at the present time (which in general requires a fine-tuning of the initial conditions), one may construct potentials which lead to "tracker" solutions where the dark energy mimics the dominant energy component until eventually coming to dominate at late times [217].

The observational constraints on a varying equation of state $w(z)$ still allow for a range of interesting behavior, as shown in Fig. 1.2. However, a scalar field with the observed energy density that does not cluster on observable scales must generically have a very small mass and absent or very weak coupling to ordinary matter. Such a situation is very unnatural as a particle physics theory, as quantum corrections will generally spoil this fine tuning [183, 163, 60].

Modifications to gravity are commonly also effected by the inclusion of an extra scalar degree of freedom which mediates a gravitational-strength fifth force. Such a fifth force is strongly constrained by solar system and pulsar tests to have a negligible effect on dynamics (see Section 20 of [41]). Thus a successful theory of modified gravity must incorporate a *screening mechanism* which leads to a small fifth force within dense structures but a large effect on cosmological scales. Such

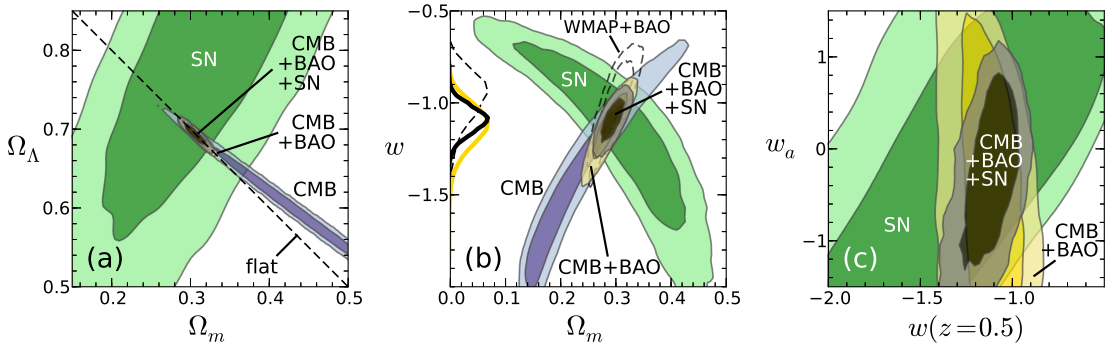

Figure 1.2: Constraints on the equation of state of dark energy and its time evolution. Dark and light shading indicate 1σ and 2σ contours, respectively. (a) Constraints in the Ω_Λ-Ω_m plane within ΛCDM. (b) Constraints on a constant w not fixed to -1. (c) Constraints on a time-dependent w with $w_a = -\frac{dw}{da}$. [41]

screening mechanisms either rely on the form of the potential (as in the *chameleon* and *symmetron* mechanism) or a nonstandard kinetic structure (as in the *Vainshtein* mechanism).

The chameleon mechanism [157] relies on a form for the scalar field potential and coupling to matter that produces an environment-dependent mass for the scalar. As illustrated in Fig. 1.3, this results in a massive scalar in high-density environments which mediates a very short-range force and a light scalar in low-density environments which mediates a long-range force. This mechanism is realized in so-called $f(R)$ theories of modified gravity [61, 59] which modify the action of GR via

$$S_{GR} = \frac{M_{\rm Pl}^2}{2}\int d^4x\sqrt{-g}R \qquad \rightarrow \qquad S_{f(R)} = \frac{M_{\rm Pl}^2}{2}\int d^4x\sqrt{-g}f(R) \qquad (1.3.3)$$

where $f(R)$ is an arbitrary function of the Ricci scalar that recovers $f(R) \simeq R$ in

high-curvature regions [50]. See [80] for a review of $f(R)$ theories.

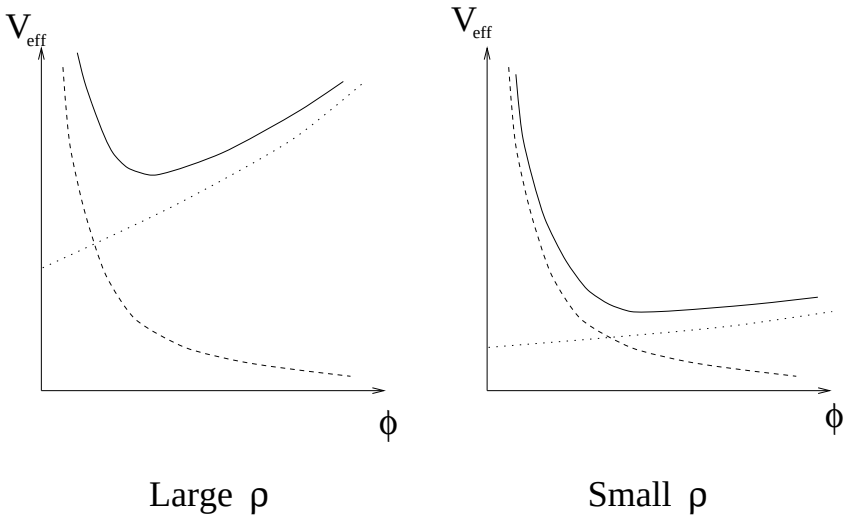

Figure 1.3: Effective potential for a chameleon field with contributions from the potential (dashed curve) and coupling to matter density ρ (dotted curve); the mass of small fluctuations about the minimum is large in high-density regions and small in low-density regions. [157]

The symmetron mechansism [141] also relies on the interplay of the potential and coupling to matter, but results in an environment-dependent coupling to matter which vanishes in high-density regions rather than an environment-dependent mass. The symmetron moves in a symmetry-breaking potential $V(\phi) = -\mu^2\phi^2/2 + \lambda\phi^4/4$ and has a universal coupling to matter $\phi^2\rho/2M^2$; this yields an environment-dependent effective potential which results in a nonzero field value $\phi = \mu/\sqrt{\lambda}$ in low-density regions and confines the field near $\phi = 0$ in high-density regions as illustrated in Fig. 1.4, thus suppressing the effects of the symmetron on the dynamics

of matter on solar system scales.

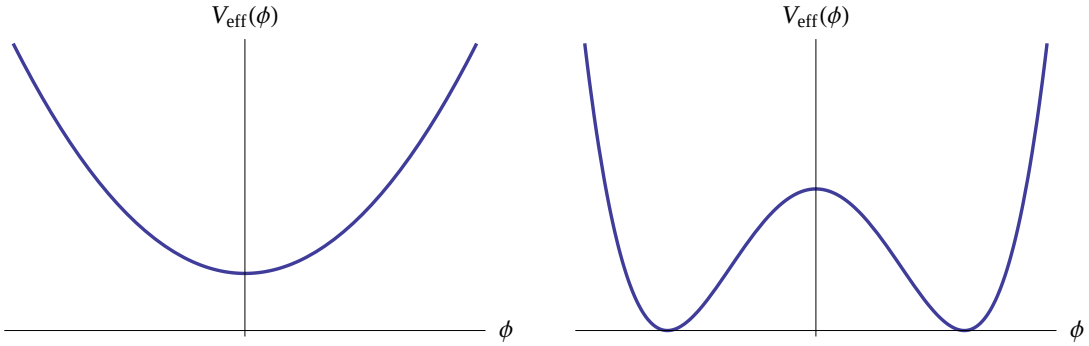

(a) Effective potential in regions of high ambient density. The VEV is 0.

(b) Effective potential in regions of low ambient density.

Figure 1.4: Effective potential for a symmetron field. The effect of the symmetron on the dynamics of matter is suppressed for small ϕ, as realized in high-density environments. [142]

It has been shown observationally in [150] and as a no-go theorem in [203] that chameleon-like scalars (including the symmetron) cannot account for the cosmic acceleration without including a dark energy component – that is, any self-acceleration in a chameleon-like theory is not a result of a true modification of gravity. The no-go theorem relies on a proof that for a theory in which the solar system is screened to the level required by observations,

- the Compton wavelength of the scalar is at most $\sim$ Mpc-scale, and thus mediates too short-range of a force to affect large scale structures, and
- the relationship between the Jordan-frame metric, in which observations are made, and the Einstein-frame metric, acceleration in which is indicative of a

dark energy component, is nearly constant over the age of the universe. That is, acceleration in the (observed) Jordan frame requires acceleration in the Einstein frame, which indicates the presence of dark energy.

This result indicates that screening mechanisms depending only on the potential and matter coupling of a single scalar field are disfavored in models attempting to explain the cosmic acceleration. The third screening mechanism we discuss here is one that relies on a modification to the kinetic energy of the fifth-force mediator.

The Vainshtein screening mechanism [198] is effected in a variety of theories with nonlinear derivative self-interactions. In low-density regions, the largest derivative term is the standard kinetic energy; the field thus approximately obeys a standard Poisson equation which results in a gravitational-strength fifth force. Unlike the chameleon mechanism, the unscreened force may have infinite range. In high-density regions the nonlinear derivative interactions dominate the standard kinetic term, causing the minimum-energy configuration to prefer small derivatives; as the force is the gradient of the scalar field, this results in a suppressed fifth force near astrophysical objects.

In Chapters 3-6 of this thesis we will investigate the theoretical and observational viability of several modified gravity theories displaying Vainshtein screening. In Chapter 7 we will broaden the scope of our study to include general theories of a scalar field with nonlinear derivative self-interactions but with no requirement that the theory realize the Vainshtein screening mechanism. We will consider the possi-

bility of distinguishing such a theory from a canonical scalar field theory through observations of topological defects.

Topological defect solutions to classical field theories have applications in many areas in physics, and in particular may have important implications for the evolution of the universe [200, 1, 171, 75]. In the early universe, such defects may have formed as the universe cooled and various gauge or global symmetry groups were broken. Some defects, such as GUT monopoles, can lead to potential cosmological problems which historically inspired the development of the theory of cosmic inflation. Other defects, such as cosmic strings, are potentially observable in the present day; for example by affecting the spectrum of perturbations observed in the microwave background and matter distributions (although defects cannot play the dominant role in structure formation). Further, the microphysics of such objects may be important in some circumstances, such as weak scale baryogenesis [48, 47, 46, 49]. Another interesting possibility arises if the strings are superconducting, as originally pointed out by Witten [209], since the evolution of a network of such superconducting cosmic strings can differ from a nonsuperconducting one. In particular, the supercurrent along loops of string can build up as the loop radiates away its energy, affecting the endpoint of loop evolution. This supercurrent can become large enough to destabilize the loop or may compete with the tension of the string loop and result in stable remnants, known as *vortons* [74], with potentially important consequences for cosmology [45, 62]. We will show in this thesis that it is possible for a domain

wall in a noncanonical theory to be indistinguishable from a canonical defect.

Chapter 2

Vainshtein-screened modified gravity theories

Vainshtein screening appears in a broad group of modified gravity theories. In this chapter we will review the history of this class of theories, leading up to the theories under investigation in the later chapters of this thesis. A number of the theories are observationally ruled out or subject to theoretical inconsistencies, but have inspired the development of many currently viable theories.

2.1 Fierz-Pauli massive gravity

The Vainshtein mechanism has its origin in the attempt to develop a consistent theory of a massive graviton. At the linearized level, as shown by Fierz and Pauli [117], there exists only one possible mass term that is both Lorentz-invariant and

does not introduce a new negative-energy degree of freedom (a "ghost"). The action includes the linearized Einstein-Hilbert action of GR (the kinetic term for a graviton $h_{\mu\nu}$), a mass term, and the standard GR coupling of the gravition to matter with stress-energy $T^{\mu\nu}$:

$$S_{FP} = \int d^4x \frac{M_{\rm Pl}^2}{4}\left[\frac{1}{2}h_{\mu\nu}\mathcal{E}^{\mu\nu,\alpha\beta}h_{\alpha\beta} - \frac{1}{2}m^2\left(h_{\mu\nu}h^{\mu\nu} - h^2\right)\right] + \frac{1}{2}h_{\mu\nu}T^{\mu\nu}\,. \qquad (2.1.1)$$

While GR describes two degrees of freedom (two spin-two helicities), the massive theory propagates five degrees of freedom - two tensors, two vectors, and a scalar. It was discovered by van Dam, Veltman and Zakharov [199, 214] that one does not recover GR when the graviton mass is taken to zero in the Fierz-Pauli massive gravity theory; light bending in the $m \to 0$ theory is different from the GR result by 25%. This result is the so-called vDVZ discontinuity and is the result of the fact that the new scalar does not decouple from matter in the $m \to 0$ limit.

It is in the context of attempting to resolve this discontinuity that the Vainshtein mechanism was first discovered [198] – presumably the linear Fierz-Pauli theory is corrected by higher-order nonlinear terms, which Vainshtein discovered grow as the graviton mass is decreased. Supposing a spherically symmetric source of mass M, a new length scale called the Vainshtein radius and given by $r_v \sim \left(\frac{M}{m^4 M_{\rm Pl}^2}\right)^{1/5}$ appears, below which nonlinearities dominate over the linear Fierz-Pauli term. As the graviton mass is taken to zero, the Vainshtein radius diverges and thus the linear theory is not a valid approximation at any distance from the source. The Vainshtein screening effect in Fierz-Pauli massive gravity is studied numerically in

[26], confirming the recovery of GR near the source.

However, it was shown by Boulware and Deser [44] that generic nonlinear completions of the Fierz-Pauli theory propagate not five but six degrees of freedom, one of which has a wrong-sign kinetic term and thus is known as the Boulware-Deser (BD) ghost. Until very recently, the presence of the BD ghost was thought to preclude any consistent theory of a massive graviton.

2.2 Dvali-Gabadadze-Porrati braneworld gravity

A partial resolution to the problem of the existence of a ghost-free theory of massive gravity comes in the form of the Dvali-Gabadadze-Porrati (DGP) braneworld gravity model [111], though it is not immediately obvious that this theory describes a massive graviton. The DGP model describes a $4+1$ (4 space and 1 time) -dimensional gravitational sector with matter confined to a $(3+1)$-dimensional brane; the action is given by

$$\begin{aligned} S_{DGP} =& \frac{M_5^3}{2}\int d^5X\sqrt{-G}R(G) + \frac{M_4^2}{2}\int d^4x\sqrt{-g}R(g) \\ &+ \int d^4x\mathcal{L}_{matter}(g, \text{matter fields}) \end{aligned} \tag{2.2.1}$$

with X and G the 5-dimensional (5D) coordinates and metric, x and g the 4-dimensional (4D) coordinates and induced 4-dimensional metric on the brane, and M_D the D-dimensional Planck mass.

The interpretation of this theory as a massive gravity theory is elucidated by

considering the effective 4-dimensional description obtained by linearizing about flat space and integrating out the bulk (see Section 10.2 of [140] for a derivation), giving the action

$$S = \int d^4x \frac{M_4^2}{4} \left[\frac{1}{2} h_{\mu\nu} \mathcal{E}^{\mu\nu,\alpha\beta} h_{\alpha\beta} - \frac{1}{2} m \left(h_{\mu\nu} \sqrt{-\Box} h^{\mu\nu} - h \sqrt{-\Box} h \right) \right] + \frac{1}{2} h_{\mu\nu} T^{\mu\nu} \tag{2.2.2}$$

with the mass parameter $m = 2M_5^3/M_4^2$. Note the similarity to the Fierz-Pauli action of Eq. (2.1.1); here, however, the mass m^2 is replaced by the operator $m\sqrt{-\Box}$. The DGP model thus describes a graviton composed of a continuum of massive states – a resonance with width m. As shown in [187], the linearized version of the DGP model suffers from the vDVZ discontinuity, but the pathology is cured at nonlinear order.

The DGP theory describes a gravitational force law that appears 4-dimensional on short distances but transitions to weaker 5-dimensional gravity at a distance $r_c \sim m^{-1}$, and thus due to the weakening of gravity in the IR is of interest as a possible solution to the CC problem. The cosmological solutions [98] bear this out: DGP cosmology has two branches of possible solutions, given by $\epsilon = \pm 1$ in the modified Friedmann equation

$$H^2 = \left(\sqrt{\frac{\rho}{3M_{\rm Pl}^2} + \frac{m^2}{4}} + \epsilon \frac{m}{2} \right)^2 . \tag{2.2.3}$$

We recover standard cosmology on both branches when $m \ll H$ (or equivalently for Hubble radii much smaller than the crossover radius to 5-dimensional behavior), but the behavior of the solutions when the Hubble radius enters the 5-dimensional

regime differs strongly between the two branches. The "normal" branch, $\epsilon = -1$, exhibits a transition to fully 5-dimensional behavior and hence effects an IR modification of gravity, but does not produce cosmic acceleration in the absence of a dark energy component. The "self-accelerating" branch, $\epsilon = +1$, transitions not to 5-dimensional gravity but to a de Sitter phase of accelerating expansion with $H \sim m$ sourced by the intrinsic curvature of the brane.

However, the DGP model is ruled out as an explanation for the late-time cosmic acceleration due to the presence of a ghost instability in the self-accelerating branch (see [164] for a review) and confrontation with observations [166, 194, 204, 116, 115]. It has been shown that the normal branch is free from ghosts [174], but is subject to observational constraints [213] requiring $m \lesssim 0.1H_0$ and thus any departure from GR is too small to be of interest.

2.3 Galileons

It is interesting to study the DGP model in a limit that distills out the nonlinearities responsible for the Vainshtein mechanism [167, 174]. This is achieved in the *decoupling* limit

$$M_4,\, M_5,\, T_{\mu\nu} \to \infty \qquad \Lambda \equiv \frac{M_5^2}{M_4} = \text{constant},\ \frac{T_{\mu\nu}}{M_4} = \text{constant} \tag{2.3.1}$$

for which the 4-dimensional graviton decouples from the scalar component corresponding to the position of the brane in the extra dimension (denoted π) whose

linearization is responsible for the vDVZ discontinuity. This limit maintains the nonlinear derivative self-interactions of π with a strength set by the mass scale Λ. The resulting scalar-tensor theory reproduces the interesting effects of DGP on scales below the Hubble radius, including the self-accelerating behavior. It is therefore interesting to consider generalizing the scalar-tensor theory obtained from the decoupling limit of DGP in search of a ghost-free self-accelerating effective field theory.

Just such a generalized theory is presented in [175], where it is noted that the cubic derivative interaction term that arises for the DGP decoupling limit π is the unique cubic interaction satisfying:

- despite being higher-derivative in the action, the equations of motion are nonetheless second-order, and
- the action is invariant under the Galilean symmetry $\pi(x) \to \pi(x) + b_\mu x^\mu + c$.

By dropping the DGP origin and including all terms consistent with these two conditions, one obtains a theory of a scalar field dubbed the "galileon" with five possible derivative self-interaction terms. The action is given by

$$S_\pi = \int d^4x \left(\sum_{i=2}^{5} \frac{\alpha_i}{\Lambda^{3(i-2)}} \mathcal{L}_i + \frac{\pi}{M_{\rm Pl}} T \right) , \tag{2.3.2}$$

where, defining the matrix $\Pi^\mu{}_\nu \equiv \partial^\mu \partial_\nu \pi$ and the notation $[A] \equiv A^\mu{}_\mu$ (for any matrix

A),

$$\mathcal{L}_2 = -\frac{1}{2}(\partial\pi)^2 \tag{2.3.3}$$

$$\mathcal{L}_3 = -\frac{3}{4}(\partial\pi)^2[\Pi] \tag{2.3.4}$$

$$\mathcal{L}_4 = -\frac{1}{2}(\partial\pi)^2\left([\Pi]^2 - [\Pi^2]\right) \tag{2.3.5}$$

$$\mathcal{L}_5 = -\frac{5}{24}(\partial\pi)^2\left([\Pi]^3 - 3[\Pi][\Pi^2] + 2[\Pi^3]\right)\ . \tag{2.3.6}$$

As hoped, this theory allows for ghost-free self-accelerating solutions that recover GR in the solar system due to the Vainshtein mechanism [175]. However, the theory is not completely free from pathologies, most notably the superluminal propagation of galileon signals inside the screened region. The extent to which this challenges the viability of galileon theories as a possible description of reality is under debate; the authors of [6] argue that such superluminality is evidence of macroscopic nonlocality and precludes the possibility that the galileons are the low-energy limit of an ultraviolet (UV)-complete theory. There are two concerns that must be addressed in order for a theory with superluminal signal propagation to be viable: the possibility of causality violation, and the non-analyticity of the S-matrix which obstructs UV completion. The first concern is addressed in [55, 28, 154]: the authors argue that the formation of causality-violating closed timelike curves requires leaving the regime of validity of the effective field theory, and thus is likely prevented by large backreaction analogously to the chronology protection conjectured by [139] in GR. The second concern is addressed by the existence of dualities mapping a galileon theory displaying Vainshtein screening and superluminal signal propagation to a

free field theory on both the classical [85, 92, 71] and quantum [153] level. Thus the S-matrix of the dual galileon theory must be analytic, and there should be no obstruction to UV completion of galileon theories.

The galileon theory is still viable given current observational constraints. The most precise constraints on modifications to gravity come from solar system and pulsar measurements, but in such an environment the effects of the galileon are expected to be very small due to screening. The prediction for orbital precession of a test body about an isolated source due to a cubic galileon (where $\alpha_4 = \alpha_5 = 0$) is within the range of detectability for near-future lunar laser ranging experiments [148, 112], but the inclusion of the quartic interaction term reduces the expected observational effects below the reach of even proposed future measurements [12]. These results are valid so long as it is consistent to neglect the effects of other nearby astrophysical bodies; in Chapter 6 of this thesis we develop the formalism to treat the n-body problem subject to a cubic galileon-mediated fifth force and raise some concerns about the validity of one-body results.

The issue of galileon radiation (of interest for binary pulsar observations) is addressed in [95, 97, 66]. Unlike gravitational waves, the galileon radiates a monopole and dipole from such systems and thus the chances of observable results are enhanced over static systems; however, the monopole, dipole, and quadrupole are found to be suppressed far below observable levels due to Vainshtein screening in the case of both cubic and quartic galileons. The formalism developed is plagued by

an uncontrolled multipole expansion – radiation in higher multipoles is enhanced versus in low multipoles, a possible indication that the treatment of this system as a small perturbation above a static, spherically-symmetric system is not valid.

Numerical solutions have been employed to confront galileon models with cosmological data in the form of redshift space distortions, type 1a supernovae, CMB, and BAO data [178, 82, 30, 10, 29, 173, 172, 31]. The results show that the cubic galileon is disfavored by a poor fit to the large-scale CMB, but the full galileon theory is favored over ΛCDM by CMB measurements alone and slightly disfavored by the combination of CMB and lower-redshift observations.

There are a number of ways investigated in the literature to generalize galileons. The original theory is only valid on flat space; it is an obvious direction to covariantize the theory of galileons [99, 102], however, this construction necessitates abandoning the Galilean symmetry in order to maintain second-order equations of motion. It can also be shown that while the DGP model only produces the cubic galileon interaction, it is possible to construct a variety of galileon-like theories in the context of higher-dimensional braneworld models [124, 126]. Other generalizations include higher-spin galileons [100], higher-derivative actions with second-order equations of motion but no Galilean symmetry [103], and supersymmetric galileons [156]. We will study in greater detail in Chapter 5 of this thesis the extension to a theory of multiple galileons [145, 100, 181, 179].

2.4 de Rham-Gabadadze-Tolley massive gravity

While the DGP theory presents a theory of a graviton with a soft mass that is free of the BD ghost, until 2010 there was no known ghost-free theory of a graviton with a hard mass. Such a theory was presented by de Rham, Gabadadze, and Tolley (dRGT) in [86, 89] – while Boulware and Deser's argument applies to generic choices of the nonlinear completion of the Fierz-Pauli mass term, the dRGT theory is the unique ghost-free (as shown by [137, 90]) choice of nonlinear completion. The dRGT theory requires the introduction of a nondynamical reference metric $f_{\mu\nu}$, which we shall take to be Minkowski, and is given by the action (as in Eq. (2.3.2), square brackets denote traces of matrices)

$$S_{dRGT} = \int d^4x\sqrt{-g}\left[\frac{M_{\rm Pl}^2}{2}R(g) + M_{\rm Pl}^2 m^2\left(\mathcal{L}_2 + \alpha_3\mathcal{L}_3 + \alpha_4\mathcal{L}_4\right)\right], \tag{2.4.1}$$

where the mass term depends on $\mathcal{K} \equiv \delta^\mu_\nu - \sqrt{g^{\mu\sigma}f_{\sigma\nu}}$ via

$$\mathcal{L}_2 = \frac{1}{2!}\left([\mathcal{K}]^2 - [\mathcal{K}^2]\right) \tag{2.4.2}$$

$$\mathcal{L}_3 = \frac{1}{3!}\left([\mathcal{K}]^3 - 3[\mathcal{K}][\mathcal{K}^2] + 2[\mathcal{K}^3]\right) \tag{2.4.3}$$

$$\mathcal{L}_4 = \frac{1}{4!}\left([\mathcal{K}]^4 - 6[\mathcal{K}]^2[\mathcal{K}^2] + 3[\mathcal{K}^2]^2 + 8[\mathcal{K}][\mathcal{K}^3] - 6[\mathcal{K}^4]\right). \tag{2.4.4}$$

The reasoning behind this choice of interaction terms is more clear in the decoupling limit: $M_{\rm Pl} \to \infty$ and $m \to 0$ with $\Lambda_3 \equiv (m^2 M_{\rm Pl})^{1/3}$ fixed. In this limit, the matrix $\mathcal{K}$ is replaced by the matrix of second derivatives of a scalar field $\partial_\mu\partial_\nu\pi$; it is then evident that the choice of the Fierz-Pauli mass term $\mathcal{L}_2$ is exactly the one that produces a total derivative term. The higher interactions thus are chosen to

have this same property. They are also precisely the interaction terms that raise the strong coupling scale from $\Lambda_5 = (M_{\rm Pl} m^4)^{1/5}$ as found by Vainshtein to the higher scale Λ_3, thus expanding the regime of validity of this theory.

We have suggestively referred to the scalar appearing in the decoupling limit as π; this scalar is in fact a galileon (as suggested by the similarity between Equations (2.3.2) and (2.4.1)). Thus, to the extent that the full massive gravity theory is probed by its decoupling limit, the interesting qualities of galileons (self-acceleration and Vainshtein screening) also apply to dRGT massive gravity. The dRGT decoupling limit also introduces a phenomenologically interesting new disformal coupling to matter $\partial_\mu \pi \partial_\nu \pi T^{\mu\nu}$. As shown in [40], the presence of this coupling precludes asymptotically flat solutions with near-source Vainshtein screening; all such solutions must have cosmological asymptotics. Interestingly, these restricted solutions are free of superluminality. The disformal coupling also produces interesting observational effects, particularly the enhancement of gravitational lensing [210].

Beyond the decoupling limit, it becomes apparent that due to the Hamiltonian constraint that removes the BD ghost, dRGT massive gravity has no nontrivial flat or closed homogeneous cosmological solutions [72]. However, both a universe with very small curvature [129] and a universe with unobservable inhomogeneity [72] remain possible within massive gravity. In the latter case, inhomogeneity enters as a result of the introduction of a new length scale m^{-1}; so long as this length scale is sufficiently large ($m \lesssim 0.1 H_0$), the observable universe will be well-approximated

by a standard homogeneous and isotropic Friedmann-Robertson-Walker (FRW) universe. Exact solutions of this type are reviewed in [201], but each requires a restrictive assumption and a general treatment will require numerical solution.

The case of an open FRW universe is more easily approached analytically, but suffers from strong coupling of the vector and scalar degrees of freedom due to their vanishing kinetic terms on the cosmological solution [131, 76]. Motivated in part by the desire to remove this pathology, a number of extensions of dRGT massive gravity have been explored. A simple extension of the theory is to consider a non-Minkowski reference metric (such as a de Sitter or FRW metric); this modified theory also has unstable FRW cosmological solutions for the physical metric [155]. The nondynamical reference metric can also be promoted to a dynamical second metric, resulting in a bimetric theory of gravity [135] which is capable of reproducing the observed expansion history [202]. One may also promote the mass to a function of the scalar to obtain the mass-varying extension [147], however, this theory does not support sufficiently long periods of self-acceleration [144]. Another extension introduces a new scalar degree of freedom, the quasidilaton [73], which enforces a scaling symmetry of the reference metric relative to the physical metric. The quasidilaton theory is unstable to scalar perturbations [132].

In Chapters 3 and 4 of this thesis we investigate the absence of the BD ghost and the presence of the strong-coupling problem about FRW cosmological solutions in the theory of a galileon coupled to massive gravity [118]. This theory improves

upon the galileon coupled to GR in that both second-order equations of motion and the Galilean symmetry are preserved when coupling to massive gravity.

One may argue that in return for all of these concerns, we have merely traded a fine-tuning of the CC for a fine-tuning of the graviton mass. However, while a small value for the CC is not technically natural and is generically ruined by large quantum corrections, a small value for the graviton mass is technically natural due to the enhanced symmetry (unbroken diffeomorphisms) when $m \to 0$ [87]. This is manifested in the decoupling limit by the fact that quantum corrections to the galileon terms are higher-derivative and thus do not correct the galileon terms themselves [174, 175]. The result is that quantum corrections to the graviton mass are bounded by

$$\delta m^2 \lesssim m^2 \left(\frac{\Lambda_3}{M_{\rm Pl}} \right) \tag{2.4.5}$$

and thus parametrically smaller than the mass. As shown in Fig. 2.1, taking quantum corrections into effect there are three distance regimes of interest in Vainshtein screening - a small region in which quantum corrections dominate, a large Vainshtein-screened region in which nonlinear scalar interactions dominate, and an asymptotic linear regime.

For an in-depth review of the topics covered in this chapter, see [140, 83].

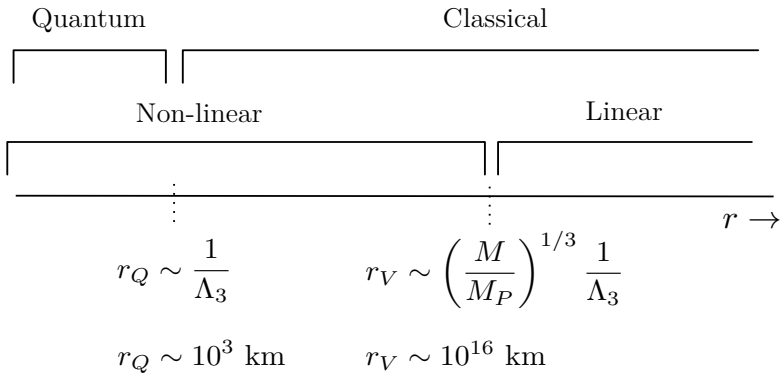

Figure 2.1: Division of distance regimes by importance of quantum effects and by linear or nonlinear dominant scalar interactions, with typical values for the solar system. [140]

Chapter 3

Ghost-freeness of massive gravity coupled to galileons

In this chapter we prove in full generality that the theory of a massive graviton coupled to a Galilean-invariant scalar field as developed in [118] propagates only the correct degrees of freedom (five degrees of freedom in the massive graviton and one in the galileon) and thus is free of the Boulware-Deser ghost.

Apart from generalizing dRGT, the construction of [118] is of interest because it provides a method of coupling the galileons to (massive) gravity while preserving the Galilean invariance. When coupling to ordinary massless gravity, non-minimal couplings must be added to ensure second-order equations of motion, and the Galilean symmetry is broken [102, 99]. In the present construction, there is no such problem, suggesting that the galileons more naturally couple to a massive graviton.

In [118], it was shown that the theory is ghost-free, for a flat bulk metric, in the decoupling limit, and for a certain simplifying choice of parameters. In this chapter, using methods similar to those of [143], we demonstrate that the full theory, for any bulk metric $G_{\mathcal{AB}}$, to all orders beyond the decoupling limit, and for all choices of parameters, has the primary constraint necessary to eliminate the Boulware-Deser ghost. This chapter is based on work done in collaboration with Garrett Goon, Kurt Hinterbichler, James Stokes, and Mark Trodden [13].

3.1 Background

It has long been known that the Fierz-Pauli action [117] provides a consistent description of the linear fluctuations of a massive graviton in flat spacetime. Nonlinear theories of massive gravity tend to propagate an extra, unphysical degree of freedom known as the Boulware-Deser (BD) ghost [44]. The presence of a ghost-like degree of freedom leads to an instability by which the vacuum decays into positive- and negative-energy states.

A general Lagrangian for nonlinear massive gravity can be formulated by introducing a nondynamical reference metric $\bar{g}_{\mu\nu}$ (e.g. the Minkowski one, $\bar{g}_{\mu\nu} = \eta_{\mu\nu}$) and constructing a potential of the form $V(g^{\mu\sigma}\bar{g}_{\sigma\nu})$. The potential explicitly breaks diffeomorphism invariance and it is expected that the theory generally propagates 12 phase-space degrees of freedom, rather than the 10 necessary to describe a massive graviton. The extra degree of freedom is the BD ghost.

The problem of finding a ghost-free nonlinear theory was only recently solved by de Rham, Gabadadze and Tolley (dRGT) [86, 89]. The dRGT theory is a 3-parameter family of potentials whose special structure ensures that there is a dynamical constraint which removes the ghost degree of freedom. This has been demonstrated by explicitly counting degrees of freedom in the Hamiltonian formalism [137, 136], and through other methods [88, 90, 170, 143].

3.2 Coupling the galileon to massive gravity

The galileon theory [175] was first explored as an extension of the 5-dimensional DGP model [111], and the full galileon theory can be shown to arise as the 4-dimensional effective theory of a 5-dimensional braneworld model by the inclusion of Lovelock terms (the unique extensions to the Einstein-Hilbert action which retain second-order equations of motion) [96]. Deriving the galileons as brane-bending modes in an extra-dimensional model ensures the Galilean symmetry, as it is descended from the bulk isometries; thus a braneworld picture is well-suited to developing extensions of the galileon theory.

Massive gravity can also be described in terms of a codimension-0 brane in a 4-dimensional bulk by disassociating the metric on the brane from the induced metric (which is taken to be nondynamical) and including interactions of the dRGT form between the two metrics. In this case, the brane-bending modes become pure gauge Stueckelberg fields that restore the diffeomorphism invariance broken by the

mass term [18]. The Stueckelberg method involves introducing four auxiliary scalars $\phi^{\mathcal{A}}(x)$ through the replacement $\bar{g}_{\mu\nu} \to \partial_\mu \phi^{\mathcal{A}} \partial_\nu \phi^{\mathcal{B}} \eta_{\mathcal{A}\mathcal{B}}$; the original theory is recovered by choosing unitary gauge $\phi^{\mathcal{A}} = \delta^{\mathcal{A}}_{\mu} x^{\mu}$.

By generalizing the brane construction of massive gravity (without specifying the bulk metric) to a D-dimensional bulk with $D \geq 4$, one obtains a theory with $D-4$ embedding fields which cannot be gauged away and these become physical Dirac-Born-Infeld (DBI) scalars coupled to the physical metric through the dRGT potential [118]. Thus the nondynamical induced metric is given in terms of the bulk coordinates $\phi^{\mathcal{A}}$ (so that now $\mathcal{A}, \mathcal{B}, \cdots$ run over D values) and bulk metric $G_{\mathcal{A}\mathcal{B}}(\phi)$ by

$$\bar{g}_{\mu\nu} = \partial_\mu \phi^{\mathcal{A}} \partial_\nu \phi^{\mathcal{B}} G_{\mathcal{A}\mathcal{B}}(\phi)\,. \tag{3.2.1}$$

Apart from the dRGT terms, curvature invariants constructed solely from $\bar{g}_{\mu\nu}$ and extrinsic curvatures of the embedding can be included in the action. The leading term in the derivative expansion is the DBI action $\sim \int \mathrm{d}^4x\sqrt{-\bar{g}}$, and higher Lovelock invariants give galileons [96, 145]. The theory will possess a galileon-like internal symmetry for every isometry of $G_{\mathcal{A}\mathcal{B}}$, and the resulting galileons will be the generalized curved space galileons discussed in [126, 124, 54].

The dynamical variables are the physical metric $g_{\mu\nu}$ and the D scalars $\phi^{\mathcal{A}}$, which appear through the induced metric (3.2.1). The action is

$$S = S_{\mathrm{EH}}[g] + S_{\mathrm{mix}}[g, \bar{g}] + S_{\mathrm{galileon}}[\bar{g}]\ . \tag{3.2.2}$$

Here $S_{\mathrm{EH}}[g]$ is the Einstein-Hilbert action for $g_{\mu\nu}$, with a possible cosmological

constant Λ,

$$S_{\rm EH}[g] = \frac{M_{\rm Pl}^2}{2}\int {\rm d}^4x\,\sqrt{-g}\,(R[g]-2\Lambda)\,. \tag{3.2.3}$$

The action mixing the two metrics is

$$S_{\rm mix}[g,\bar{g}] = -\frac{M_{\rm Pl}^2 m^2}{8}\sum_{n=1}^{3}\beta_n S_n\left(\sqrt{g^{-1}\bar{g}}\right)\,, \tag{3.2.4}$$

where $\sqrt{g^{-1}\bar{g}}$ is the matrix square root of the matrix $g^{\mu\sigma}\bar{g}_{\sigma\nu}$, and $S_n(M)$ of a matrix M are the symmetric polynomials[1] $S_n(M) = M^{[\mu_1}_{\ \ \mu_1}\cdots M^{\mu_n]}_{\ \ \mu_n}$. The β_n are three free parameters (one combination of which is redundant with the mass m). $S_{\rm galileon}[\bar{g}]$ stands for any Lagrangian constructed from diffeomorphism invariants of $\bar{g}$ (and extrinsic curvatures of the embedding) whose equations of motion remain second order in time derivatives. The possible terms in $S_{\rm galileon}[\bar{g}]$ are the Lovelock invariants and their boundary terms (see [96] and Sec. IV.B of [145] for a discussion). The structure of the dRGT-DBI coupled system (3.2.2) is nearly identical to that of ghost-free bigravity [135], the difference being that one of the two metrics is induced from a target space, and so it fundamentally depends on the embedding scalars.

[1] Our anti-symmetrization weight is $[\mu_1\ldots\mu_n] = \frac{1}{n!}(\mu_1\cdots\mu_n+\cdots)$. See appendix A of [143] for more details on the symmetric polynomials.

3.3 Vierbein formulation

Following [143], due to the presence of matrix square roots we will find it convenient to write the theory in terms of vierbein variables[2], which can be thought of as the square root of the metric. We write the physical metric and induced metric in terms of vierbeins $E^A = E_\mu{}^A \mathrm{d}x^\mu$, $\bar{E}^A = \bar{E}_\mu{}^A \mathrm{d}x^\mu$,

$$g_{\mu\nu} = E_\mu{}^A E_\nu{}^B \eta_{AB}, \quad \bar{g}_{\mu\nu} = \bar{E}_\mu{}^A \bar{E}_\nu{}^B \eta_{AB}, \tag{3.3.1}$$

where η_{AB} is the 4-dimensional Minkowski metric. For the induced metric $\bar{g}_{\mu\nu}$, we write the vierbein in an upper triangular form

$$\bar{E}_\mu{}^B = \begin{pmatrix} \bar{N} & \bar{N}^i \bar{e}_i{}^a \\ 0 & \bar{e}_i{}^a \end{pmatrix} . \tag{3.3.2}$$

Here $\bar{N}$ and $\bar{N}^i$ are ADM lapse and shift variables, and $\bar{e}_i{}^a$ is an upper triangular spatial dreibein for the spatial part of the induced metric and $\bar{e}^i{}_a$ its inverse transpose (in what follows $i, j, \ldots$ are spatial coordinate indices raised and lowered with the spatial metric $\bar{g}_{ij}$, and $a, b, \ldots$ are spatial Lorentz indices raised and lowered with δ_{ab}). These are obtained in terms of $\phi^{\mathcal{A}}$ by solving

$$\begin{aligned} \bar{g}_{00} &= \dot{\phi}^{\mathcal{A}} \dot{\phi}^{\mathcal{B}} G_{\mathcal{A}\mathcal{B}}(\phi) = -\bar{N}^2 + \bar{N}^i \bar{N}_i \\ \bar{g}_{0i} &= \dot{\phi}^{\mathcal{A}} \partial_i \phi^{\mathcal{B}} G_{\mathcal{A}\mathcal{B}}(\phi) = \bar{N}_i \\ \bar{g}_{ij} &= \partial_i \phi^{\mathcal{A}} \partial_j \phi^{\mathcal{B}} G_{\mathcal{A}\mathcal{B}}(\phi) = \bar{e}_i{}^a \bar{e}_j{}^b \delta_{ab} \ . \end{aligned} \tag{3.3.3}$$

[2]See also [105, 108] for covariant methods of degree of freedom counting in the vierbein formulation of massive gravity.

The upper triangular vierbein (3.3.2) has 10 components, and is merely a repackaging of the 10 components of $\bar{g}_{\mu\nu}$ (which in turn depend on the $\phi^{\mathcal{A}}$).

For the physical metric $g_{\mu\nu}$, we parameterize its 16-component vierbein as a local Lorentz transformation (LLT) Λ, which has 6 components, times a vierbein $\hat{E}$ which is constrained in some way so that it has only 10 components,

$$E_\mu{}^A = \Lambda^A{}_B \hat{E}_\mu{}^B \,. \tag{3.3.4}$$

The freedom to choose the constraints for $\hat{E}$ allows us to make different aspects of the theory manifest. The mixing term (3.2.4), in terms of vierbeins, takes the form

$$\begin{aligned}
S_{\text{mix}} &\equiv -\frac{M_{\text{Pl}}^2 m^2}{8} \sum_{n=1}^{3} \frac{\beta_n}{n!(4-n)!} S_{\text{mix}}^{(n)}, \\
S_{\text{mix}}^{(1)} &= \int \epsilon_{ABCD} \bar{E}^A \wedge E^B \wedge E^C \wedge E^D, \\
S_{\text{mix}}^{(2)} &= \int \epsilon_{ABCD} \bar{E}^A \wedge \bar{E}^B \wedge E^C \wedge E^D, \\
S_{\text{mix}}^{(3)} &= \int \epsilon_{ABCD} \bar{E}^A \wedge \bar{E}^B \wedge \bar{E}^C \wedge E^D.
\end{aligned} \tag{3.3.5}$$

The dynamical vierbein has 16 components, 6 more than the metric. If we choose the 6 constraints which $\hat{E}$ must satisfy to be the symmetry condition,

$$\hat{E}_{\mu[A} \bar{E}^\mu{}_{B]} = 0, \tag{3.3.6}$$

then we can show using the arguments in [143] (see also [104] for subtleties) that the extra 6 fields in Λ are auxiliary fields which are eliminated by their own equations of motion, setting $\Lambda = 1$, and the resulting theory is dynamically equivalent to the metric formulation (3.2.2).

Instead, we take $\hat{E}$ to be of upper triangular form

$$\hat{E}_\mu{}^A = \begin{pmatrix} N & N^i e_i{}^a \\ 0 & e_i{}^a \end{pmatrix} . \tag{3.3.7}$$

Here the spatial dreibein $e_i{}^a$ is arbitrary, containing 9 components. The LLT Λ in (3.3.4) depends now on 3 boost parameters p^a and can be written as

$$\Lambda(p)^A{}_B = \begin{pmatrix} \gamma & p^b \\ p_a & \delta^a_b + \frac{1}{1+\gamma} p^a p_b \end{pmatrix} , \tag{3.3.8}$$

where $\gamma \equiv \sqrt{1 + p^a p_a}$. Using this decomposition, the 16-component vierbein $E_\mu{}^A$ is parameterized in terms of the three components of p^a, one N, three components of N^i and the nine components of $e_i{}^b$.

3.4 Hamiltonian analysis

We start the Hamiltonian analysis by Legendre transforming with respect to the spatial vierbein $e_i{}^a$, defining canonical momenta $\pi^i{}_a = \frac{\partial \mathcal{L}}{\partial \dot{e}_i{}^a}$. Since S_{mix} contains no time derivatives of the physical metric, and S_{galileon} has no dependence on the physical metric at all, the expressions for the canonical momenta are the same as their GR counterparts. In particular, there will be three primary constraints

$$\mathcal{P}_{ab} = e_{i[a}\pi^i{}_{b]} = 0 . \tag{3.4.1}$$

In GR, these are first class constraints which generate local rotations.

The Einstein-Hilbert part of the action takes the form[3]

$$S_{\rm EH} = \int \mathrm{d}^4x\, \pi^i{}_a \dot{e}_i{}^a - \frac{1}{2}\lambda^{ab}\mathcal{P}_{ab} - N\mathcal{C}\left(e,\pi\right) - N^j\mathcal{C}_j\left(e,\pi\right). \tag{3.4.2}$$

The anti-symmetric λ^{ab} holds the three Lagrange multipliers for the three primary constraints (3.4.1). The N and N^i appear as Lagrange multipliers enforcing respectively the Hamiltonian and momentum constraints of GR: $\mathcal{C} = 0,\ \mathcal{C}_i = 0$.

We now look at the mixing terms (3.3.5). The contributions to $\mathcal{L}_{\rm mix}$ are of the form $\sim \epsilon^{\mu\nu\rho\sigma}\epsilon_{ABCD}E_\mu{}^A E_\nu{}^B \bar{E}_\rho{}^C \bar{E}_\sigma{}^D$, containing various numbers of copies of E and $\bar{E}$. From (3.3.2), (3.3.7) and (3.3.8), we see that the $\mu = 0$ components of $E_\mu{}^A$ and $\bar{E}_\mu{}^A$ are strictly linear in their respective lapses and shifts and the $\mu = i$ components are independent of the lapse and shift. Therefore, due to the anti-symmetry of the epsilons, the entire mixing term is linear in the lapses and shifts, so we may write

$$\begin{aligned}\mathcal{L}_{\rm mix} = &-N\mathcal{C}_{\rm mix}(e,\bar{e},p) - N^i\mathcal{C}_{{\rm mix},i}(e,\bar{e},p) - \bar{N}\bar{\mathcal{C}}_{\rm mix}(e,\bar{e},p)\\ &- \bar{N}^i\bar{\mathcal{C}}_{{\rm mix},i}(e,\bar{e},p) - \mathcal{H}_{\rm mix}(e,\bar{e},p)\ .\end{aligned} \tag{3.4.3}$$

The lapse and shift remain as Lagrange multipliers, and the p^a appear algebraically. We now solve the constraint enforced by N^i for the p^a: $\mathcal{C}_i + \mathcal{C}_{{\rm mix},i} = 0 \Rightarrow$

[3]See [107] or Appendix B of [143] for details of the Hamiltonian formulation of GR in vierbein form.

$p^a = p^a(e, \bar{e}, \pi)$. Plugging back into the action we obtain

$$\begin{aligned} S = \int \mathrm{d}^4x\, \pi^i{}_a \dot{e}_i{}^a - \frac{1}{2}\lambda^{ab}\mathcal{P}_{ab} - N\left[\mathcal{C}\left(e,\pi\right) + \mathcal{C}_{\mathrm{mix}}(e,\bar{e},\pi)\right] \\ - \bar{N}\bar{\mathcal{C}}_{\mathrm{mix}}(e,\bar{e},\pi) - \bar{N}^i\bar{\mathcal{C}}_{\mathrm{mix},i}(e,\bar{e},\pi) \\ - \mathcal{H}_{\mathrm{mix}}(e,\bar{e},\pi) + \mathcal{L}_{\mathrm{galileon}}(\bar{e},\bar{N},\bar{N}^i)\ . \end{aligned} \tag{3.4.4}$$

It remains to Legendre transform with respect to the scalars $\phi^{\mathcal{A}}$, which appear through the dependence of $\bar{N}$, $\bar{N}^i$ and $\bar{e}_i{}^a$, as determined by (3.3.3). In order to avoid dealing with the complications of diffeomorphism invariance, we first fix unitary gauge, setting the first four fields equal to the space-time coordinates: $\phi^\mu = x^\mu$ (this can be done consistently in the action, since the missing equations of motion are implied by the remaining equations). The Lagrangian (3.4.4) then depends on the remaining $D-4$ scalars and their time derivatives. Crucially, we see from (3.3.3) that while $\bar{N}$ and $\bar{N}_i$ depend on time derivatives of the scalars, the $\bar{e}_i{}^a$'s do not, and this in turn implies that the momenta conjugate to the scalars are independent of the dynamical lapse N. Thus, when the scalar velocities are eliminated in terms of the momenta, the action will remain linear in N. (If this were not the case, the lapse would no longer be a Lagrange multiplier, but would instead become an auxiliary field which does not impose a constraint on the remaining variables.) The phase space is spanned by the nine independent components of $e_i{}^a$, the physical scalars, and the canonical momenta. Since the interaction terms break the local rotation invariance of GR, the three primary constraints (3.4.1) associated with the local rotations will generate secondary constraints and form three second class pairs,

thus removing three degrees of freedom. The constraint enforced by N is precisely the special primary constraint needed to remove the Boulware-Deser sixth degree of freedom, leaving five degrees of freedom for the massive graviton. Analogously to what happens in massive gravity, we expect this special primary constraint to generate a secondary constraint to eliminate the ghost's conjugate momentum [136].

We have implicitly assumed that S_{galileon} can be written in such a way that the $D-4$ unitary gauge scalar fields appear with at most first time derivatives, so that we may define canonical momenta in the usual way. This is not immediately obvious, because the higher-order galileons in S_{galileon} possess higher-derivative interactions. However, the higher-derivative interactions within S_{galileon} are special in that they generate equations of motion which are no higher than second order in time. This means it should be possible, after integrations by parts, to express these Lagrangians in terms of first time derivatives only (though we shouldn't expect to be able to do the same with both the spatial and time derivatives simultaneously). For example, take the case of a flat 5D target space, so that there is a single physical scalar ϕ. The unitary gauge induced metric is $\bar{g}_{\mu\nu} = \eta_{\mu\nu} + \partial_\mu\phi\,\partial_\nu\phi$. The first higher-derivative galileon is the cubic, coming from the extrinsic curvature term

$$S_K \sim \int \mathrm{d}^4x\sqrt{-\bar{g}}\bar{K} \sim \int \mathrm{d}^4x \frac{\partial_\mu\partial_\nu\phi\,\partial^\mu\phi\,\partial^\nu\phi}{1+(\partial\phi)^2} \ . \tag{3.4.5}$$

Looking at the structure of the possible higher-order time derivatives, the only

offending term is

$$\frac{\ddot{\phi}\dot{\phi}^2}{1+(\partial\phi)^2} \subset \mathcal{L}_K \ . \tag{3.4.6}$$

Expanding the denominator in powers of $(\partial\phi)^2$ we see that every term in this expansion is of the form $\ddot{\phi}\dot{\phi}^n(\vec{\nabla}\phi)^{2m}$ for some integer m and n. Integrating by parts, we can express each one in terms of first time derivatives only: $\ddot{\phi}\dot{\phi}^n(\vec{\nabla}\phi)^{2m} \sim \frac{\mathrm{d}}{\mathrm{d}t}(\dot{\phi}^{n+1})(\vec{\nabla}\phi)^{2m} \sim \dot{\phi}^{n+1}\frac{\mathrm{d}}{\mathrm{d}t}(\vec{\nabla}\phi)^{2m}$. The same can be done with the higher galileons and with a curved bulk (see for example the Hamiltonian analysis of [215, 193] in the nonrelativistic case).

3.5 Implications

There exists [124, 126, 125] a wide range of novel scalar field theories with interesting properties such as Vainshtein screening and non-renormalization theorems in common with the original galileon models of [167, 175]. These properties hold out the hope that such models may be of use both in particle physics and as a possible way to modify gravity in the infrared. However, coupling such fields to general relativity in a way that preserves their symmetries and second-order equations of motion seems to be impossible [102]. Instead, galileon-like scalar fields seem to most naturally couple to dRGT massive gravity [118].

The consistency of such a proposal rests on the preservation of the hard-won ghost-free structure of the dRGT theory. In this chapter, we have shown for the first

time that a theory of nonlinear massive gravity coupled to DBI scalars in such a way as to preserve the generalized Galilean shift symmetry and the property of having second-order equations of motion is ghost free. Our proof is based on the vierbein formulation of massive gravity, in which the Hamiltonian analysis simplifies. Our analysis shows that the dRGT-DBI system provides a consistent framework in which models of interest to cosmology [144] may be developed.

Chapter 4

Strong coupling in massive gravity – galileon cosmology

As introduced in Chapter 2, modifying gravity by the introduction of an additional scalar, called the galileon, has interesting cosmological consequences: the galileon theory allows for the possibility of an accelerating cosmology without introducing any dark energy. However, in order to covariantize galileons while maintaining second order equations of motion one must break the defining assumption of Galilean symmetry [102, 99]. On the other hand, the dRGT theory is a covariant theory of a massive graviton whose longitudinal degree of freedom in the decoupling limit is a galileon [86]. This comes at the cost that a flat or closed homogeneous and isotropic self-accelerating cosmological solution is forbidden.

Although the dRGT theory possesses a self-accelerating solution with negatively

curved spatial slices [129], the study of fluctuations on top of this background has shown that the kinetic terms for the vector and scalar perturbations vanish [131], indicating that they are strongly coupled. The vanishing of these terms can be remedied by departing from isotropic and homogeneous cosmologies [130, 77] or by introducing new degrees of freedom. There are many ways to achieve the latter option, and several possibilities have been explored in the so-called quasidilaton [73, 134, 132, 113] and mass-varying extensions of dRGT [72, 147, 132]. (See [78] for a review of these aspects of cosmological solutions in various versions of massive gravity.)

In this chapter we perform a study of cosmological perturbations for the natural extension of dRGT introduced in [118] – massive gravity galileons – in which Dirac-Born-Infeld (DBI) scalars couple to the massive graviton in such a way that the scalars possess generalized Galilean shift symmetries [118]. This theory has been shown to be ghost free in the decoupling limit [118] and in full generality using the vierbein formalism [13] (see also [159]), and admits a self-accelerating branch that is a generalization of that discovered for massive gravity itself [144]. We study fluctuations around the self-accelerating branch and show that the kinetic terms for the scalar and vector modes vanish, just as they do in pure dRGT theory. This chapter is based on work done in collaboration with Kurt Hinterbichler, James Stokes, and Mark Trodden [15].

4.1 Massive gravity – galileon theory

The construction of massive gravity coupled to galileons is carried out using an extension of the probe brane approach [96, 145, 125, 126, 124, 54] for constructing general galileon models and the bimetric approach for constructing the dRGT non-linear massive gravity theory [138, 135]. We introduce a physical metric $g_{\mu\nu}$ and a second, induced metric $\bar{g}_{\mu\nu}$ which is the pull-back through a dynamical embedding $\phi^A(x)$ into a 5-dimensional Minkowski space with metric $\eta_{AB} = \mathrm{diag}(-1, 1, 1, 1, 1)$,

$$\bar{g}_{\mu\nu} = \eta_{AB}\partial_\mu\phi^A\partial_\nu\phi^B \ . \tag{4.1.1}$$

The action contains three kinds of terms:

$$S = S_{\rm EH}[g] + S_{\rm mix}[g, \bar{g}] + S_{\rm galileon}[\bar{g}] \ . \tag{4.1.2}$$

The first part $S_{\rm EH}[g]$ is the Einstein-Hilbert action for $g_{\mu\nu}$

$$S_{\rm EH}[g] = \frac{M_{\rm Pl}^2}{2}\int \mathrm{d}^4x\,\sqrt{-g}\,R[g] \ . \tag{4.1.3}$$

The second part is the action mixing the two metrics,

$$S_{\rm mix}[g, \bar{g}] = M_{\rm Pl}^2 m^2 \int \mathrm{d}^4x\sqrt{-g}(\mathcal{L}_2 + \alpha_3\mathcal{L}_3 + \alpha_4\mathcal{L}_4) \ , \tag{4.1.4}$$

where

$$\begin{aligned}
\mathcal{L}_2 &= \frac{1}{2}\left([\mathcal{K}]^2 - [\mathcal{K}^2]\right) \ , \\
\mathcal{L}_3 &= \frac{1}{6}\left([\mathcal{K}]^3 - 3[\mathcal{K}][\mathcal{K}^2] + 2[\mathcal{K}^3]\right) , \\
\mathcal{L}_4 &= \frac{1}{24}\left([\mathcal{K}]^4 - 6[\mathcal{K}]^2[\mathcal{K}^2] + 3[\mathcal{K}^2]^2 + 8[\mathcal{K}][\mathcal{K}^3] - 6[\mathcal{K}^4]\right) \ ,
\end{aligned}$$

and where the brackets are traces of powers of the matrix $\mathcal{K}^{\mu}{}_{\nu} = \delta^{\mu}{}_{\nu} - \sqrt{g^{\mu\sigma}\bar{g}_{\sigma\nu}}$. The final part is the DBI galileon action $S_{\rm galileon}[\bar{g}]$ consisting of the Lovelock invariants constructed from $\bar{g}$, and their boundary terms (see [96, 127, 126] and Sec. IV.B of [145]; we use normalizations consistent with [127, 126]),

$$S_{\rm galileon} = \Lambda^4 \int \mathrm{d}^4x\sqrt{-\bar{g}}\Big\{ -a_2 + \frac{a_3}{\Lambda}[\bar{K}] - \frac{a_4}{\Lambda^2}\left([\bar{K}]^2 - [\bar{K}^2]\right) + \frac{a_5}{\Lambda^3}\left([\bar{K}]^3 - 3[\bar{K}][\bar{K}^2] + 2[\bar{K}^3]\right)\Big\}, \tag{4.1.5}$$

where $\bar{K}_{\mu\nu}$ is the extrinsic curvature of the brane embedding $\phi^A(x)$ into the flat 5-dimensional Minkowski space and indices are raised with $\bar{g}^{\mu\nu}$ (since the bulk is flat, we may use Gauss-Codazzi to eliminate all intrinsic curvatures in favor of extrinsic curvatures).

Note that we have set the cosmological constant and a possible tadpole term in $S_{\rm galileon}$ to zero. This ensures the existence of a flat space solution with constant π. Restoring these terms does not change our essential conclusion.

4.2 Background cosmology and self-accelerating solutions

For our purposes, we take a Friedmann-Robertson-Walker (FRW) ansatz for the physical metric

$$\mathrm{d}s^2 = -N^2(t)\mathrm{d}t^2 + a^2(t)\Omega_{ij}\mathrm{d}x^i\mathrm{d}x^j \ , \quad \Omega_{ij} = \delta_{ij} + \frac{\kappa}{1-\kappa r^2}x^i x^j \ , \tag{4.2.1}$$

where $\kappa < 0$ is the spatial curvature.

As shown in [144], this model does not admit nontrivial cosmological solutions for a flat FRW ansatz with a homogeneous fiducial metric, just as pure dRGT massive gravity does not [72], and there are no solutions for $\kappa > 0$ since the fiducial Minkowski metric cannot be foliated by closed slices. (There are, however, known solutions to pure dRGT massive gravity with FRW physical metric and and inhomogeneous Stueckelberg sector [72, 128], that is, solutions where the physical metric is FRW but the fiducial metric is not also FRW in the same coordinates.)

The embedding (the Stueckelbergs) is chosen so that the fiducial metric has the symmetries of an open FRW spacetime [129],

$$\phi^0 = f(t)\sqrt{1-\kappa\vec{x}^2}, \quad \phi^i = \sqrt{-\kappa}f(t)x^i, \quad \phi^5 \equiv \pi(t)\ . \tag{4.2.2}$$

where $f(t)$ plays the role of a Stueckelberg field which restores time reparametrization invariance. The induced metric then takes the form

$$\bar{g}_{\mu\nu}dx^\mu dx^\nu = \left(-\dot{f}(t)^2 + \dot{\pi}(t)^2\right)dt^2 - \kappa f(t)^2\Omega_{ij}(\vec{x})dx^i dx^j. \tag{4.2.3}$$

Note that we can obtain the extended massive gravity mass terms from the dRGT mass terms by replacing $\bar{g}_{\mu\nu}$ with $\bar{g}_{\mu\nu} + \partial_\mu\pi\partial_\nu\pi$.

This ansatz leads to the mini-superspace action

$$S_{\rm EH} = 3M_{\rm Pl}^2\int \mathrm{d}t\ \left[-\frac{\dot{a}^2 a}{N} + \kappa N a\right]\ , \tag{4.2.4}$$

$$S_{\rm mix} = 3M_{\rm Pl}^2\int \mathrm{d}t\, m^2\left[NF(a,f) - G(a,f)\sqrt{\dot{f}^2 - \dot{\pi}^2}\right]\ , \tag{4.2.5}$$

where

$$F(a,f) = a(a-\sqrt{-\kappa}f)(2a-\sqrt{-\kappa}f) + \frac{\alpha_3}{3}(a-\sqrt{-\kappa}f)^2(4a-\sqrt{-\kappa}f) + \frac{\alpha_4}{3}(a-\sqrt{-\kappa}f)^3 \ , \tag{4.2.6}$$

$$G(a,f) = a^2(a-\sqrt{-\kappa}f) + \alpha_3 a(a-\sqrt{-\kappa}f)^2 + \frac{\alpha_4}{3}(a-\sqrt{-\kappa}f)^3 \ . \tag{4.2.7}$$

Varying with respect to N, we obtain the Friedmann equation,

$$\frac{H^2}{N^2} + \frac{\kappa}{a^2} + m^2\frac{F(a,f)}{a^3} = 0 \ . \tag{4.2.8}$$

The equations obtained by varying the action with respect to f and π, respectively, are

$$\frac{\delta S}{\delta f} = 3M_{\rm Pl}^2 m^2 \frac{\partial G}{\partial a}\left(\frac{\dot{a}}{\dot{f}}\sqrt{\dot{f}^2-\dot{\pi}^2} - N\sqrt{-\kappa}\right) + \frac{\dot{\pi}}{\dot{f}}\dot{\Pi} = 0 \ , \tag{4.2.9}$$

$$\frac{\delta S}{\delta \pi} = -\dot{\Pi} = 0 \ , \tag{4.2.10}$$

where we have defined the quantity

$$\Pi = \left(3M_{\rm Pl}^2 m^2 G + a_2\Lambda^4\left(\sqrt{-\kappa}f\right)^3\right)\frac{\dot{\pi}}{\sqrt{\dot{f}^2-\dot{\pi}^2}} - 3a_3\Lambda^3\left(\sqrt{-\kappa}\right)^3 f^2\left(\frac{\dot{\pi}}{\sqrt{\dot{f}^2-\dot{\pi}^2}}\right)^2 + 6a_4\Lambda^2\left(\sqrt{-\kappa}\right)^3 f\left(\frac{\dot{\pi}}{\sqrt{\dot{f}^2-\dot{\pi}^2}}\right)^3 - 6a_5\Lambda\left(\sqrt{-\kappa}\right)^3\left(\frac{\dot{\pi}}{\sqrt{\dot{f}^2-\dot{\pi}^2}}\right)^4 \ . \tag{4.2.11}$$

The acceleration equation obtained by varying with respect to a is redundant, due to the time reparametrization invariance of the action.

In contrast to GR, these equations enforce a constraint: the combination $\dot{f}\frac{\delta S}{\delta f} + \dot{\pi}\frac{\delta S}{\delta \pi}$ becomes

$$\frac{\partial G(a,f)}{\partial a}\left(\dot{a}\sqrt{\dot{f}^2-\dot{\pi}^2} - \sqrt{-\kappa}N\dot{f}\right) = 0 \ , \tag{4.2.12}$$

the analogue of which for pure massive gravity is responsible for the well-known absence of flat FRW solutions in that theory.

There exist two branches of solutions depending on whether the constraint equation is solved by setting $\frac{\partial G}{\partial a} = 0$ or instead by setting $\dot{a}\sqrt{\dot{f}^2 - \dot{\pi}^2} - \sqrt{-\kappa}N\dot{f} = 0$. In this work we shall focus on the former choice, since this corresponds to de Sitter space – the self-accelerating branch of the theory [144], in which the metric takes the same form as the self-accelerating solution of the original massive gravity theory. Defining

$$X \equiv \frac{\sqrt{-\kappa}f}{a} \,, \tag{4.2.13}$$

we find an algebraic equation for f that can be written in the form $J_\phi = 0$, where

$$J_\phi \equiv 3 - 2X + \alpha_3(1-X)(3-X) + \alpha_4(1-X)^2 \,. \tag{4.2.14}$$

The solutions read

$$f(t) = \frac{1}{\sqrt{-\kappa}} X_\pm a(t) \,, \qquad X_\pm \equiv \frac{1 + 2\,\alpha_3 + \alpha_4 \pm \sqrt{1 + \alpha_3 + \alpha_3^2 - \alpha_4}}{\alpha_3 + \alpha_4} \,. \tag{4.2.15}$$

These are the same self-accelerated solutions that were found in pure massive gravity [129]. The solution for the extra galileon field π can then be determined by solving (4.2.10).

4.3 Perturbations

We now turn to the primary issue addressed in this paper – the behavior of perturbations around this background cosmological solution. To obtain the quadratic

action for perturbations, we work in unitary gauge for the Stueckelberg fields ϕ^0 and ϕ^i and expand the metric and π fields to second order in fluctuations around the background. We write the metric as $g_{\mu\nu} = g^{(0)}_{\mu\nu} + \delta g_{\mu\nu}$, with

$$\delta g_{\mu\nu} = \begin{pmatrix} -2N^2\Phi & NaB_i \\ NaB_j & a^2 h_{ij} \end{pmatrix} . \tag{4.3.1}$$

Here, Φ, B_i and h_{ij} are the small perturbations, N and a are the background lapse and scale factor, and we henceforth raise and lower Latin indices with respect to Ω_{ij}.

The vector perturbation B_i can be decomposed into transverse and longitudinal components via

$$B_i = B_i^T + \partial_i B \ , \quad D^i B_i^T = 0, \tag{4.3.2}$$

where D_i denotes the covariant derivative with respect to Ω_{ij}. The tensor perturbations h_{ij} decompose into a transverse traceless component h_{ij}^{TT}, a transverse vector E_i^T, a longitudinal component E, and a trace Ψ as follows:

$$h_{ij} = 2\Psi\Omega_{ij} + \left(D_i D_j - \frac{1}{3}\Omega_{ij}\triangle \right) E + \frac{1}{2}(D_i E_j^T + D_j E_i^T) + h_{ij}^{TT} \ , \tag{4.3.3}$$

where $\triangle \equiv D^i D_i$, and the transverse traceless conditions read

$$D^i h_{ij}^{TT} = h_i^{TT\, i} = 0, \quad D^i E_i^T = 0 \ . \tag{4.3.4}$$

We denote the remaining dynamical scalar field – the galileon perturbation – by τ, via

$$\phi^5 = \pi + \tau \ . \tag{4.3.5}$$

4.3.1 Preliminaries

Before writing the full quadratic actions for the various perturbations, we first write some intermediate expressions obtained from the expansions of the mass terms (4.1.4). This will serve to highlight the manner in which the kinetic terms vanish, and illustrate the similarities with pure dRGT.

For convenience, we introduce the quantities

$$s = \sqrt{1 - (\dot{\pi}/\dot{f})^2} \ , \quad r = \frac{\dot{f}a}{N\sqrt{-\kappa}f} \ , \tag{4.3.6}$$

and we will continue to use J_ϕ to denote the quantity (4.2.14) which vanishes on the equations of motion.

Expanding the mass term to linear order in the fluctuations yields

$$S_{\rm mix} = S^{(0)}_{\rm mix} + \int dx^4 N a^3 \sqrt{\Omega} \Bigg[- \left(\Phi + \frac{1}{2}h\right)\rho_g + \frac{1}{2}M_{\rm Pl}^2 m_g^2 (1 - rs) X h J_\phi + M_{\rm Pl}^2 m_g^2 (r\dot{\pi}/\dot{f}^2 s) Y \dot{\tau} \Bigg] \ , \tag{4.3.7}$$

where we have defined

$$\rho_g \equiv -M_{Pl}^2 m_g^2 (1 - X) \left[3(2 - X) + \alpha_3 (1 - X)(4 - X) + \alpha_4 (1 - X)^2\right] , \tag{4.3.8}$$

$$Y \equiv X(1 - X) \left[3 + 3\alpha_3 (1 - X) + \alpha_4 (1 - X)^2\right] \ . \tag{4.3.9}$$

When the background equations of motion for the Stueckelberg fields are satisfied, the terms linear in the metric match the corresponding terms of pure massive gravity. This suggests that we follow the massive gravity analysis of [131] and define

$$\tilde{S}_{\rm mix}[g_{\mu\nu}, \tau] \equiv S_{\rm mix}[g_{\mu\nu}, \tau] + \int {\rm d}^4 x \sqrt{-g} \rho_g \equiv M_{\rm Pl}^2 m_g^2 \int d^4 x N a^3 \sqrt{\Omega} \tilde{\mathcal{L}}_{\rm mix} \ . \tag{4.3.10}$$

Expanding to second order in perturbations we have,

$$\tilde{\mathcal{L}}^{(0)}_{\rm mix} = -rsY, \tag{4.3.11}$$

$$\tilde{\mathcal{L}}^{(1)}_{\rm mix} = 3(1-rs)XJ_\phi\Psi + (r\dot{\pi}/\dot{f}^2 s)Y\dot{\tau}, \tag{4.3.12}$$

$$\begin{aligned}\tilde{\mathcal{L}}^{(2)}_{\rm mix} =& \frac{1}{2}\frac{r}{s}\frac{1}{\dot{f}^2 s^2}Y\dot{\tau}^2 + \frac{1}{2}\left(6\Phi\Psi + \frac{B_i^T B^{Ti}}{1+rs}\right)XJ_\phi + 3\frac{r}{s}\frac{\dot{\pi}}{\dot{f}^2}XJ_\phi\dot{\tau}\Psi \\ &+ \frac{\dot{\pi}}{\sqrt{-\kappa}\dot{f}f}\left(\frac{r}{1+rs}\right)XJ_\phi\tau\triangle B - \frac{1}{2\kappa f^2}\left[\left(\frac{1-r^2}{1+rs}\right)XJ_\phi + \frac{r}{s}Y\right]\tau\triangle\tau \\ &+ \frac{1}{8}(1-rs)\left(12\Psi^2 - 2h_{ij}^{TT}h^{TTij} + E_j^T\triangle E^{Tj}\right)XJ_\phi \\ &+ \frac{1}{8}m_g^{-2}M_{GW}^2\left(24\Psi^2 - h_{ij}^{TT}h^{TTij} + \frac{1}{2}E_j^T\triangle E^{Tj}\right),\end{aligned} \tag{4.3.13}$$

where we have defined a quantity which will turn out to be the graviton mass term:

$$m_g^{-2}M_{GW}^2 \equiv XJ_\phi + (1-rs)X^2\left[1+\alpha_3(2-X)+\alpha_4(1-X)\right]\ . \tag{4.3.14}$$

Here we have not imposed any equations of motion on the background. We note that all of the terms in (4.3.13) which depend upon Φ or B_i are proportional to J_ϕ, and therefore vanish on the de Sitter self-accelerating branch, on which $J_\phi = 0$. As we will see, this implies the vanishing of the graviton scalar and vector kinetic terms on this background.

4.3.2 Tensor perturbations

We now write the full second-order action obtained from expanding (4.1.2) and decomposing the perturbations according to (4.3.1) and (4.3.2), (4.3.3).

The tensor perturbations take the same form as in pure massive gravity, but

with a different time-dependent mass term,

$$S^{(2)}_{\rm tensor} = \frac{M_{\rm Pl}^2}{8}\int {\rm d}^4x\sqrt{\Omega}\,Na^3\Big[\frac{1}{N^2}\dot{h}^{TTij}\dot{h}^{TT}_{ij} + \frac{1}{a^2}h^{TTij}(\triangle - 2\kappa)h^{TT}_{ij} - M^2_{GW}h^{TTij}h^{TT}_{ij}\Big], \tag{4.3.15}$$

where M^2_{GW}, in terms of the definitions (4.3.6), (4.2.13) made above, takes the following value on the de Sitter self-accelerating branch,

$$M^2_{GW} = \pm(rs-1)m_g^2X_\pm^2\sqrt{1+\alpha_3+\alpha_3^2-\alpha_4}\,. \tag{4.3.16}$$

As in pure massive gravity, the tensor perturbation maintains the correct sign for both the kinetic and gradient terms. However, the new mass term implies a more complicated region of parameter space in which the tensors are non-tachyonic, $M^2_{GW} > 0$ (the sign of the mass term is given by the sign of $\pm(rs-1)$). Note, however, that even if this term is negative, so that we have a tachyonic instability, then barring any fine tuning such instabilities are of order the Hubble scale if we have chosen $m \sim H$ to ensure late-time acceleration of the correct magnitude. This agrees qualitatively with the result found in pure massive gravity.

4.3.3 Vector perturbations

Since the vector field B_i^T obtained from δg_{0i} does not appear in the Lagrangian with any time derivatives, it can be eliminated as an auxiliary field. Leaving the background fields arbitrary for the moment, we find the solution

$$B_i^T = \frac{a(1+rs)\,(-\triangle - 2\kappa)}{2\,[(1+rs)(-\triangle - 2\kappa) + 2a^2J_\phi m^2X]\,N}\dot{E}_i^T. \tag{4.3.17}$$

This matches the result of pure dRGT theory $B_i^T = \frac{a}{2N}\dot{E}_i^T$ when the Stueckelberg equation of motion for the de Sitter self-accelerating branch is imposed, $J_\phi = 0$. It is instructive, however, to leave the backgrounds arbitrary so that we can explicitly see the kinetic term vanish. Substituting the general expression for the non-dynamical vector we obtain

$$S^{(2)}_{\rm vector} = \frac{M_{\rm Pl}^2}{8}\int d^4x\sqrt{\Omega}\, a^3 N\Bigg\{\mathcal{T}_V(\dot{E}_i^T)^2 - \left[\frac{1}{2}M_{GW}^2(-\triangle - 2\kappa) + J_\phi k^2 m^2(1-rs)\right](E_i^T)^2\Bigg\}\,, \tag{4.3.18}$$

where

$$\mathcal{T}_V = \frac{a^2 J_\phi m^2 X\,(-\triangle - 2\kappa)}{[(1+rs)(-\triangle - 2\kappa) + 2a^2 J_\phi m^2 X]\,N^2}\,. \tag{4.3.19}$$

The vanishing of the vector kinetic terms is now obvious on the de Sitter self-accelerating branch where $J_\phi = 0$. The vector Lagrangian has the same form as pure dRGT theory, only with a different time-dependent mass,

$$S^{(2)}_{\rm vector} = -\frac{M_{\rm Pl}^2}{16}\int d^4x\sqrt{\Omega}\, a^3 N M_{GW}^2(-\triangle - 2\kappa)(E_i^T)^2. \tag{4.3.20}$$

4.3.4 Scalar perturbations

The analysis of the scalar perturbations simplifies considerably on the de Sitter self-accelerating branch since all the terms mixing scalar degrees of freedom from the graviton with the fluctuation of the galileon vanish when $J_\phi = 0$, as can be seen from the expression (4.3.13). The scalars Φ and B coming from perturbations of δg_{00} and δg_{0i} appear without time derivatives and we may eliminate them as

auxiliary fields. We obtain (this time imposing the self-accelerating background equation of motion $J_\phi = 0$)

$$\Phi = \frac{\kappa\triangle}{6a^2H^2}E - \frac{\triangle}{6HN}\dot{E} - \frac{\kappa}{a^2H^2}\Psi + \frac{1}{HN}\dot{\Psi} \tag{4.3.21}$$

$$B = \frac{\triangle}{6aH}E + \frac{a}{2N}\dot{E} - \frac{1}{aH}\Psi \tag{4.3.22}$$

which are the same as in pure dRGT theory. The calculation of the graviton scalar quadratic action mirrors the dRGT case and we find that the kinetic terms vanish and the action once again has the same form as pure dRGT, only with a modified time-dependent mass,

$$S^{(2)}_{\rm scalar} = \frac{M_{\rm Pl}^2}{2}\int d^4x\sqrt{\Omega}\,a^3N\left(6M_{GW}^2\Psi^2 + \frac{1}{6}M_{GW}^2\triangle(-\triangle - 3\kappa)E^2\right). \tag{4.3.23}$$

We now turn to the expansion of the galileon action (4.1.5), using (4.3.5). We start by expanding the lowest galileon, the DBI term (the one proportional to a_2 in (4.1.5)) to quadratic order in τ. We obtain $S_{\rm DBI} = -a_2\Lambda^4\int d^4xNa^3\sqrt{\Omega}\mathcal{L}_{\rm DBI}$, where

$$\mathcal{L}^{(0)}_{\rm DBI} = rsX^4\ , \tag{4.3.24}$$

$$\mathcal{L}^{(1)}_{\rm DBI} = -\left(\frac{r}{s}\frac{\dot{\pi}}{\dot{f}^2}\dot{\tau}\right)X^4\ , \tag{4.3.25}$$

$$\mathcal{L}^{(2)}_{\rm DBI} = -\frac{1}{2}\frac{r}{s}\left(\frac{1}{\dot{f}^2s^2}\dot{\tau}^2 + \frac{1}{\kappa f^2}\tau\triangle\tau\right)X^4\ . \tag{4.3.26}$$

From $\mathcal{L}^{(2)}_{\rm DBI}$ we see that the effect of including the DBI Lagrangian is to shift $Y \to Y + (a_2\Lambda^4/m^2M_{\rm Pl}^2)X^4$ in the quadratic action (4.3.13). Note that on the de Sitter self-accelerating branch, where $J_\phi = 0$, this is equivalent to shifting the brane tension by

$$\Lambda^4 \to \tilde{\Lambda}^4 = \Lambda^4 + \frac{m^2M_{\rm Pl}^2}{a_2}\frac{Y_\pm}{X_\pm^4}\ . \tag{4.3.27}$$

We therefore see that on the self-accelerating de Sitter branch, the galileon has the correct-sign kinetic term provided

$$\frac{m^2 M_{\rm Pl}^2}{a_2 \Lambda^4} \frac{Y_\pm}{X_\pm^4} > -1 \ . \tag{4.3.28}$$

It is clear that this constraint can always be satisfied by choosing $a_2\Lambda^4$ appropriately large. Note that the background Stueckelberg and galileon fields do not lead to any simplification for the DBI quadratic action.

The higher galileon terms in (4.1.5) can be similarly expanded to quadratic order. After imposing the background equation for the Stueckelberg/galileon and its time derivatives, we obtain $S_{\rm galileon} = \Lambda^4 \int d^4x N a^3 \sqrt{\Omega} \mathcal{L}_{\rm galileon}$, where

$$\begin{aligned}
\mathcal{L}^{(2)}_{\rm galileon} = & -\frac{r}{\dot{f}^2 s^3}\left[-\frac{1}{2}a_2 + 3\frac{a_3}{\Lambda}\left(\frac{\dot{\pi}}{sf\dot{f}}\right) - 9\frac{a_4}{\Lambda^2}\left(\frac{\dot{\pi}}{sf\dot{f}}\right)^2 + 12\frac{a_5}{\Lambda^3}\left(\frac{\dot{\pi}}{sf\dot{f}}\right)^3\right] X^4\dot{\tau}^2 \\
& - \frac{r}{s}\frac{1}{\kappa f^2}\left[\frac{1}{2}a_2 + \frac{a_3}{\Lambda}\frac{\dot{\pi}}{sf\dot{f}} - \frac{a_4}{\Lambda^2}\frac{3\dot{\pi}^4 + 11\dot{f}^2\dot{\pi}^2 - 2\dot{f}^4}{s^2 f^2 \dot{f}^4}\right. \\
& \left. + 6\frac{a_5}{\Lambda^3}\frac{3\dot{\pi}^4 + 2\dot{f}^2\dot{\pi}^2 + 2\dot{f}^4}{s^3 f^3 \dot{f}^5}\dot{\pi}\right] X^4 \tau \triangle \tau \ .
\end{aligned} \tag{4.3.29}$$

The conditions for stability can now be read off by requiring that these kinetic terms have the correct sign.

4.4 Implications

We have examined the nature of cosmological perturbations around the self-accelerating branch of the massive gravity galileon theory of [118], in which the galileon fields couple covariantly to massive gravity while simultaneously retaining

both their symmetry properties and their second-order equations of motion. This construction provides a more general framework within which we may ask self-consistent questions about the implications of both massive gravity and galileon models. Such an approach is important both for the wider goal of understanding the general implications of modified gravity models, and also for probing the extent to which particular features of massive gravity are peculiar to the specific restrictive structure of that theory.

One of the more striking results of dRGT massive gravity is that the kinetic terms for both vector and scalar perturbations vanish around the phenomenologically interesting self-accelerating branch of the theory. The main result of our analysis is that the vanishing of these kinetic terms is preserved around the analogous de Sitter branch in the more general class of theories, suggesting that this is a generic result tied to the existence of self-accelerating homogeneous solutions in theories with this general structure. This is partly upheld by ghost-free bimetric gravity, for which there are two branches of FRW solutions: one for which the ratio of Hubble constants for the two metrics is constant, and one for which it is non-constant. The first branch is the analogue of the solution studied here, and exhibits the same vanishing of kinetic terms for one vector and one scalar degree of freedom; on the second branch, however, all 7 degrees of freedom are dynamical [67]. Furthermore, we have verified that the tensor perturbations are ghost-free, and that while the details of the analysis of their mass terms differs from that in pure

massive gravity, any tachyonic modes are similarly unstable on Hubble timescales.

An obvious extension of this work is to study the behavior of the same perturbations around the other branch of cosmological solutions identified in [144] (this work is underway). One may also wish to search for the equivalent to the pure dRGT massive gravity solutions which display flat, approximately FRW cosmological solutions at the cost of an inhomogeneous Stueckelberg sector as in [72, 128], about which the kinetic terms for scalar perturbations no longer vanish [211, 165]. It will also be interesting to ask whether the fluctuations of the galileon around these accelerating solutions can be kept subluminal, in contrast to the situation around flat space [127].

Chapter 5

Instabilities of spherical solutions with multiple galileons and $SO(N)$ symmetry

There has been much recent interest in theories of gravity arising from scenarios with extra spatial dimensions. Many examples of these are based on the Dvali-Gabadadze-Porrati (DGP) model [111, 110] – a $(4+1)$-dimensional theory with action consisting simply of separate Einstein-Hilbert terms in the bulk and on a codimension-1 brane, to which standard model particles are also confined. The model results in a 4D gravitational force law at sufficiently small scales, which transitions to a 5D gravitational force law at a crossover length scale $r_c \sim M_{\rm Pl}^2/M_5^3$, determined by the 5D and 4D gravitational couplings M_5 and $M_{\rm Pl}$ respectively. To

yield interesting cosmological dynamics, this crossover scale is usually chosen to be of order the horizon size.

Much of the phenomenology of the DGP model is captured by its decoupling limit $M_{\rm Pl},\ M_5 \to \infty$ with the strong-coupling scale $\Lambda_5 \sim M_5^2/M_{\rm Pl}$ kept fixed [167, 174]. In this limit, the difference between DGP gravity and general relativity is encoded in the behavior of a scalar degree of freedom, π. The dynamics of this scalar are invariant under internal Galilean transformations $\pi \to \pi + c + b_\mu x^\mu$, with c a constant and b_μ a constant vector. This symmetry proves to be extremely restrictive, with a leading order self-interaction term that is a higher-derivative coupling cubic in π, and yet yields second-order equations of motion. Higher-order couplings with these properties were derived independently of the DGP model [175, 102, 99, 176] and dubbed "galileons." See [63, 192, 161, 160, 158, 212, 70, 79, 81] for cosmological studies of galileon theories.

It is natural to explore induced gravity models in codimension greater than one [109, 119, 162, 84, 91, 152, 68, 69, 93, 94], and recently multi-galileon actions arising in the relevant 4-dimensional decoupling limit have been derived [145, 100, 181, 179]. The theories studied in [145] are invariant under individual Galilean transformations of the π fields, and also under an internal $SO(N)$ symmetry rotating the fields into one another, thus forbidding the existence of terms containing an odd number of π fields, in contrast to the codimension one DGP case. In this chapter we explore the nature of spherically symmetric solutions in theories with an $SO(N)$

internal symmetry among the galileon fields, and couplings to matter that respect this symmetry. This chapter is based on work done in collaboration with Kurt Hinterbichler, Justin Khoury, and Mark Trodden [14].

Spherical solutions for a more general bi-galileon action were discussed in [180], for the specific case of a linear coupling $\sim \pi T$ to matter, where T is the trace of the matter energy-momentum tensor. This form of coupling arises from decoupling limits of DGP-like theories, because π arises through a conformal mixing with the graviton. However, while this coupling is therefore the natural form to consider in the case of a single galileon field, it breaks the new internal symmetry satisfied by multiple galileons (and breaks the Galilean symmetry if the matter is dynamical). We instead study general non-derivative couplings to matter fields which respect the $SO(N)$ internal symmetry.

At the background level, our solution can always be rotated to lie along a single field direction, say π_1, while the other field variables remain trivial, thus exhibiting spontaneous symmetry breaking. The solution exhibits Vainshtein screening [198, 101], characteristic of galileon theories: we find $\pi_1 \sim r$ sufficiently close to the source, whereas $\pi_1 \sim 1/r$ far away, with the crossover scale determined by a combination of the galileon self-interaction scale and the coupling to the source. However, when we turn to the stability of spherically symmetric solutions under small perturbations, we find that, sufficiently close to the source, perturbations in π_1 suffer from gradient instabilities along the angular directions. Morever, they propa-

gate superluminally along both the radial and angular directions (in the regime that angular perturbations are stable). Perturbations in the remaining $N-1$ galileon fields are stable but propagate superluminally in the radial direction.

The gradient instability and superluminal propagation found here for the π_1 field are multi-field generalizations of single galileon instabilities [175]. Our findings thus present significant hurdles for $SO(N)$ galileon models with non-derivative matter coupling. One of the main lessons to be drawn is that more general matter couplings, including derivative interactions, are necessary for the phenomenological viability of $SO(N)$ multi-galileon theories. For instance, the coupling $\sim \partial_\mu \pi^I \partial_\nu \pi_I T^{\mu\nu}$ naturally arises from brane-world constructions [96, 145] and maintains both the Galilean and the internal rotation symmetries.

5.1 Multi-galileon theory from extra dimensions

In codimension N, the 4-dimensional effective theory contains N fields π^I, $I = 1 \cdots N$, representing the N brane-bending modes of the full $(4+N)$-dimensional theory. The extended symmetry of the vacuum Lagrangian is

$$\delta\pi^I = \omega^I{}_\mu x^\mu + \epsilon^I + \omega^I{}_J \pi^J \ , \tag{5.1.1}$$

where $\omega^I{}_\mu$, ϵ^I and $\omega^I{}_J$ are constant transformation parameters. (See [145] for the geometric setup and origin of this symmetry). This transformation consists of a Galilean invariance acting on each of the π^I fields, and an $SO(N)$ rotation symme-

try under which π_I transforms as a vector. The unique 4-dimensional Lagrangian density respecting this is [181, 145]

$$\mathcal{L}_\pi = -\frac{1}{2}\partial_\mu\pi^I\partial^\mu\pi_I - \lambda\left[\partial_\mu\pi^I\partial_\nu\pi^J\left(\partial_\lambda\partial^\mu\pi_J\partial^\lambda\partial^\nu\pi_I - \partial^\mu\partial^\nu\pi_I\Box\pi_J\right)\right],$$

where λ is a coupling with dimension $[\text{mass}]^{-6}$, containing the strong interaction mass scale. The I, J indices are raised and lowered with δ_{IJ}.

It remains to couple this theory to matter. The natural coupling we might consider, the lowest dimension coupling that preserves the Galilean and internal rotation symmetries, is $\sim \partial_\mu\pi^I\partial_\nu\pi_I T^{\mu\nu}$. This is the coupling that naturally arises from brane matter in the construction of [96, 145]. However, for static nonrelativistic sources $T^{\mu\nu} \sim \rho\delta_0^\mu\delta_0^\nu$, and since $\partial_0\pi = 0$ for static solutions there are no nontrivial spherically symmetric solutions with this coupling.

Linear couplings $\mathcal{L}_{\text{linear}} \sim \pi T$ arise naturally from DGP-like setups, since the π's conformally mix with the graviton. These lead to spherical solutions [180], but break the $SO(N)$ internal symmetry.

We therefore do not consider these couplings further, and instead concentrate on the most general non-derivative coupling that preserves the $SO(N)$ symmetry.

$$\mathcal{L}_{\text{coupling}} = \frac{T}{2}P(\pi^2)\,, \tag{5.1.2}$$

where P is an arbitrary function of the invariant $\pi^2 \equiv \pi^I\pi_I$.

5.2 Spherically symmetric solutions

Our focus is on the existence and viability of spherically symmetric solutions sourced by a delta function mass distribution[1]

$$T = -M\delta^3(r) \ . \tag{5.2.1}$$

The equations of motion, including the coupling (5.1.2), are

$$\begin{aligned} MP'\left(\pi^2(0)\right)\pi^I(0)\delta^3(\vec{r}) = \Box\pi^I - \lambda\big[\Box\pi^I\left(\partial_\mu\partial_\nu\pi_J\partial^\mu\partial^\nu\pi^J - \Box\pi^J\Box\pi_J\right) \\ + 2\partial_\mu\partial_\nu\pi^I\left(\partial^\mu\partial^\nu\pi_J\Box\pi^J - \partial^\mu\partial_\lambda\pi_J\partial^\nu\partial^\lambda\pi^J\right)\big] \ , \end{aligned} \tag{5.2.2}$$

where $P'(X) \equiv \mathrm{d}P/\mathrm{d}X$. Restricting to spherically symmetric configurations $\pi^I(r)$, this reduces to

$$\frac{1}{r^2}\frac{\mathrm{d}}{\mathrm{d}r}\left[r^3\left(y^I + 2\lambda y^I y^2\right)\right] = MP'\left(\pi^2(0)\right)\pi^I(0)\delta^3(\vec{r}) \ , \tag{5.2.3}$$

where

$$y^I \equiv \frac{1}{r}\frac{\mathrm{d}\pi^I}{\mathrm{d}r} \ , \tag{5.2.4}$$

and $y^2 \equiv y^I y_I$. Note that, due to the shift symmetry of the Lagrangian, the equations of motion of galileon fields always take the form of a total derivative. Thus we can integrate once to obtain the equations of motion

$$y^I + 2\lambda y^I y^2 = \frac{M}{4\pi r^3}P'\left(\pi^2(0)\right)\pi^I(0) \ . \tag{5.2.5}$$

[1]Note that stable, nontrivial solutions without a source do not exist [114].

Dividing these equations by each other, we obtain the relations

$$\frac{\mathrm{d}\pi^I/\mathrm{d}r}{\mathrm{d}\pi^J/\mathrm{d}r} = \frac{\pi^I(0)}{\pi^J(0)} \ , \tag{5.2.6}$$

which, when integrated from the origin, gives

$$\frac{\pi^I(r)}{\pi^J(r)} = \frac{\pi^I(0)}{\pi^J(0)} \ . \tag{5.2.7}$$

The various components of the solution are therefore always proportional to each other. Thus, by a global $SO(N)$ rotation, we can rotate the solution into one direction in field space, say the $I = 1$ direction, so that the solution takes the form $\pi^1 \equiv \pi$ and $\pi^I = 0$ for $I \neq 1$. This model therefore exhibits a kind of spontaneous symmetry breaking of the internal $SO(N)$ symmetry, since any nontrivial solution must pick a direction in field space.

Equation (5.2.5) now takes the form

$$y + 2\lambda y^3 = \frac{M}{4\pi r^3} P'\left(\pi^2(0)\right)\pi(0) \ . \tag{5.2.8}$$

As r ranges from zero to infinity, the left-hand side is monotonic, and is positive or negative depending on the sign of $P'\left(\pi^2(0)\right)\pi(0)$. For there to be a continuous solution for y as a function of r, the left-hand side must be invertible when it is positive (negative). For a solution to exist, this requires (for nontrivial λ)

$$\lambda > 0 \ . \tag{5.2.9}$$

Thus y is also positive (negative), is monotonic with r, and ranges from zero to (negative) infinity as r ranges from infinity to zero. This in turn implies that $\mathrm{d}\pi/\mathrm{d}r$ does not cross zero, and hence π is monotonic.

Equation (5.2.8) yields a solution for y, and hence $\mathrm{d}\pi/\mathrm{d}r$, as a function of r and the parameters of the theory. Integrated from $r = 0$ to infinity, this will give a relation between $\pi(0)$ and the asymptotic value of the field $\pi(\infty)$. The asymptotic field value is essentially a modulus of the theory – it will be set by whatever cosmological expectation value is present. It is a physically meaningful parameter as it affects the coupling to the source by determining $\pi(0)$.

Near the source, where the nonlinear term dominates, the solution is linear in r,

$$\pi_{r\ll r_*}(r) \sim \pi(0) + \left[\frac{M}{8\pi\lambda}P'\left(\pi^2(0)\right)\pi(0)\right]^{1/3} r \ , \tag{5.2.10}$$

whereas far from the source, where the linear term dominates, the solution goes like $1/r$,

$$\pi_{r\gg r_*}(r) \sim \pi(\infty) - \frac{M}{4\pi}P'\left(\pi^2(0)\right)\pi(0)\frac{1}{r} \ , \tag{5.2.11}$$

where the transition between these regimes occurs at the radius

$$r_* \sim \left(\lambda M^2\left[P'\left(\pi^2(0)\right)\pi(0)\right]^2\right)^{1/6} \ . \tag{5.2.12}$$

Note that this crossover radius, and hence the distance at which nonlinearities become important, depends on the modulus $\pi(0)$. The equation of motion for $\pi(r)$ is readily solved numerically, and the solution obtained is plotted schematically in Fig. 5.1.

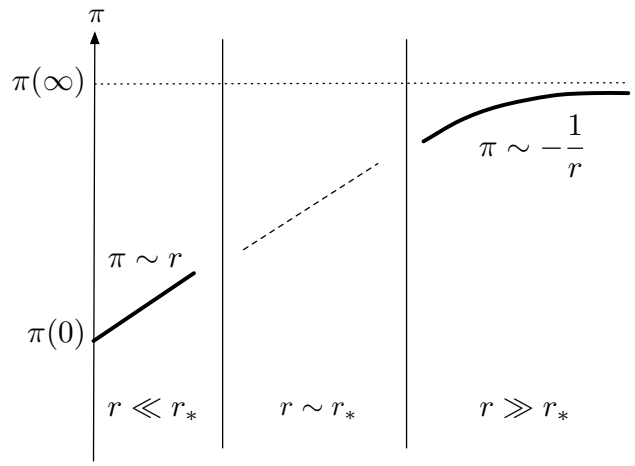

Figure 5.1: Schematic sketch of the solution for $\pi(r)$.

5.3 Perturbations: stability and subluminality

While the existence of static, spherically-symmetric configurations is encouraging, there are, of course, other important checks that our solution must pass to be physically viable. Specifically, following [175], we must study the stability of these spherically-symmetric solutions and to determine the speed at which fluctuations propagate, since superluminal propagation can be an obstacle to finding an ultra-violet completion of the effective theory [6].

We expand the field in perturbations around the background solution π_0^I,

$$\pi^I = \pi_0^I + \delta\pi^I \ . \tag{5.3.1}$$

Away from the source, the linearized equations of motion for the perturbations are

of the form

$$-K_I^t(r)\partial_t^2\delta\pi^I+\frac{1}{r^2}\partial_r\left(r^2K_I^r(r)\partial_r\delta\pi^I\right)+K_I^\Omega(r)\partial_\Omega^2\delta\pi^I=0\ , \tag{5.3.2}$$

where the coefficients $K_I^t(r)$, $K_I^r(r)$ and $K_I^\Omega(r)$ depend on r through the background field $\pi^I(r)$. We find

$$\begin{aligned}
K_1^t&=\frac{1}{3r^2}\frac{\mathrm{d}}{\mathrm{d}r}\left[r^3\left(1+18\lambda y^2\right)\right]\ ,\\
K_1^r&=1+6\lambda y^2\ ,\\
K_1^\Omega&=\frac{1}{2r}\frac{\mathrm{d}}{\mathrm{d}r}\left[r^2\left(1+6\lambda y^2\right)\right]\ ,\\
K_{I\neq1}^t&=\frac{1}{3r^2}\frac{\mathrm{d}}{\mathrm{d}r}\left[r^3\left(1+6\lambda y^2\right)\right]\ ,\\
K_{I\neq1}^r&=1+2\lambda y^2\ ,\\
K_{I\neq1}^\Omega&=\frac{1}{2r}\frac{\mathrm{d}}{\mathrm{d}r}\left[r^2\left(1+2\lambda y^2\right)\right]\ .
\end{aligned} \tag{5.3.3}$$

Applying the implicit function theorem to the function $F(y,r)=y+2\lambda y^3-\frac{M}{4\pi r^3}P'\left(\pi^2(0)\right)\pi(0)=0$, we have

$$\frac{\mathrm{d}y}{\mathrm{d}r}=-\frac{\partial_rF}{\partial_yF}=-\frac{3}{r}\frac{y+2\lambda y^3}{1+6\lambda y^2}\ . \tag{5.3.4}$$

This allows us to eliminate $\mathrm{d}y/\mathrm{d}r$ from (5.3.3):

$$
\begin{aligned}
K_1^t &= \frac{\left(1-6\lambda y^2\right)^2}{1+6\lambda y^2}\,, \\
K_1^r &= 1+6\lambda y^2\,, \\
K_1^\Omega &= \frac{1-6\lambda y^2}{1+6\lambda y^2}\,, \\
K_{I\neq 1}^t &= \frac{1+12\lambda^2 y^4}{1+6\lambda y^2}\,, \\
K_{I\neq 1}^r &= 1+2\lambda y^2\,, \\
K_{I\neq 1}^\Omega &= \frac{1+2\lambda y^2}{1+6\lambda y^2}\,.
\end{aligned}
\tag{5.3.5}
$$

Stability of the spherically symmetric background solutions against small perturbations requires $K>0$ for all K's. The $I\neq 1$ directions in field space are stable, but the π^1 direction exhibits a gradient instability sufficiently close to the source along the angular directions. In other words, $K_1^\Omega<0$ near the source. Therefore, localized perturbations can be found near the source that lower the energy of the solution through their gradients. This instability plagues very short-wavelength fluctuations, right down to the UV cutoff, so decay rates are dominated by the shortest distances in the theory and cannot be reliably computed within the effective theory.

Equations (5.3.5) also allow us to compute the speeds of propagation of our

small perturbations, in both the radial and angular directions. These are given by

$$
\begin{aligned}
(c^2)_1^r &= \frac{K_1^r}{K_1^t} = \left(\frac{1+6\lambda y^2}{1-6\lambda y^2}\right)^2 , \\
(c^2)_1^\Omega &= \frac{K_1^\Omega}{K_1^t} = \frac{1}{1-6\lambda y^2} , \\
(c^2)_{I\neq 1}^r &= \frac{K_{I\neq 1}^r}{K_{I\neq 1}^t} = \frac{(1+2\lambda y^2)\,(1+6\lambda y^2)}{1+12\lambda^2 y^4} , \\
(c^2)_{I\neq 1}^\Omega &= \frac{K_{I\neq 1}^\Omega}{K_{I\neq 1}^t} = \frac{1+2\lambda y^2}{1+12\lambda^2 y^4} .
\end{aligned}
\tag{5.3.6}
$$

Note that $(c^2)_1^r > 1$, and hence these perturbations always propagate superluminally. The same is true of $(c^2)_1^\Omega$, in regions where these perturbations are stable. The speed $(c^2)_{I\neq 1}^r$ is always superluminal, and $(c^2)_{I\neq 1}^\Omega$ is always subluminal. Whether superluminal propagation of signals is problematic for a low-energy effective theory is still an arguable issue, but it seems that at the least it may preclude the possibility of embedding the theory in a local, Lorentz-invariant UV completion [6].

5.4 Other constraints

It is interesting to note in passing that if a mechanism exists to tame the instabilities we have identified, then precision tests of gravity within the solar system already place useful constraints on multi-galileon theories. The galileon is screened at radii below the Vainshtein radius r_*, given by Equation (5.2.12), restoring the behavior of general relativity. Requiring the solar system to be screened to $r \sim 10^{16}$ m thus yields a constraint on λ and $\pi(0)$. However, lunar laser ranging data constrain the departure from the gravitational potential predicted by GR to satisfy $\frac{\delta\Phi}{\Phi} <$

2.4×10^{-11} (at radius $r = 3.84 \times 10^{10}$ cm), and we may translate this into a constraint on a different combination of λ and $\pi(0)$.

For example, consider the choice of $P(X)M_{\rm Pl} \sim \sqrt{\pi^I \pi_I}$, giving a linear coupling between the radial π field and matter. In the interesting case when the constraints are saturated, and detection of an effect is therefore imminent, the relevant constraint simply becomes

$$\frac{1}{\lambda^{1/6}} \lesssim 10^{-9} \text{ eV} \ . \tag{5.4.1}$$

Note that this is an extremely low cutoff for the effective theory, as is also found in the DGP model.

5.5 Implications

We have derived spherically-symmetric solutions in an $SO(N)$ multi-galileon theory with general, non-derivative couplings to matter. These solutions exhibit a Vainshtein screening effect, characteristic of galileon models. However, a study of the behavior of fluctuations around these solutions shows that one of the fields has imaginary sound speed along the angular directions, signaling an instability to anisotropic modes of arbitrarily short wavelength. Moreover fluctuations inevitably propagate superluminally.

These results raise serious concerns about the phenomenological viability of $SO(N)$ multi-galileon theories. (Of course, this does not preclude their effectiveness in early universe physics [56, 70], for instance during inflation, as long as they

become massive or decouple before the present epoch.) A key input in our analysis is the restriction to non-derivative coupling to matter. The main lesson to be drawn is that more general, derivative couplings are necessary. For instance, the lowest-dimensional coupling invariant under the Galilean and internal rotation symmetries is $\sim \partial_\mu \pi^I \partial_\nu \pi_I T^{\mu\nu}$. This coupling in fact naturally arises in the higher-codimension brane picture [96]. As mentioned earlier, the galileon fields are oblivious to static, spherically-symmetric sources in this case; thus exhibiting a screening mechanism. However, they will be excited by orbital motion, and we leave a study of the phenomenological implication of this coupling to future work.

Our analysis also highlights a distinct advantage to explicitly breaking the symmetry (5.1.1), for example through the introduction of a sequence of regulating branes of different codimensions, as in the cascading gravity case [84, 91, 8]. The explicit breaking of $SO(N)$ symmetry allows for more general terms in the action, which can lead to a healthier phenomenology [180].

Finally, should a creative cure for our instabilities be found, then we have demonstrated that precision solar system tests of gravity set interesting constraints on multi-galileon theories.

Chapter 6

Galileon forces in the solar system

In exploring the possible space of allowed modifications to general relativity (GR), one of the most stringent constraints is provided by precision tests within the solar system, which agree with GR to a high degree [207]. If one is interested, for example, in infrared modifications of GR, in which late-time cosmic acceleration may be addressed, then one must satisfy these constraints while simultaneously seeking dynamics that depart strongly from GR on large scales. Thus, a viable modified gravity theory that explains cosmic acceleration is expected to display a screening mechanism that results in the behavior of the theory in high-density regions differing significantly from that on cosmological scales, where densities are relatively low.

In this chapter we wish to initiate the analytic study of long-range forces medi-

ated by galileons, a class of scalar particles appearing in various attempts to modify gravity at large distances and exhibiting what is known as the Vainshtein screening mechanism. (See [175] for the derivation of the action used here and [198, 101] for discussion of the Vainshtein screening mechanism. Also see [146] for numerical work on the static Vainshtein-screened 2-body problem.) Possible astrophysical tests of galileon theories are discussed in [57, 210, 112, 97, 66, 95], and the theory and its many extensions [102, 99, 96, 100, 179, 106, 145, 14, 127, 156, 126, 197, 124, 54, 125, 216, 123, 122, 118] have been of particular interest due to their cosmological consequences. This chapter is based on work done in collaboration with Yi-Zen Chu and Mark Trodden [12].

The primary hurdle to understanding both gravitational and Vainshtein-screened forces is the presence of the nonlinear graviton and galileon self-interactions. In GR, gravitational forces within the solar system cannot be computed exactly but they can be treated perturbatively, because the Einstein-Hilbert Lagrangian $\frac{M_{\rm Pl}^2}{2}\sqrt{|g|}\mathcal{R}$ written in a weakly curved spacetime

$$g_{\mu\nu} \equiv \eta_{\mu\nu} + \frac{h_{\mu\nu}}{M_{\rm Pl}}, \qquad M_{\rm Pl} \equiv \frac{1}{\sqrt{8\pi G_N}},$$

is a series taking the schematic form $\sum_{n=2}^{\infty} \partial^2 h^n / M_{\rm Pl}^{n-2}$. (That is, higher nonlinearities contain exactly two derivatives but higher powers of $h/M_{\rm Pl}$.) To lowest order, $h/M_{\rm Pl}$ scales as the typical Newtonian potential $G_N m/r \ll 1$ generated by the masses in the solar system, where G_N is Newton's constant, m is a typical mass and r is the distance from the mass. Thus, each increasing order in nonlinearity

scales as $h/M_{\rm Pl} \ll 1$, and is hence a small perturbation relative to the previous order. Moreover, the 1/(distance) form of the Newtonian potential, and its nonlinear (and relativistic) corrections, is valid for any separation distance from a massive body within the solar system. In GR it is the Schwarzschild radius of the mass in question (when $h/M_{\rm Pl} \sim 1$) that characterizes when nonlinearities will dominate the dynamics. Even for the sun, the most massive object in our solar system, its Schwarzschild radius is a mere 3 km while its physical radius is 7×10^5 km.

However, because the mass scale Λ associated with the nonlinear self-interactions of galileons π is much smaller than the mass scale $M_{\rm pl} \sim 1/\sqrt{G_N}$ associated with gravitational interactions, the force law produced by galileons does not remain the same for all relevant separation distances. To see this, we first note that the galileon Lagrangian written in flat spacetime takes the schematic form

$$\sum_{n=2}^{5} (\partial\pi)^2 (\partial^2\pi)^{n-2} / \Lambda^{3(n-2)} \ ,$$

where the degree of nonlinearity is measured by the powers of $\partial^2\pi/\Lambda^3$ in a given term. Galileons couple to the trace of the stress-energy of matter, with an interaction Lagrangian $\pi T/M_{\rm Pl}$. For an isolated static body of mass M, we may define $1/\Lambda^3 \equiv (M_{\rm Pl}/M) r_v^3$, where r_v is the Vainshtein radius of the object. Far away from M the galileon potential is the familiar $\pi/M_{\rm Pl} \sim M/(M_{\rm Pl}^2 r)$ form. However, when one gets closer to the source M than $r \lesssim r_v$ – i.e. once $(M_{\rm Pl}/M) r_v^3 \partial^2\pi \sim 1$ – the nonlinearities will begin to dominate the dynamics. Typically, for galileons to be relevant cosmologically, $\Lambda \sim (M_{\rm Pl} H_0^2)^{1/3} \sim 1/10^3$ km (H_0 is the current Hubble

parameter). This means the sun's Vainshtein radius $r_v \sim 10^3$ light years and solar system dynamics takes place deep within the nonlinear regime of the sun's (hypothetical) galileon field. Furthermore, the solar system is a multi-body system; to develop a quantitative understanding of its dynamics it is also necessary to compute self-consistently the galileon forces exerted by the rest of the planetary bodies in the presence of the sun. For instance, properly calculating the earth-moon galileon force is important if one wishes to use precision lunar laser ranging measurements to constrain the galileon's existence.

In this work, we approximate the sun and its planetary companions as point masses and assume that the solar system is held together primarily by weak field gravity described by GR – we will assume galileon forces are subdominant. We will focus only on the modification of solar system dynamics due to galileons, and thus attempt to solve the galileon theory in exactly flat spacetime. This is justified as the interaction of galileons and gravity can be taken into account perturbatively, and we will show that these corrections are subdominant. However, we do not take into account the effects of cosmological boundary conditions as in [27].

To capture the effects of nonlinearities we will first solve the galileon field $\bar{\pi}$ due to the sun. We proceed to solve for the static Green's function of the galileon fluctuations about $\bar{\pi}$, and then use a field theoretic framework to examine the effective action of these point masses. This effective action framework is very similar in spirit to that developed in [120] for the two-body problem in GR (and extended

in [64] to the n-body case). We will exploit the fact that the solar system is a nonrelativistic system and therefore, to zeroth order, the galileon potential between two point masses $M_{1,2}$ is simply $M_1 M_2/M_{\rm Pl}^2$ multiplied by the static Green's function of the galileon wave equation linearized about $\bar{\pi}$. Recently, in [66], this static potential was solved exactly for the purely cubic galileon theory. Here, we will extend that work and find an exact solution for the maximally quartic galileon case. Using these exact solutions, we will also demonstrate how one may compute the general galileon force law using the perturbation theory approach developed in [65].

This chapter will be organized as follows: in Section 6.1.1 we introduce the galileon theory and discuss the galileon force sourced by the sun, including the resulting planetary perihelion precession. In Section 6.1.2 we obtain the full static propagator for galileon interactions in the presence of a large central mass for both the minimum and maximum quartic interaction strengths allowed by stability requirements, and then extend these results to more generic parameter values using perturbation theory. In Section 6.2.1 we explain the power counting of Feynman diagrams in the field-theoretic framework and present the resulting form for the effective action as an expansion in two small parameters. In Section 6.2.2 we provide concrete results in the region outside the Vainshtein radius of the large central source, followed in Section 6.2.3 by a discussion of why this calculation should not be trusted in the region inside the Vainshtein radius. We discuss the results in

Section 6.3.

6.1 Force laws

6.1.1 The background

Galileon theory

We wish to examine the following theory to understand how Vainshtein-screened scalar forces impact the dynamics of astrophysical systems:

$$S \equiv S_\pi + S_{\text{point particles}}\,. \tag{6.1.1}$$

As derived in [175], S_π encodes the dynamics of a scalar field π with derivative self-interactions consistent with a Galilean shift symmetry $\pi \to \pi + b_\mu x^\mu + c$, and yields second-order equations of motion. The action is given by

$$S_\pi = \int d^4x \left(\sum_{i=2}^{5} \frac{\alpha_i}{\Lambda^{3(i-2)}} \mathcal{L}_i + \frac{\pi}{M_{\text{Pl}}} T \right)\,, \tag{6.1.2}$$

where, defining the matrix $\Pi^{\mu}{}_{\nu} \equiv \partial^{\mu}\partial_{\nu}\pi$ and the notation $[A] \equiv A^{\mu}{}_{\mu}$ (for any matrix A),

$$\mathcal{L}_2 = -\frac{1}{2}\partial\pi\cdot\partial\pi \tag{6.1.3}$$

$$\mathcal{L}_3 = -\frac{1}{2}[\Pi]\partial\pi\cdot\partial\pi \tag{6.1.4}$$

$$\mathcal{L}_4 = -\frac{1}{4}\left([\Pi]^2\,\partial\pi\cdot\partial\pi - 2[\Pi]\partial\pi\cdot\Pi\cdot\partial\pi - \left[\Pi^2\right]\partial\pi\cdot\partial\pi + 2\,\partial\pi\cdot\Pi^2\cdot\partial\pi\right) \tag{6.1.5}$$

$$\begin{aligned}\mathcal{L}_5 = -\frac{1}{5}\Big(&[\Pi]^3\,\partial\pi\cdot\partial\pi - 3\,[\Pi]^2\,\partial\pi\cdot\Pi\cdot\partial\pi - 3[\Pi]\left[\Pi^2\right]\partial\pi\cdot\partial\pi + 6[\Pi]\partial\pi\cdot\Pi^2\cdot\partial\pi \\ &+ 2\left[\Pi^3\right]\partial\pi\cdot\partial\pi + 3\left[\Pi^2\right]\partial\pi\cdot\Pi\cdot\partial\pi - 6\,\partial\pi\cdot\Pi^3\cdot\partial\pi\Big).\end{aligned} \tag{6.1.6}$$

We have chosen the coupling to matter $(\pi/M_{\rm Pl})\,T$, which arises naturally from DGP-like models and is the lowest-order coupling term. This choice is Galilean-invariant in flat spacetime and for an external source; away from these assumptions the Galilean symmetry is broken but the theory is nevertheless interesting as the simplest realization of the Vainshtein screening mechanism. Another possible coupling which arises in the decoupling limit of massive gravity is the disformal coupling $(\partial_\mu\pi\partial_\nu\pi/M_{\rm Pl}^4)\,T^{\mu\nu}$. This coupling is parametrically smaller than the coupling to the trace of the stress-energy tensor so long as the galileon is sub-Planckian and quantum corrections to the galileon terms are irrelevant ($\alpha_q = \partial^2/\Lambda^2 \ll 1$ [145]):

$$\frac{\partial_\mu\pi\partial_\nu\pi}{M_{\rm Pl}^4}T^{\mu\nu} \sim \frac{\pi}{M_{\rm Pl}}T\left(\alpha_q\left(\frac{\Lambda}{M_{\rm Pl}}\right)^2\frac{\pi}{M_{\rm Pl}}\right) \tag{6.1.7}$$

The disformal coupling is not only higher order, it is also zero in the case of a static, nonrelativistic source such as we consider here. As discussed in [210], however, this coupling is important for lensing calculations (for which the lowest-order coupling

is zero).

We consider as matter a collection of point particles whose motion is left arbitrary, aside from a large central mass $M_\odot$ which is pinned at the origin:

$$S_{\text{point particles}} = -M_\odot \int dt_M - \sum_{a=1}^{N} m_a \int dt_a \sqrt{-\eta_{\mu\nu} v_a^\mu v_a^\nu}\,. \tag{6.1.8}$$

Via the standard definition $T_{\mu\nu} = -\frac{2}{\sqrt{-\eta}} \frac{\delta S_{\text{PP}}}{\delta \eta^{\mu\nu}}$ the trace of the stress-energy tensor to which the galileon couples is

$$T = -M_\odot \delta^3(\vec{x}) - \sum_{a=1}^{N} m_a \delta^3(\vec{x} - \vec{x}_a(t)) \sqrt{1 - v_a(t)^2}\,. \tag{6.1.9}$$

Strategy Our approach to understanding galileon forces between well-separated bodies lying deep within the Vainshtein radius of the central mass $M_\odot$ is as follows. We shall first solve for the galileon profile $\bar{\pi}$ generated by $M_\odot$. This means setting to zero all the $\{m_a\}$ and solving the resulting π-equation from the variation of (6.1.1) (note that the shift symmetry ensures that the equation of motion is a total derivative, and thus can be integrated to obtain an algebraic equation for $\bar{\pi}'$ [175])

$$\alpha_2 \left(\frac{\bar{\pi}'}{r}\right) + 2\frac{\alpha_3}{\Lambda^3}\left(\frac{\bar{\pi}'}{r}\right)^2 + 2\frac{\alpha_4}{\Lambda^6}\left(\frac{\bar{\pi}'}{r}\right)^3 = \frac{M_\odot}{4\pi M_{\text{Pl}} r^3}\,, \tag{6.1.10}$$

which we rewrite as

$$y + 2y^2 + 2xy^3 = \frac{1}{8z^3} \tag{6.1.11}$$

in terms of $y \equiv \frac{\alpha_3}{\alpha_2 \Lambda^3}\left(\frac{\bar{\pi}'}{r}\right)$, $x \equiv \frac{\alpha_2 \alpha_4}{\alpha_3^2}$, and $z^3 \equiv \frac{\pi \alpha_2^2}{2\alpha_3}\left(\frac{r}{r_v}\right)^3$. The cubic equation for y has only one solution that is both real and satisfies the boundary condition that $y(z \to 0) = 0$:

$$y = 2\frac{\sqrt{1 - \frac{3}{2}x}}{3x}\left[\begin{Bmatrix}\cos\\ \cosh\end{Bmatrix}\left(\frac{\theta(z)}{3}\right) - \begin{Bmatrix}\cos\\ \cosh\end{Bmatrix}\left(\frac{\theta(0)}{3}\right)\right]\,, \tag{6.1.12}$$

where

$$\theta(z) = \begin{Bmatrix} \cos^{-1} \\ \cosh^{-1} \end{Bmatrix} \left(\frac{-32 + 72x + 27x^2 z^{-3}}{32\left(1 - \frac{3}{2}x\right)^{3/2}} \right) \tag{6.1.13}$$

and cos or cosh is chosen such that $\theta(z)$ is real.

We then carry out perturbation theory about $\bar{\pi}$, replacing in (6.1.1)

$$\pi(t, \vec{x}) = \bar{\pi}(r) + \phi(t, \vec{x})\,. \tag{6.1.14}$$

Isolating the quadratic-in-ϕ terms of (6.1.1), we obtain the general form

$$S_{\text{kin}} \equiv -\frac{1}{2} \int d^4x \sqrt{-\eta} \left[-K_t(r)(\partial_t \phi)^2 + K_r(r)(\partial_r \phi)^2 + K_\Omega(r)(\partial_\Omega \phi)^2 \right] ,$$

where $K_t(r)$, $K_r(r)$ and $K_\Omega(r)$ are functions of the background field $\bar{\pi}(r)$ given by (with occurrences of $\partial_r y$ eliminated using the equation of motion)

$$\begin{aligned} K_t(r) &= \alpha_2 \left(\frac{1 + 4y + 12(1-x)y^2 + 24\left(x - 2\frac{\alpha_2^2 \alpha_5}{\alpha_3^3}\right) y^3 + 12\left(3x^2 - 4\frac{\alpha_2^2 \alpha_5}{\alpha_3^3}\right) y^4}{1 + 4y + 6xy^2} \right) \\ K_r(r) &= \alpha_2 \left(1 + 4y + 6xy^2\right) \\ K_\Omega(r) &= \alpha_2 \left(\frac{1 + 2y + 2(2-3x)y^2}{1 + 4y + 6xy^2} \right) . \end{aligned} \tag{6.1.15}$$

For an arbitrary static, spherically-symmetric background, we may re-express the action as the kinetic term of a massless scalar field in a curved spacetime (see [28] for a prior example of this procedure), namely

$$S_{\text{kinetic}} = -\frac{1}{2} \int d^4x \sqrt{-\tilde{g}} \tilde{g}^{\mu\nu} \partial_\mu \phi \partial_\nu \phi \,, \tag{6.1.16}$$

with the effective metric

$$\tilde{g}_{\mu\nu} \equiv \text{diag}\left(-\sqrt{\frac{K_r}{K_t}} K_\Omega, \sqrt{\frac{K_t}{K_r}} K_\Omega, r^2 \sqrt{K_t K_r}, r^2 \sin^2\theta \sqrt{K_t K_r} \right) . \tag{6.1.17}$$

The first order of business is then to solve the static Green's function of the resulting massless scalar wave operator,

$$\widetilde{\Box}_x G\left(\vec{x},\vec{y}\right) = \widetilde{\Box}_y G\left(\vec{x},\vec{y}\right) = -\frac{\delta^{(3)}(\vec{x}-\vec{y})}{\sqrt[4]{-\tilde{g}(x)}\sqrt[4]{-\tilde{g}(y)}}\,. \tag{6.1.18}$$

where $\widetilde{\Box} \equiv \widetilde{g}^{\mu\nu}\widetilde{\nabla}_\mu\widetilde{\nabla}_\nu$ and $\widetilde{\nabla}$ is the covariant derivative with respect to the effective metric in Eq. (6.1.17). Strictly speaking, to probe the dynamical content of our scalar equation linearized about $\bar{\pi}$, one would need to solve the full time-dependent retarded Green's function $G_{\rm ret}(x,y)$. However, this is not an easy task. Therefore, because we are interested primarily in the forces between planetary bodies moving at speeds much less than unity (relative to the solar system's center of energy), we shall in this chapter seek its static limit,

$$G(\vec{x},\vec{y}) \equiv \int_{-\infty}^{\infty} dx^0 G_{\rm ret}(x,y) = \int_{-\infty}^{\infty} dy^0 G_{\rm ret}(x,y)\ .$$

Before proceeding, let us observe from (6.1.10) that the quintic galileon self-interactions do not contribute to the background field $\bar{\pi}$. In fact, as discussed in [175], any time-independent galileon π trivially satisfies the portion of the equations arising from $\mathcal{L}_5$. This (as expressed by the α_5-independence of K_r and K_Ω) means the static Green's function obtained for $\alpha_4 = 0$ in [66] and the maximally quartic case we shall consider in Section 6.1.2 are also solutions in the presence of an arbitrary nonzero α_5. The quintic interactions become relevant, however, for the full time-dependent Green's function.

Precession of Mercury

We begin by asking: what is the contribution to the precession of perihelia of planetary orbits due to the galileon field of the sun? This has been calculated in [148] for galileons with only the cubic interaction term; here we extend the calculation to the case of the full galileon theory with cubic, quartic, and quintic interactions. To zeroth order, the galileon field in the solar system is primarily governed by the field due to the sun, (6.1.10). As the orbits of the planets are well within the sun's Vainshtein radius, the most nonlinear term dominates and hence the background solution is (up to an additive constant) well approximated by

$$\bar{\pi} = \frac{M_\odot r}{2(\pi\alpha_4)^{1/3} M_{\rm Pl} r_v^2}\,. \tag{6.1.19}$$

Thus, we wish to consider the perihelion precession induced by a potential

$$\Psi = -\frac{GM_\odot}{r} + \frac{\bar{\pi}}{M_{\rm Pl}} \sim GM_\odot\left(-\frac{1}{r} + Cr\right), \qquad C = \frac{8\pi}{2(\pi\alpha_4)^{1/3} r_v^2}\,. \tag{6.1.20}$$

Following the standard procedure for such calculations as found in any GR textbook, we find that to second order in the eccentricity e for a planet with semi-major axis a, the perihelion precession induced by the galileons relative to that induced by GR is

$$\frac{\Delta\phi_{\rm galileon}}{\Delta\phi_{\rm GR}} = -\frac{8\pi^{2/3}}{3\alpha_4^{1/3}}\frac{a^3}{r_s r_v^2}\,, \tag{6.1.21}$$

with r_s the Schwarzschild radius of the sun. The galileon-induced precession thus decreases the precession per orbit from GR by an amount suppressed by the distance ratio $a^3/(r_s r_v^2)$. For the Sun-Mercury system, this is an effect at $\mathcal{O}(10^{-10})\Delta\phi_{GR}$, and

hence is unobservable by all current and near-future methods of measurement. Note that this is the correct result only if the quartic interaction term dominates the cubic one at the orbit of the planet in question, or in other words, when $r_{\text{Mercury}} \ll r_{34}$ (see (6.1.25) below). If we wish to consider the crossover from this behavior to the cubic-dominated precession which is several orders of magnitude larger, we must consider the full galileon force law.

This precession calculation treats every object in the solar system, other than the sun itself, as a test body with negligible mass. However, due to the highly nonlinear nature of the galileon field in the solar system, it is important to go beyond this one-body problem. We proceed henceforth to investigate the dynamics of objects due to galileon interactions between such objects within the background field of a large central mass.

6.1.2 Forces between smaller masses

To lowest order in galileon self-interactions, the scalar force between two test masses in the presence of the sun can be determined from the curved-space Green's function with the effective metric as obtained from (6.1.15) and (6.1.17). We seek a full Green's function solution as an expansion in spherical harmonics via the ansatz

$$G(\vec{r},\vec{r}') = \sum_{\ell=0}^{\infty}\sum_{m=-\ell}^{\ell} R_{>,\ell}(r_>)R_{<,\ell}(r_<)Y_\ell^m(\Omega)Y_\ell^m(\Omega')^*\,, \tag{6.1.22}$$

where $r_>$ and $r_<$ are, respectively, the larger and smaller of r and r'. Henceforth, $R_\ell(r)$ should be understood to mean the piecewise-defined function that is $R_{>,\ell}$

when $r = r_>$ and $R_{<,\ell}$ when $r = r_<$. The main obstacle to finding a solution is then whether or not the radial equation

$$\left[K_r(r)R''_\ell(r) + K_r(r)\left(2 + \frac{rK'_r(r)}{K_r(r)}\right)\frac{1}{r}R'_\ell(r) - K_\Omega(r)\frac{\ell(\ell+1)}{r^2}R_\ell(r)\right]R_\ell(r') = -\frac{1}{r^2}\delta(r-r') \tag{6.1.23}$$

is solvable. Because $\bar{\pi}''$ in the K_is can be exchanged for $y = \bar{\pi}'/r$ via the equation of motion, (6.1.23) depends on the background field solely through y, for arbitrary choices of the parameters α_i.

First note that the stability requirement that all the K_is be positive restricts the viable parameter space to

$$\alpha_2 > 0 \qquad \alpha_3 \geq \sqrt{\frac{3}{2}\alpha_2\alpha_4} \qquad \alpha_4 \geq 0 \qquad \alpha_5 \leq \frac{3\alpha_4^2}{4\alpha_3}\ , \tag{6.1.24}$$

as discussed in [175] (this analysis is modified for a spacetime which is not asymptotically Minkowski - see [27]). We will focus on the case where $\alpha_5 = 0$, since the quintic term has little effect on the analysis – it does not affect the background solution and only appears in K_t and hence is irrelevant for the static Green's function.

Note also that there are three different distance regimes relevant to the problem. The first is the regime far from the sun (*i.e.*, the central mass) beyond which the nonlinearities are unimportant, the second is the intermediate-distance regime where the cubic term dominates the dynamics, and the final one is the near-source regime where the quartic term dominates over the cubic term in determining the dynamics. The linear-nonlinear transition happens at a scale r_{23} and the cubic-

quartic transition at a second scale r_{34}, as defined by:

$$r_{23}^3 = \frac{\alpha_3 M}{\alpha_2^2 M_{\rm Pl} \Lambda^3}\,, \qquad\qquad r_{34}^3 = x^2 r_{23}^3\,, \tag{6.1.25}$$

where it is convenient to define a new parameter x controlling the relative importances of the cubic and quartic terms, via

$$0 \leq x \equiv \frac{\alpha_2 \alpha_4}{\alpha_3^2} \leq \frac{2}{3}\,. \tag{6.1.26}$$

The bounds on the magnitude of x are a consequence of the stability conditions above.

In Fig. 6.1 we plot the components of the effective metric for a range of different values of x in the allowed range, and in Fig. 6.2 we demonstrate the effects on the radial and angular sound speeds for these same values. As is well-known for the galileons, radial waves propagate superluminally; note that larger quartic interaction strength correlates with faster maximum propagation speed. It is unclear whether such superluminality presents a problem for the viability of the theory; [6] argues that it is an indicator that the theory cannot be UV completed and is macroscopically nonlocal, whereas [55, 53, 28, 154, 20] argue that causality is preserved despite superluminal signal propagation and hence the theory is no less safe than GR under the Hawking Chronology Protection Principle. Additionally, [85] shows that for a specific choice of parameters, the galileon theory (with accompanying Vainshtein mechanism and superluminal signals) is dual to a free field theory, and thus has an analytic S-matrix and is causal.

It is also apparent from Fig. 6.2 that near the large central mass, the angular galileon modes propagate highly *sub*luminally for galileon theories with a nonzero quartic term. As discussed in [175], this limits the validity of the static approximation we have made: the static limit is valid in the regime where the galileon propagation speed is much faster than the speed with which astrophysical objects move. Clearly then, near the sun for example, it is necessary to solve the fully time-dependent system.

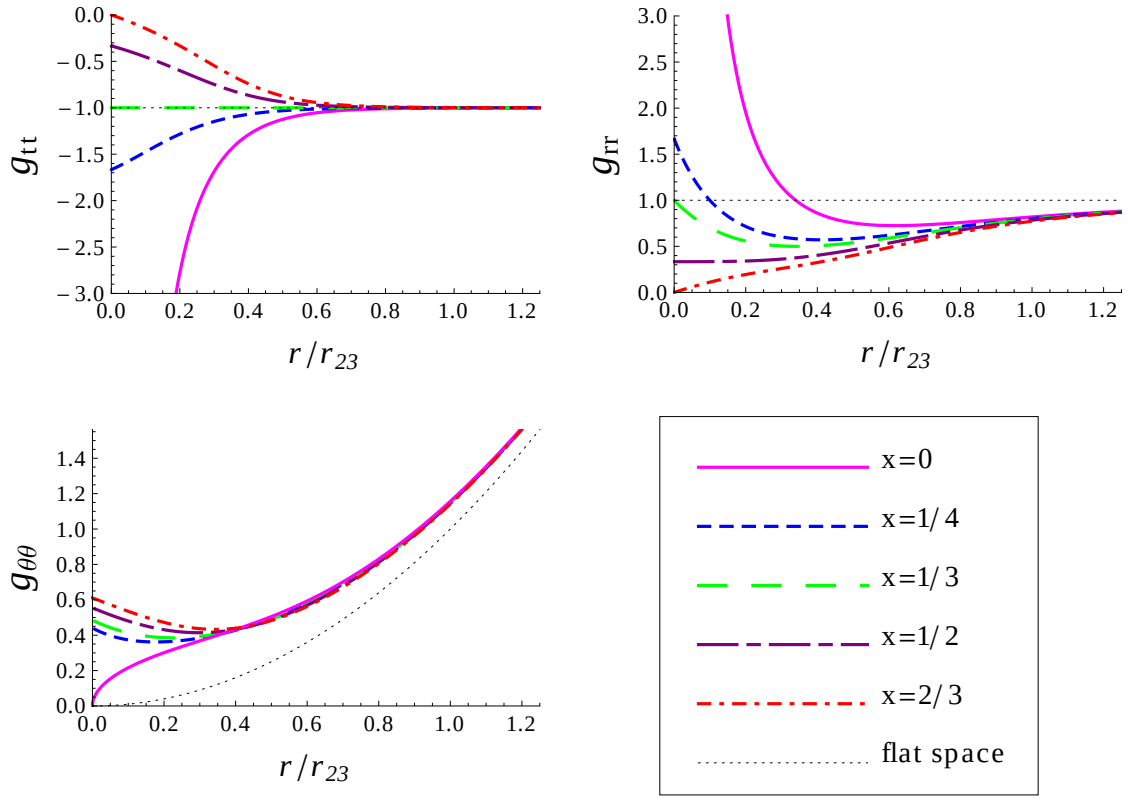

Figure 6.1: The effective metric seen by galileon fluctuations about the spherically-symmetric background for various relative strengths $x \equiv \alpha_2\alpha_4/\alpha_3^2$ of the cubic and quartic terms.

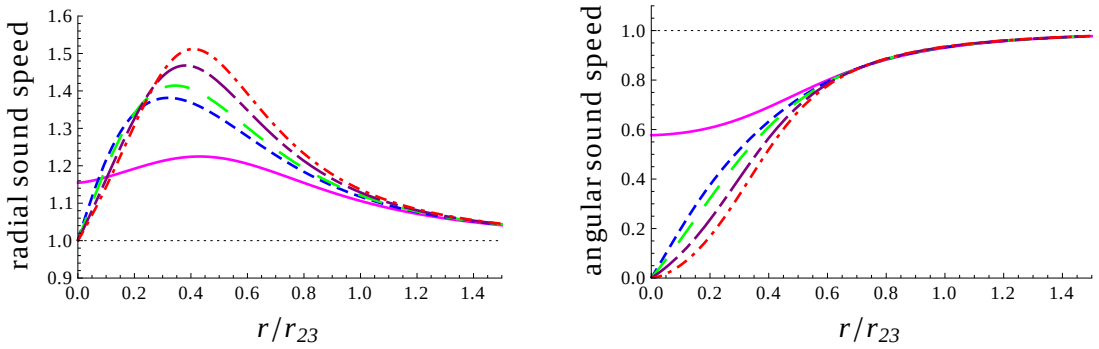

Figure 6.2: The propagation speed of galileon fluctuations about the spherically-symmetric background for various relative strengths of the cubic and quartic terms. Color coding is as in Fig. 6.1.

While explicitly solving (6.1.23) is not possible for general parameter choices, the special values for which we can make progress are when x lies at the edges of its allowed range: $x = 0,\ 2/3$. The choice $x = 0$ is the already-solved case of only cubic interactions ($r_{34} \to 0$). To explore the new phenomena exhibited when the quartic term is present, we therefore consider the choice of maximal quartic term, $x = \frac{2}{3}$. First, however, we review the results for cubic galileons.

Cubic galileons

Our first step is to find the (static) cubic galileon propagator - the Green's function of the wave equation linearized about $\bar{\pi}$. For $\alpha_4 = \alpha_5 = 0$, the terms in (6.1.15)

become

$$S_{\rm kin} = \int d^4x \left[\phi\left(\frac{2}{\Lambda^3}\Box\bar{\pi}\Box - \frac{2}{\Lambda^3}\nabla^\mu\nabla^\nu\bar{\pi}\nabla_\mu\nabla_\nu + \frac{1}{2}\Box\right)\phi\right] \tag{6.1.27}$$
$$= \int d^4x\Bigg[\left(3+\frac{2}{\Lambda^3}\Box\bar{\pi}\right)(\partial_t\phi)^2 - \left(3+\frac{4}{\Lambda^3}\frac{\bar{\pi}'}{r}\right)(\partial_r\phi)^2$$
$$- \left(3+\frac{2}{\Lambda^3}(\bar{\pi}''+\frac{\bar{\pi}'}{r})\right)(\partial_\Omega\phi)^2\Bigg],$$

with the background $\bar{\pi}$ obtained by solving the quadratic equation in (6.1.10) with the boundary condition $\bar{\pi}'(r\to\infty)=0$:

$$\frac{\bar{\pi}'}{r} = \frac{\alpha_2\Lambda^3}{4\alpha_3}\left(-1+\sqrt{1+\frac{2}{\pi}\left(\frac{r_{23}}{r}\right)^3}\right). \tag{6.1.28}$$

This equation can be integrated to obtain

$$\bar{\pi}(z) = -\left(\frac{2}{\pi}\right)^{2/3}\frac{M}{8\alpha_2 M_{\rm Pl} r_{23}}\left[\frac{\Gamma\left(\frac{1}{3}\right)^2}{2^{1/3}\Gamma\left(\frac{2}{3}\right)} + \sqrt{z}\left(z^{3/2} - 4\,{}_2F_1\left(-\frac{1}{2},\frac{1}{6},\frac{7}{6},-z^3\right)\right)\right], \tag{6.1.29}$$

in terms of the dimensionless radial variable $z \equiv \left(\frac{\pi}{2}\right)^{1/3}\frac{r}{r_{23}}$.

As we shall now see, viewing ϕ as a massless scalar propagating in a curved geometry makes some of the relevant questions conceptually clear. Firstly, it is known that – see, for instance, [133, 186, 185] – signals in curved space do not propagate solely on the light cone; there is also a tail of signals propagating everywhere within the light cone. Secondly, it makes superluminal propagation of fluctuations inside the Vainshtein radius manifest.

For the case at hand, using the solution (6.1.28), the relevant functions are easily read off, and in the limits $r \gg r_{23}$ (outside Vainshtein) and $r \ll r_{23}$ (inside

Vainshtein), they are given by the approximate expressions

$$\begin{aligned} K_t(r) &\sim \begin{cases} \alpha_2 & r \gg r_{23} \\ \frac{3}{4}\alpha_2 z^{-3/2} & r \ll r_{23} \end{cases}, \\ K_r(r) &\sim \begin{cases} \alpha_2 & r \gg r_{23} \\ \alpha_2 z^{-3/2} & r \ll r_{23} \end{cases}, \\ K_\Omega(r) &\sim \begin{cases} \alpha_2 & r \gg r_{23} \\ \frac{1}{4}\alpha_2 z^{-3/2} & r \ll r_{23} \end{cases}. \end{aligned} \tag{6.1.30}$$

Hence, the effective metric approaches the flat one far outside the Vainshtein radius, whereas deep inside the Vainshtein radius

$$\tilde{g}_{\mu\nu} = \sqrt{\frac{3}{2\pi}}\alpha_2 \left(\frac{r_{23}}{r}\right)^{3/2} \mathrm{diag}\left(-\frac{1}{3},\, \frac{1}{4},\, r^2,\, r^2 \sin^2\theta\right). \tag{6.1.31}$$

It is now immediately apparent that well outside the Vainshtein radius, fluctuations propagate precisely luminally, as in flat space. Well inside the Vainshtein radius, the behavior of null geodesics tells us that

$$c_r^2 = -\frac{\tilde{g}_{tt}}{\tilde{g}_{rr}} = \frac{K_r}{K_t} \qquad c_\theta^2 = -r^2\frac{\tilde{g}_{tt}}{\tilde{g}_{\theta\theta}} = \frac{K_\Omega}{K_t} \tag{6.1.32}$$

and in particular, the radial fluctuations propagate superluminally ($c_r^2 = \frac{4}{3}$) and the angular fluctuations propagate subluminally ($c_\theta^2 = \frac{1}{3}$).

Although at zeroth order the propagator well outside the Vainshtein radius is simply the flat-space propagator, it is less straightforward to calculate the propagator well inside the Vainshtein radius, for which we must solve for the Green's

function of the differential operator $\tilde{g}^{\mu\nu}\tilde{\nabla}_\mu\tilde{\nabla}_\nu$, obeying (see (6.1.18))

$$\left(-3\partial_t^2+4\partial_r^2+\frac{2}{r}\partial_r+\frac{\vec{L}^2}{r^2}\right)G\left(\vec{r},\vec{r}'\right)\ =-\frac{2}{\alpha_2}\sqrt{2\pi}\left(\frac{r}{r_{23}}\right)^{3/2}\delta^3\left(\vec{r}-\vec{r}'\right)\,. \quad (6.1.33)$$

For simplicity we will focus on the static propagator. As already alluded to, this treatment assumes that the static force law is a good description of the dynamics despite the existence of galileon wave tails propagating inside, not on, the light-cone. Strictly speaking this assumption needs to be checked via an actual calculation. However, we argue, on physical grounds, that this is a valid assumption as long as the speed of propagation of galileons is much larger than the velocity of the astrophysical objects whose dynamics we wish to study.

We begin by defining a new variable

$$\vec{\rho}=\sqrt{z}\hat{r}\,, \quad (6.1.34)$$

where $\hat{r}\equiv\vec{r}/|\vec{r}|$. In terms of this variable, we now define a rescaled Green's function

$$g(\vec{\rho},\vec{\rho}')=\frac{G(\vec{r},\vec{r}')}{\rho\rho'}\ ,\qquad \rho\equiv|\vec{\rho}|\,, \quad (6.1.35)$$

which we find obeys Poisson's equation for a point mass in the new variable ρ; namely $-\delta^{ij}(\partial/\partial\rho^i)(\partial/\partial\rho^j)G=\delta^3(\vec{r}-\vec{r}')$. Thus, the rescaled $g(\rho,\rho')$ has the standard flat-space propagator solution and therefore the galileon propagator

$$\langle\phi(r)\phi(r')\rangle_{\rm static}=i\delta(t-t')G(r,r') \quad (6.1.36)$$

must contain the term

$$\left(\frac{\pi}{2}\right)^{1/3}\frac{i\delta(t-t')}{2\pi\alpha_2 r_{23}}\frac{\rho\rho'}{|\vec{\rho}-\vec{\rho}'|}\,. \quad (6.1.37)$$

As discussed in detail in [66], the full propagator also must include homogeneous solutions to impose the boundary condition that when one of the endpoints is taken to coincide with the central large mass, the propagator merely renormalizes the mass in the background solution. Taking this into account we have [66]

$$\langle\phi(r)\phi(r')\rangle = \left(\frac{\pi}{2}\right)^{1/3} \frac{i\delta(t-t')}{2\pi\alpha_2 r_{23}} \left[\frac{\rho\rho'}{|\vec{\rho}-\vec{\rho}'|} - \rho - \rho' + \frac{\Gamma\left(\frac{1}{6}\right)\Gamma\left(\frac{1}{3}\right)}{6\sqrt{\pi}}\right]. \tag{6.1.38}$$

Although it is extremely useful to have a closed form solution for this propagator, we will see in the remainder of the chapter that calculating the dynamics of objects subject to this force beyond first order is technically quite difficult.

For completeness we also record here the exact solution (valid for all radii) derived in [66]:

$$\begin{aligned} G_3\left(\vec{r},\vec{r}'\right) = {} & \left(\frac{\pi}{2}\right)^{1/3} \frac{1}{4\pi\alpha_2 r_{23}} \left(\frac{\Gamma\left[\frac{1}{3}\right]\Gamma\left[\frac{1}{6}\right]}{3\sqrt{\pi}} - 2\sqrt{z_>}\,{}_2F_1\left[\frac{1}{6},\frac{1}{2};\frac{7}{6};-z_>^3\right]\right) \\ & + \left(\frac{\pi}{2}\right)^{1/3} \frac{1}{\alpha_2 r_{23}} \sum_{\ell=1}^{\infty}\sum_{m=-\ell}^{\ell} \frac{Y_\ell^m[\theta,\phi]Y_\ell^m[\theta',\phi']^*}{2\ell+1} z_<^{\frac{\ell+1}{2}} \\ & \times {}_2F_1\left[\frac{1}{6}-\frac{\ell}{6},\frac{1}{2}+\frac{\ell}{2};\frac{7}{6}+\frac{\ell}{3};-z_<^3\right]\left(2z_>^{-\frac{\ell}{2}}\,{}_2F_1\left[\frac{\ell}{6}+\frac{1}{3},-\frac{\ell}{2};\frac{5}{6}-\frac{\ell}{3};-z_>^3\right]\right. \\ & \left. + \frac{\ell!\,\Gamma\left[-\frac{1}{6}(2\ell+1)\right]}{\sqrt{\pi}\,\Gamma\left[\frac{1}{3}(2\ell+1)\right]} z_>^{\frac{\ell+1}{2}}\,{}_2F_1\left[\frac{1}{6}-\frac{\ell}{6},\frac{1}{2}+\frac{\ell}{2};\frac{7}{6}+\frac{\ell}{3};-z_>^3\right]\right). \end{aligned} \tag{6.1.39}$$

Maximally quartic galileons

Choosing now the $x = \frac{2}{3}$ case, the background solution then obeys the equation

$$\frac{\bar{\pi}'}{r} = \frac{\alpha_2\Lambda^3}{2\alpha_3}\left(-1+\sqrt[3]{1+\frac{3}{2\pi}\left(\frac{r_{23}}{r}\right)^3}\right). \tag{6.1.40}$$

This expression can be integrated to yield

$$\bar{\pi}(\tilde{z}) = -\left(\frac{3}{2\pi}\right)^{2/3} \frac{M}{4\alpha_2 M_{\rm Pl} r_{23}} \left[\frac{\Gamma\left(\frac{1}{3}\right)^2}{3\Gamma\left(\frac{2}{3}\right)} + \tilde{z}\left(\tilde{z} - 2\,{}_2F_1\left(-\frac{1}{3}, \frac{1}{3}; \frac{4}{3}; -\tilde{z}^3\right)\right)\right], \tag{6.1.41}$$

where we have chosen the integration constant to impose $\bar{\pi}(r \to \infty) = 0$ and introduced the new variable $\tilde{z} \equiv \left(\frac{2\pi}{3}\right)^{1/3} \frac{r}{r_{23}}$. Note that this $\tilde{z}$ is a rescaling of z defined for the $x = 0$ case.

The functions K_i which appear in the static Green's function equation are, in terms of our new variable $\tilde{z}$,

$$K_r(\tilde{z}) = \frac{\alpha_2}{\tilde{z}^2}(1+\tilde{z}^3)^{2/3}\,, \qquad\qquad K_\Omega(\tilde{z}) = \frac{\alpha_2 \tilde{z}}{(1+\tilde{z}^3)^{1/3}}\,. \tag{6.1.42}$$

Substituting these into (6.1.23) it is then possible to obtain two independent solutions

$$\begin{aligned} R_1(\tilde{z}) &= {}_2F_1\left(\frac{\ell+1}{3}, -\frac{\ell}{3}, \frac{2}{3}, -\tilde{z}^3\right) \\ R_2(\tilde{z}) &= \tilde{z}\,{}_2F_1\left(\frac{1-\ell}{3}, \frac{\ell+2}{3}, \frac{4}{3}, -\tilde{z}^3\right), \end{aligned} \tag{6.1.43}$$

so that the full radial dependence of the Green's function for each mode ℓ takes the form

$$\begin{aligned} g_\ell(\tilde{z}, \tilde{z}') &\equiv R_{>,\ell}(\tilde{z}_>) R_{<,\ell}(\tilde{z}_<) \\ &= \Big(R_1(\tilde{z}_>) + C_{2>} R_2(\tilde{z}_>)\Big)\Big(C_{1<} R_1(\tilde{z}_<) + C_{2<} R_2(\tilde{z}_<)\Big). \end{aligned} \tag{6.1.44}$$

In this form we have already imposed continuity at $r = r'$. To fix the constants $C_{2>}$, $C_{1<}$ and $C_{2<}$, we shall need to impose the following boundary conditions.

Discontinuous first derivative Firstly, the first derivative of $g_\ell(\tilde{z},\tilde{z}')$ with respect to $\tilde{z}$ needs to be discontinuous at $\tilde{z}=\tilde{z}'$, so that its second derivative gives us the needed $\delta(\tilde{z}-\tilde{z}')$. Specifically, by integrating $\widetilde{\Box}G(\tilde{z},\tilde{z}')=\delta^{(3)}(\tilde{z}-\tilde{z}')/\sqrt[4]{|g(\tilde{z})g(\tilde{z}')|}$ with respect to $\tilde{z}$ about the point $\tilde{z}=\tilde{z}'$, one may show that

$$r'^2K_r(r')\left(\partial_{r_>}-\partial_{r_<}\right)\left(R_\ell(r)R_\ell(r')\right)\big|_{r=r'}=-1\,. \tag{6.1.45}$$

At this point,

$$C_{2<}=C_{1<}C_{2>}+\left(\frac{2\pi}{3}\right)^{1/3}\frac{1}{\alpha_2 r_{23}(1+\tilde{z}'^3)^{2/3}(R_1\partial_{\tilde{z}}R_2-\partial_{\tilde{z}}R_1R_2)}\bigg|_{\tilde{z}=\tilde{z}'}\,. \tag{6.1.46}$$

Note that the second term of Eq. (6.1.46) is a constant by the equations of motion obeyed by the radial mode functions R_i – the differential equation obeyed by $q_i(\tilde{z})\equiv(1+\tilde{z}^3)^{1/3}R_i(\tilde{z})$ contains no first derivative terms. In fact, we have normalized R_i such that $(1+\tilde{z}'^3)^{2/3}(R_1\partial_{\tilde{z}}R_2-\partial_{\tilde{z}}R_1R_2)=1$. Hence

$$C_{2<}=C_{1<}C_{2>}+\left(\frac{2\pi}{3}\right)^{1/3}\frac{1}{\alpha_2 r_{23}}\,. \tag{6.1.47}$$

Observer at infinity Next, for fixed $\tilde{z}_<$, the static Green's function must vanish as $\tilde{z}_>\to\infty$, for all $\ell\geq 0$. Using the identity

$$\begin{aligned}{}_2F_1(\alpha,\beta;\gamma;\tilde{z})=&\frac{\Gamma[\gamma]\Gamma[\beta-\alpha]}{\Gamma[\beta]\Gamma[\gamma-\alpha]}(-\tilde{z})^{-\alpha}\,{}_2F_1\left(\alpha,\alpha+1-\gamma;\alpha+1-\beta;\frac{1}{\tilde{z}}\right)\\&+\frac{\Gamma[\gamma]\Gamma[\alpha-\beta]}{\Gamma[\alpha]\Gamma[\gamma-\beta]}(-\tilde{z})^{-\beta}\,{}_2F_1\left(\beta,\beta+1-\gamma;\beta+1-\alpha;\frac{1}{\tilde{z}}\right)\end{aligned} \tag{6.1.48}$$

on $g_\ell(\tilde{z},\tilde{z}')$ in Eq. (6.1.44) results in (for $\tilde{z}\gg 1$) two terms of the form $\widetilde{C}_1\tilde{z}_>^\ell$ and $\widetilde{C}_2\tilde{z}_>^{-\ell-1}$. These are the familiar flat-space radial solutions. Requiring that

$\lim_{\tilde{z}_>\to\infty} g_\ell(\tilde{z},\tilde{z}') \to 0$ means $\widetilde{C}_1 = 0$, which in turn leads us to

$$C_{2>} = -\frac{\Gamma\left(\frac{2}{3}\right)\Gamma\left(1+\frac{\ell}{3}\right)}{\Gamma\left(\frac{4}{3}\right)\Gamma\left(\frac{\ell+1}{3}\right)}\,. \tag{6.1.49}$$

Monopole solution The $\tilde{z}\to 0$ boundary condition we must satisfy is

$$\delta\bar{\pi}(\tilde{z}') = -\frac{\delta M}{M_{\rm Pl}} G(0,\tilde{z}') \tag{6.1.50}$$

where $\delta\bar{\pi}(r')$ indicates the $\mathcal{O}(\delta M)$ part of $\bar{\pi}(M+\delta M)$. That is, since the static Green's function is the field observed at $\tilde{z}'$ produced by a static point source at $\tilde{z}$, when $\tilde{z}=0$ this should simply amount to shifting the total mass of the point mass already present at the origin.

Furthermore, since the background is spherically symmetric, $g_\ell(0,r')$ should only be nonzero for $\ell = 0$. This gives the condition

$$\begin{aligned}
&C_{1<}(\ell=0)\left[1 + C_{2>}(\ell=0)\tilde{z}'\,{}_2F_1\left(\frac{1}{3},\frac{2}{3},\frac{4}{3},-\tilde{z}'^3\right)\right] \\
&= \frac{1}{3}\left(\frac{2\pi}{3}\right)^{1/3}\frac{\Gamma\left(\frac{1}{3}\right)^2}{\Gamma\left(\frac{2}{3}\right)}\frac{1}{\alpha_2 r_{23}}\left[1 - 3\frac{\Gamma\left(\frac{2}{3}\right)}{\Gamma\left(\frac{1}{3}\right)^2}\tilde{z}'\left(2\,{}_2F_1\left(-\frac{1}{3},\frac{1}{3},\frac{4}{3},-\tilde{z}'^3\right) - \sqrt[3]{1+\tilde{z}'^3}\right)\right].
\end{aligned} \tag{6.1.51}$$

One can check that the $\tilde{z}'$-dependent parts are equal, and thus

$$C_{1<}(\ell=0) = \frac{1}{3}\left(\frac{2\pi}{3}\right)^{1/3}\frac{\Gamma\left(\frac{1}{3}\right)^2}{\Gamma\left(\frac{2}{3}\right)}\frac{1}{\alpha_2 r_{23}}\,, \qquad C_{1<}(\ell>0) = 0\,. \tag{6.1.52}$$

Result Hence the full static propagator for the maximally quartic galileon is

$$
\begin{aligned}
G_4(r,r') = \left(\frac{2\pi}{3}\right)^{1/3} \frac{1}{\alpha_2 r_{23}} \Bigg\{ \frac{1}{4\pi} \left[\frac{\Gamma\left(\frac{1}{3}\right)^2}{3\Gamma\left(\frac{2}{3}\right)} - \tilde{z}_{>}\, {}_2F_1\left(\frac{1}{3},\frac{2}{3},\frac{4}{3},-\tilde{z}_{>}^3\right)\right] \\
+ \sum_{\ell=1}^{\infty} \sum_{m=-\ell}^{\ell} \Bigg[{}_2F_1\left(-\frac{\ell}{3},\frac{\ell+1}{3},\frac{2}{3},-\tilde{z}_{>}^3\right) \\
- \ell \frac{\Gamma\left(\frac{2}{3}\right)\Gamma\left(\frac{\ell}{3}\right)}{\Gamma\left(\frac{1}{3}\right)\Gamma\left(\frac{\ell+1}{3}\right)} \tilde{z}_{>}\, {}_2F_1\left(\frac{1-\ell}{3},\frac{\ell+2}{3},\frac{4}{3},-\tilde{z}_{>}^3\right) \Bigg] \\
\times \tilde{z}_{<}\, {}_2F_1\left(\frac{1-\ell}{3},\frac{\ell+2}{3},\frac{4}{3},-\tilde{z}_{<}^3\right) Y_\ell^m(\Omega) Y_\ell^m(\Omega')^* \Bigg\}.
\end{aligned}
\tag{6.1.53}
$$

Unlike in the cubic case, we did not find a closed-form Green's function in the near-source limit.

Generic quartic term from perturbation theory

By exploiting the effective metric picture, we now adopt reasoning similar to that leading up to Equations (53) and (56) of [65] to illustrate how one may perturbatively solve the static Green's function near the points $x = 0$ and $x = 2/3$, using the exact solutions we have obtained there. Let us set $x = \epsilon$ and $x = 2/3 - \epsilon$ (near $x = 0$ and $x = 2/3$ respectively), where $0 < \epsilon \ll 1$. Then the effective metric in (6.1.17) may be written as a power series in ϵ, namely

$$
\tilde{g}_{\mu\nu} = \tilde{\bar{g}}_{\mu\nu} + \epsilon h_{\mu\nu} + \mathcal{O}(\epsilon^2)\,, \tag{6.1.54}
$$

where $\tilde{\bar{g}}_{\mu\nu}$ is the effective metric for either $x = 0$ or $x = 2/3$. Denote the exact Green's function solutions at either $x = 0$ or $x = 2/3$ as $\bar{G}(\vec{r}_1, \vec{r}_2)$ and the solution for arbitrary $x = \epsilon$ or $x = 2/3 - \epsilon$ as $G(\vec{r}_1, \vec{r}_2)$. First we consider the following

integral

$$\int d^3r\partial_\mu \left(|\tilde{g}|^{\frac{1}{2}} \bar{G}\left(\vec{r}_1,\vec{r}\right) \tilde{g}^{\mu\nu}\partial_\nu G\left(\vec{r},\vec{r}_2\right) - |\tilde{\tilde{g}}|^{\frac{1}{2}} G\left(\vec{r}_1,\vec{r}\right) \tilde{\tilde{g}}^{\mu\nu}\partial_\nu \bar{G}\left(\vec{r},\vec{r}_2\right)\right) . \tag{6.1.55}$$

Here, the derivatives are with respect to the 4-coordinate r, and all the metric-related quantities are evaluated at $\vec{r}$. Since both geometries $\tilde{g}$ and $\tilde{\tilde{g}}$ are independent of time, the time derivative term ($\mu = 0$) is automatically zero. Therefore (6.1.55) is really the integral of a total spatial divergence, and if we assume the Green's functions fall off sufficiently quickly at infinity (6.1.55) is identically zero. On the other hand, if we carry out the ∂_μ derivatives, for example $\partial_\mu \left(|\tilde{g}|^{\frac{1}{2}} \bar{G}\tilde{\nabla}^\mu G\right) = |\tilde{g}|^{\frac{1}{2}} \left(\tilde{\nabla}_\mu \bar{G}\tilde{\nabla}^\mu G + \bar{G}\widetilde{\Box}_r G\right)$, and proceed to employ the equations $\widetilde{\widetilde{\Box}}\bar{G} = -\delta^3(\vec{r}_1 - \vec{r}_2)/|\tilde{\tilde{g}}|^{1/2}$, $\widetilde{\Box} G = -\delta^3(\vec{r}_1 - \vec{r}_2)/|\tilde{g}|^{1/2}$, and the time-independence of the Green's functions, we deduce that G and $\bar{G}$ obey the integral equation

$$\begin{aligned} G\left(\vec{r}_1,\vec{r}_2\right) &= \bar{G}\left(\vec{r}_1,\vec{r}_2\right) \\ &- \int d^3r \left(|\tilde{g}|^{\frac{1}{2}} \tilde{g}^{ij}\partial_i \bar{G}\left(\vec{r}_1,\vec{r}\right) \partial_j G\left(\vec{r},\vec{r}_2\right) - |\tilde{\tilde{g}}|^{\frac{1}{2}} \tilde{\tilde{g}}^{ij}\partial_i G\left(\vec{r}_1,\vec{r}\right) \partial_j \bar{G}\left(\vec{r},\vec{r}_2\right)\right) . \end{aligned} \tag{6.1.56}$$

By iterating this integral equation and expanding the full metric in terms of the "background metric" $\tilde{\tilde{g}}_{\alpha\beta}$ and the perturbation $h_{\alpha\beta}$, we see that up to $\mathcal{O}(\epsilon)$, the static Green's function reads

$$G\left(\vec{r}_1,\vec{r}_2\right) = \bar{G}\left(\vec{r}_1,\vec{r}_2\right) - \epsilon \int d^3r |\tilde{\tilde{g}}|^{\frac{1}{2}} \partial_i \bar{G}\left(\vec{r}_1,\vec{r}\right) \left(\frac{1}{2}\tilde{\tilde{g}}^{\mu\nu}h_{\mu\nu}\tilde{\tilde{g}}^{ij} - h^{ij}\right) \partial_j \bar{G}\left(\vec{r},\vec{r}_2\right) , \tag{6.1.57}$$

where the perturbation with upper indices is defined as $h^{ij} \equiv \tilde{\tilde{g}}^{i\mu}\tilde{\tilde{g}}^{j\nu}h_{\mu\nu}$. We remark in passing that, by iterating (6.1.56) repeatedly, perturbation theory can be carried

out, in principle, to arbitrary order in ϵ. The background Green's function is an expansion in spherical harmonics with coefficients $R_{>,\ell}(r_>)R_{<,\ell}(r_<)$, where

$$\underline{\mathbf{x}=\mathbf{0}:} \tag{6.1.58}$$

$$R_{<,\ell=0}(r_<) = \left(\frac{\pi}{2}\right)^{1/3} \frac{1}{\alpha_2 r_{23}} \frac{\Gamma\left(\frac{1}{3}\right)\Gamma\left(\frac{7}{6}\right)}{\Gamma\left(\frac{1}{2}\right)}$$

$$R_{<,\ell\neq 0}(r_<) = \left(\frac{\pi}{2}\right)^{1/3} \frac{1}{\alpha_2 r_{23}(2\ell+1)} z_<^{\frac{\ell+1}{2}}\, {}_2F_1\left(\frac{1-\ell}{6}, \frac{\ell+1}{2}, \frac{2\ell+7}{6}, -z_<^3\right)$$

$$R_{>,\ell}(r_>) = 2z_>^{-\frac{\ell}{2}}\, {}_2F_1\left(\frac{\ell+2}{6}, -\frac{\ell}{2}, \frac{5-2\ell}{6}, -z_>^3\right)$$
$$+ \frac{\ell!\,\Gamma\left(-\frac{1}{6}(2\ell+1)\right)}{\sqrt{\pi}\,\Gamma\left(\frac{1}{3}(2\ell+1)\right)} z_>^{\frac{\ell+1}{2}}\, {}_2F_1\left(\frac{1-\ell}{6}, \frac{\ell+1}{2}, \frac{2\ell+7}{6}, -z_>^3\right)$$

$$\underline{\mathbf{x}=\frac{\mathbf{2}}{\mathbf{3}}:} \tag{6.1.59}$$

$$R_{<,\ell=0}(r_<) = \left(\frac{2\pi}{3}\right)^{1/3} \frac{1}{\alpha_2 r_{23}} \frac{\Gamma\left(\frac{1}{3}\right)\Gamma\left(\frac{4}{3}\right)}{\Gamma\left(\frac{2}{3}\right)}$$

$$R_{<,\ell\neq 0}(r_<) = \left(\frac{2\pi}{3}\right)^{1/3} \frac{1}{\alpha_2 r_{23}} \tilde{z}_<\, {}_2F_1\left(\frac{1-\ell}{3}, \frac{\ell+2}{3}, \frac{4}{3}, -\tilde{z}_<^3\right)$$

$$R_{>,\ell}(r_>) = {}_2F_1\left(-\frac{\ell}{3}, \frac{\ell+1}{3}, \frac{2}{3}, -\tilde{z}_>^3\right)$$
$$- \frac{\Gamma\left(\frac{2}{3}\right)\Gamma\left(1+\frac{\ell}{3}\right)}{\Gamma\left(\frac{4}{3}\right)\Gamma\left(\frac{\ell+1}{3}\right)} \tilde{z}_>\, {}_2F_1\left(\frac{1-\ell}{3}, \frac{\ell+2}{3}, \frac{4}{3}, -\tilde{z}_>^3\right).$$

Via the orthonormality of the spherical harmonics, integrating-by-parts the angular derivatives, using the eigenvalue equation for the Y_ℓ^ms, and changing the radial integration variable to z (or $\tilde{z}$), we arrive at the formula

$$G(\vec{r}_1,\vec{r}_2) = \bar{G}(\vec{r}_1,\vec{r}_2) - \epsilon \sum_{\ell,m} Y_\ell^m(\Omega_1) Y_\ell^m(\Omega_2)^* \Big(R_{>,\ell}(r_1) R_{>,\ell}(r_2) I_{>>,\ell} \tag{6.1.60}$$
$$+ R_{>,\ell}(r_>) R_{<,\ell}(r_<) I_{><,\ell} + R_{<,\ell}(r_1) R_{<,\ell}(r_2) I_{<<,\ell} \Big) + \mathcal{O}(\epsilon^2)\,.$$

Only one-dimensional integrals remain. Defining $M^{(r)}$ to be the radial $ij = rr$

and $\Omega^{AB}M^{(\Omega)}$ to be the angular $ij = AB$ components of the (diagonal) matrix $|\tilde{\bar{g}}|^{\frac{1}{2}}\left(\frac{1}{2}\tilde{\bar{g}}^{\mu\nu}h_{\mu\nu}\tilde{\bar{g}}^{ij} - h^{ij}\right)$, where $\Omega^{AB} = \mathrm{diag}(1, 1/\sin^2\theta)$ is the inverse metric on a 2-sphere, we find that

$$I_{>>,\ell} \equiv \int_0^{z_<} dz \left[\left(\partial_z R_{<,\ell}(z)\right)^2 M^{(r)}(z) + \ell(\ell+1)\left(R_{<,\ell}(z)\right)^2 M^{(\Omega)}(z)\right] \tag{6.1.61}$$

$$I_{><,\ell} \equiv \int_{z_<}^{z_>} dz \left[\partial_z R_{>,\ell}(z) M^{(r)}(z) \partial_z R_{<,\ell}(z) + \ell(\ell+1) R_{>,\ell}(z) M^{(\Omega)}(z) R_{<,\ell}(z)\right] \tag{6.1.62}$$

$$I_{<<,\ell} \equiv \int_{z_>}^{\infty} dz \left[\left(\partial_z R_{>,\ell}(z)\right)^2 M^{(r)}(z) + \ell(\ell+1)\left(R_{>,\ell}(z)\right)^2 M^{(\Omega)}(z)\right] . \tag{6.1.63}$$

For $x = \epsilon$, we have $z \equiv \left(\frac{\pi}{2}\right)^{1/3}\frac{r}{r_{23}}$ and

$$M^{(r)}(z) = \frac{\alpha_2 r_{23}}{6(4\pi)^{1/3}}\sqrt{\frac{z}{1+z^3}}\left[2\left(1+z^3\right)\left(\sqrt{1+z^{-3}}-1\right)-1\right] \tag{6.1.64}$$

$$M^{(\Omega)}(z) = \frac{\alpha_2 r_{23}}{6(4\pi)^{1/3}}\frac{1}{\sqrt{1+z^{-3}}}\left[\left(2-z^{-3}\right)\sqrt{1+z^{-3}} - \frac{3}{4z^3(1+z^3)} - 2\right] . \tag{6.1.65}$$

For $x = 2/3 - \epsilon$, we have $\tilde{z} \equiv \left(\frac{2\pi}{3}\right)^{1/3}\frac{r}{r_{23}}$ and

$$M^{(r)}\left(\tilde{z}\right) = \frac{\alpha_2 r_{23}}{(18\pi)^{1/3}}\frac{1}{\sqrt[3]{1+\tilde{z}^3}}\left[3\tilde{z}^3\left(\sqrt[3]{1+\tilde{z}^{-3}}-1\right)-1\right] \tag{6.1.66}$$

$$M^{(\Omega)}\left(\tilde{z}\right) = \frac{\alpha_2 r_{23}}{(18\pi)^{1/3}}\frac{1}{\sqrt[3]{1+\tilde{z}^{-3}}\left(1+\tilde{z}^3\right)}\left[3\left(1+\tilde{z}^3\right)\left(\sqrt[3]{1+\tilde{z}^{-3}}-1\right)-1\right] . \tag{6.1.67}$$

For $\ell = 0$, the integrals (6.1.63), (6.1.62) and (6.1.61) can be evaluated exactly. Referring to (6.1.58) and (6.1.59), we see that $R_{<,0}$ is a constant for both $x = 0, 2/3$.

This means the only nonzero integral is $I_{<<,\ell=0}$, which is given by

$$I_{<<,\ell=0}(x\approx 0)=\left(\frac{2}{\pi}\right)^{1/3}\frac{\alpha_2 r_{23}}{18}\left(\sqrt{\frac{z_>}{1+z_>^3}}+\frac{3}{z_>}-4\frac{\Gamma\left(\frac{1}{3}\right)\Gamma\left(\frac{4}{3}\right)}{2^{1/3}\Gamma\left(\frac{2}{3}\right)}R_{>,0}(z_>)\right) \tag{6.1.68}$$

$$I_{<<,\ell=0}\left(x\approx 2/3\right)=\left(\frac{3}{2\pi}\right)^{1/3}\frac{\alpha_2 r_{23}}{3}\left(\frac{3}{\sqrt[3]{1+\tilde{z}_>^3}}-\frac{\tilde{z}_>}{\sqrt[3]{\left(1+\tilde{z}_>^3\right)^2}}\right.$$
$$\left.-2\frac{\Gamma\left(\frac{1}{3}\right)\Gamma\left(\frac{4}{3}\right)}{\Gamma\left(\frac{2}{3}\right)}R_{>,0}(\tilde{z}_>)\right). \tag{6.1.69}$$

These expressions enable us to perform a check on the Green's function perturbation theory: the $\ell=0$ piece of the static Green's function, when $r_<\to 0$, should now correspond to the $\mathcal{O}(\epsilon)$-accurate coefficient of $\delta M/M_{\rm Pl}$ of the background solution $\bar{\pi}$ of the central mass, upon shifting it by $M\to M+\delta M$. One may confirm this by inserting in (6.1.60) the expressions in (6.1.58), (6.1.59), (6.1.68) and (6.1.69); and comparing the result with the following expressions for $\bar{\pi}$. When $x=\epsilon$, the $\mathcal{O}(\epsilon)$ correction to Eq. (6.1.29) is given by

$$\bar{\pi}(z)=\bar{\pi}_{x=0}(z)-\epsilon\left(\frac{2}{\pi}\right)^{2/3}\frac{M}{36\alpha_2 M_{\rm Pl}r_{23}}\left[\frac{\Gamma\left(\frac{1}{3}\right)^2}{2^{1/3}\Gamma\left(\frac{2}{3}\right)}\right.$$
$$\left.+\sqrt{z}\left(\frac{3}{2}z^{3/2}-\frac{1}{2}\sqrt{1+z^3}-4\,{}_2F_1\left(-\frac{1}{2},\frac{1}{6},\frac{7}{6},-z^3\right)\right)-\frac{3}{4z}\right]. \tag{6.1.70}$$

Similarly, when $x=\frac{2}{3}-\epsilon$, the $\mathcal{O}(\epsilon)$ correction to Eq. 6.1.41 is given by

$$\bar{\pi}(\tilde{z})=\bar{\pi}_{x=2/3}(\tilde{z})-\epsilon\left(\frac{3}{2\pi}\right)^{2/3}\frac{M}{6\alpha_2 M_{\rm Pl}r_{23}}\left[\frac{\Gamma\left(\frac{1}{3}\right)^2}{3\Gamma\left(\frac{2}{3}\right)}+\tilde{z}\left(\frac{3}{2}\tilde{z}-{}_2F_1\left(\frac{1}{3},\frac{2}{3},\frac{4}{3},-\tilde{z}^3\right)\right)\right.$$
$$\left.-\frac{3}{2}\left(1+\tilde{z}^3\right)^{2/3}\right]. \tag{6.1.71}$$

For $\ell \geq 1$, the integrals in (6.1.61), (6.1.62), and (6.1.63) consist of terms with products of two ${}_2F_1$s and $r^a(1+r^3)^b$, where a and b are integers or rational numbers. They likely cannot be performed exactly, but it is possible that, in the limits $r_1, r_2 \ll r_{23}$ and $r_1, r_2 \gg r_{23}$ – by writing the ${}_2F_1$s appropriately so that they may be replaced with the first few terms of their Taylor series – an approximate expression may be obtained. We leave these technical issues to possible future work.

6.2 Nonlinearities

Having now obtained (exactly or perturbatively, depending on the choice of parameters) the propagator for galileons in the presence of a large central mass, we wish to study perturbatively the motion of astrophysical objects subject to the full nonlinear galileon force. We will proceed using the field theoretic effective action framework derived for GR for a two-body system in [120] and generalized to n-body systems in [64]. For simplicity, we will henceforth restrict the analysis to only the cubic interactions ($x = 0$ case).

6.2.1 Diagrammatic construction of perturbation theory

With a closed-form static propagator well within and well outside the Vainshtein radius in hand, we now consider the construction of the perturbative expansion. The approach we will use is familiar from quantum field theory – we will construct an effective action by integrating out $\phi = \pi - \bar{\pi}$, leaving an action dependent only

on the positions and velocities of the point particles:

$$e^{iS_{\text{eff}}[\vec{x}_a,\vec{v}_a]} = \int \mathcal{D}\phi\, e^{iS[\phi,\vec{x}_a,\vec{v}_a]}\,. \tag{6.2.1}$$

The functional integral can be performed up to an irrelevant overall factor $\mathcal{N}$ by

$$e^{iS_{\text{eff}}[\vec{x}_a,\vec{v}_a]} = \mathcal{N}\exp\left[iS_{\text{int}}\left[\frac{1}{i}\frac{\delta}{\delta J}\right]\right]\exp\left[-\frac{1}{2}\int d^4x d^4y J(x)\langle\phi(x)\phi(y)\rangle J(y)\right]\Bigg|_{J=0}\,, \tag{6.2.2}$$

where the interaction part of the action $S_{\text{int}}\left[\frac{1}{i}\frac{\delta}{\delta J}\right]$ is defined as $S_{\text{int}} = S - S_{\text{kin}}$, with all occurrences of ϕ replaced by $\frac{1}{i}\frac{\delta}{\delta J}$. Expanding the interaction exponential then leads to an infinite series of terms, which can be represented graphically as Feynman diagrams. The dictionary of what each graphical object means mathematically is given in Table 6.1. Complete diagrams are created by Wick contracting each occurrence of ϕ with a corresponding occurrence of ϕ in another diagram piece. Note that, since we are interested in the classical galileon force, we neglect all loop diagrams and consider only tree-level diagrams. This procedure is completely equivalent to the Born approximation, and in particular, one need not worry about properly defining the measure for the path integral for noncanonical field theories.

The classical effective action is thus given by

$$e^{iS_{\text{eff}}} = e^{\sum(\text{fully-connected tree-level diagrams})}\,. \tag{6.2.3}$$

It is important to understand how each Feynman diagram scales with the physical scales of the problem at hand, so that we may identify the relevant expansion parameters to organize our calculations and also understand the domain of their

validity. We begin by noting that, since the galileon only appears as a propagator, it is appropriate to consider it to scale as the square root of the propagator in Eq. (6.1.38):

$$\phi \sim \sqrt{\langle \phi\phi \rangle} \sim \frac{v^{1/2}}{r_v^{3/4} r^{1/4}} \,. \tag{6.2.4}$$

Were we to be interested in the results of our calculation in a world without a spin-2 graviton, it would be necessary to understand the analogue of the virial theorem for a purely scalar force. Technically, the virial theorem should be derived by requiring that the kinetic energy of the test masses scale in the same way as the one-graviton exchange (potential) between the large central mass and a test mass. Thus, the purely galileon virial velocity is derived as

$$S_0 \equiv m v_{\rm gal} r \sim \frac{mM}{M_{\rm Pl}^2 v_{\rm gal}} \left(\frac{r}{r_v}\right)^{3/2} \qquad \Rightarrow \qquad v_{\rm gal}^2 \sim \frac{M}{M_{\rm Pl}^2 r} \left(\frac{r}{r_v}\right)^{3/2} . \tag{6.2.5}$$

However, we are obviously motivated by the eventual goal of including gravity, and so it is appropriate here to invoke the standard GR virial theorem where necessary:

$$v_{\rm GR}^2 \sim \frac{M}{M_{\rm Pl}^2 r} \,. \tag{6.2.6}$$

In the case of test masses well outside the Vainshtein radius, the virial theorem for the galileon case matches that of the GR case, and the propagator is the standard flat-space one.

The diagrams that result, what they represent, and how they scale under both versions of the virial theorem are collected in Table 6.1 for both inside and outside the Vainshtein radius. The effective action is given by the sum of diagrams that

propagator	$r \ll r_v$	$r \gg r_v$
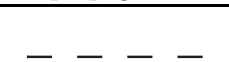	$\left(\frac{\pi}{2\alpha_2\alpha_3}\right)^{1/3} \frac{i\delta(t-t')}{2\pi r_v}\left[\frac{\rho\rho'}{\lvert\vec{\rho}-\vec{\rho}'\rvert} - \rho - \rho' + \frac{\Gamma\left(\frac{1}{6}\right)\Gamma\left(\frac{1}{3}\right)}{6\sqrt{\pi}}\right]$	$\frac{i\delta(t-t')}{4\pi\alpha_2\lvert\vec{r}-\vec{r}'\rvert}$
diagram	Feynman rule	scaling
	$-\frac{i}{2}\int d^4x\sqrt{-\tilde{g}}\tilde{g}^{00}\partial_0\phi\partial_0\phi$	v^2
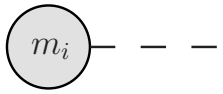	$-i\int dt\frac{m_i}{M_{\rm Pl}}\phi$	$\widetilde{S}_0^{1/2}$
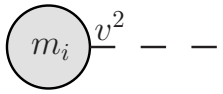	$-i\int dt\frac{m_i}{M_{\rm Pl}}v_i^2\phi$	$\widetilde{S}_0^{1/2}v^2$
	$-\frac{iM_{\rm Pl}r_v^3}{M}\int d^4x(\partial_i\phi)^2\nabla^2\phi$	$\widetilde{S}_0^{-1/2}\epsilon$
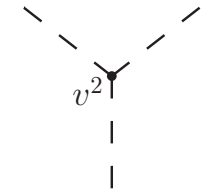	$-\frac{iM_{\rm Pl}r_v^3}{M}\int d^4x\left[(\partial_i\phi)^2\partial_0^2\phi + (\partial_0\phi)^2\nabla^2\phi\right]$	$\widetilde{S}_0^{-1/2}\epsilon v^2$

Table 6.1: Ingredients for power counting and calculation of diagrams in the effective action.

can be constructed from these basic pieces, and arranges itself into an expansion in two parameters:

$$S_{\rm eff} = \widetilde{S}_0(1 + v^2 + \cdots)(1 + \epsilon + \cdots)\,, \tag{6.2.7}$$

with the values of $\widetilde{S}_0$ and ϵ depending on the choice of virial theorem and on the

distance regime via

$$\widetilde{S}_0 = \begin{cases} S_0 \frac{m}{M} & r \ll r_v \text{ with } v_{\rm gal} \text{ or } r \gg r_v \\ S_0 \frac{m}{M} \left(\frac{r}{r_v}\right)^{3/2} & r \ll r_v \text{ with } v_{\rm GR} \end{cases}, \qquad \epsilon = \begin{cases} \frac{m}{M} & r \ll r_v \\ \frac{m}{M} \left(\frac{r_v}{r}\right)^3 & r \gg r_v \end{cases}. \tag{6.2.8}$$

Note that well within the Vainshtein radius and using the GR virial theorem, the overall amplitude of the effective action $\widetilde{S}_0$ is suppressed relative to the GR amplitude by a factor of $\left(\frac{r}{r_v}\right)^{3/2}$. This is one manifestation of the screening mechanism within the Vainshtein radius. Also note that the second expansion parameter is, indeed, small, given that the masses whose dynamics we are considering are small compared to that sourcing the background. However, as we will discuss later in more detail, when distance hierarchies are taken into account this parameter can become large in some regions of interest for comparison with astrophysical observations. This problem is not present outside the Vainshtein radius due to the additional small factor of $\left(\frac{r_v}{r}\right)^3$.

We can now justify our consideration of galileons in flat space by arguing that, at least deep within the Vainshtein radius of the sun, galileon-graviton interactions are suppressed relative to galileon self-interactions by multiplicative factors of ϵ, v^2 and/or (r/r_v). If we denote the graviton propagator by a double wavy line, the effective interaction between planets orbiting the sun is, at first order in $h/M_{\rm Pl}$, described by the Feynman graphs

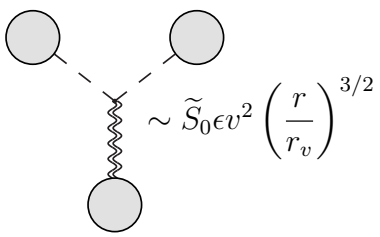

and

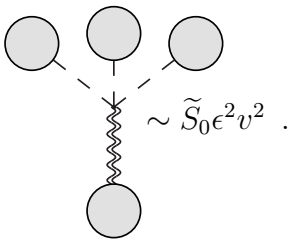

Diagrams with more graviton lines would be suppressed by higher powers of $G_{\rm N} m_i / r \sim v^2$. To arrive at these scaling relations, we first covariantize the action in Eq. (6.1.2), replacing partial derivatives with covariant ones, and expand about flat spacetime: $g_{\mu\nu} = \eta_{\mu\nu} + h_{\mu\nu}/M_{\rm pl}$. Then, because gravity is dominant over galileon forces here, we use the GR virial theorem.

Additionally, we can confirm that the correction to the gravitational force of the sun on the planets due to galileon-graviton interactions is small due to Vainshtein screening. This is done by (perturbatively) solving for $h_{\mu\nu}(x)/M_{\rm Pl}$ by expanding the covariantized action in Eq. (6.1.2) about flat spacetime and evaluating on the galileon background $\pi = \bar{\pi}$.

Explicitly, the correction coming from the $(h/M_{\rm Pl})(\partial\bar{\pi})^2$ interaction is given by

$$\frac{1}{M_{\rm Pl}} \langle h_{\mu\nu}(x) \rangle_{\bar{\pi}\bar{\pi}} = \int d^4y \left[\frac{\alpha_2}{2} \left(\eta^{\alpha\kappa}\eta^{\beta\lambda} - \frac{1}{2}\eta^{\alpha\beta}\eta^{\kappa\lambda} \right) \langle h_{\mu\nu}(x) h_{\alpha\beta}(y) \rangle \partial_\kappa \bar{\pi}(y) \partial_\lambda \bar{\pi}(y) \right] \tag{6.2.9}$$

$$\sim \Psi_h \frac{\bar{\pi}}{M_{\rm Pl}} \left(\frac{r}{r_v} \right)^{\{3/2,2\}} \tag{6.2.10}$$

for {purely cubic, nonzero quartic} galileon theories. Here, $\Psi_h \sim G_{\rm N} M_\odot / r$ is the Newtonian gravitational potential of the sun. Because the first order general relativistic correction to $h_{\mu\nu}(x)/M_{\rm Pl}$ begins at $\mathcal{O}(\Psi_h^2)$, we see that galileon-graviton

interactions are suppressed as long as $\frac{\bar{\pi}}{M_{\rm Pl}}\left(\frac{r}{r_v}\right)^{\{3/2,2\}} \ll \Psi_h$.

Similarly, the $(h/M_{\rm Pl})\partial^2\bar{\pi}(\partial\bar{\pi})^2/\Lambda^3$ interaction term yields a correction that reads

$$\frac{1}{M_{\rm Pl}}\langle h_{\mu\nu}(x)\rangle_{\bar{\pi}\bar{\pi}\bar{\pi}} = \int d^4y \Bigg[\frac{\alpha_3}{2\Lambda^3}\left(\eta^{\alpha\rho}\eta^{\beta\sigma}\eta^{\kappa\lambda} + \eta^{\alpha\beta}\eta^{\kappa\rho}\eta^{\lambda\sigma} - 2\eta^{\alpha\rho}\eta^{\kappa\beta}\eta^{\lambda\sigma}\right) \times \langle h_{\mu\nu}(x)h_{\alpha\beta}(y)\rangle\partial_\kappa\partial_\lambda\bar{\pi}(y)\partial_\rho\bar{\pi}(y)\partial_\sigma\bar{\pi}(y)\Bigg] \tag{6.2.11}$$

$$\sim \Psi_h\frac{\bar{\pi}}{M_{\rm Pl}}\left(\frac{r}{r_v}\right)^{\{0,1\}} \tag{6.2.12}$$

and the $(h/M_{\rm Pl})(\partial^2\bar{\pi})^2(\partial\bar{\pi})^2/\Lambda^6$ interaction term (which is of course absent in the purely cubic galileon theory) gives us

$$\begin{aligned}\frac{1}{M_{\rm Pl}}&\langle h_{\mu\nu}(x)\rangle_{\bar{\pi}\bar{\pi}\bar{\pi}\bar{\pi}} \\ &= \int d^4y\Big[\left(-\frac{\alpha_4}{4\Lambda^6}\right)\langle h_{\mu\nu}(x)h_{\alpha\beta}(y)\rangle\Big(M^{\alpha\beta\gamma\delta\kappa\lambda\rho\sigma}\partial_\gamma\partial_\delta\bar{\pi}(y)\partial_\rho\partial_\sigma\bar{\pi}(y)\partial_\kappa\bar{\pi}(y)\partial_\lambda\bar{\pi}(y) \\ &\qquad + N^{\alpha\beta\gamma\delta\kappa\lambda\rho\sigma}\partial_\gamma\partial_\delta\partial_\sigma\bar{\pi}(y)\partial_\kappa\bar{\pi}(y)\partial_\lambda\bar{\pi}(y)\partial_\rho\bar{\pi}(y)\Big)\Big] \qquad (6.2.13) \\ &\sim \Psi_h\frac{\bar{\pi}}{M_{\rm Pl}}\,, \qquad (6.2.14)\end{aligned}$$

with

$$\begin{aligned} M^{\alpha\beta\gamma\delta\kappa\lambda\rho\sigma} =& -2\eta^{\alpha\kappa}\eta^{\beta\lambda}\eta^{\gamma\delta}\eta^{\rho\sigma} - \frac{1}{2}\eta^{\alpha\beta}\eta^{\gamma\delta}\eta^{\kappa\lambda}\eta^{\rho\sigma} - 2\eta^{\alpha\beta}\eta^{\gamma\delta}\eta^{\kappa\sigma}\eta^{\lambda\rho} + 6\eta^{\alpha\kappa}\eta^{\beta\gamma}\eta^{\delta\lambda}\eta^{\rho\sigma} \\ & - 8\eta^{\alpha\kappa}\eta^{\beta\rho}\eta^{\gamma\lambda}\eta^{\delta\sigma} + 3\eta^{\alpha\beta}\eta^{\gamma\lambda}\eta^{\delta\rho}\eta^{\kappa\sigma} - \frac{1}{2}\eta^{\alpha\beta}\eta^{\gamma\sigma}\eta^{\delta\rho}\eta^{\kappa\lambda} + \eta^{\alpha\gamma}\eta^{\beta\delta}\eta^{\kappa\lambda}\eta^{\rho\sigma} \\ & + 2\eta^{\alpha\gamma}\eta^{\beta\delta}\eta^{\kappa\sigma}\eta^{\rho\lambda} + 3\eta^{\alpha\lambda}\eta^{\beta\kappa}\eta^{\gamma\sigma}\eta^{\delta\rho} - 2\eta^{\alpha\delta}\eta^{\beta\rho}\eta^{\gamma\lambda}\eta^{\kappa\sigma} \end{aligned} \tag{6.2.15}$$

$$\begin{aligned} N^{\alpha\beta\gamma\delta\kappa\lambda\rho\sigma} =& -\eta^{\alpha\beta}\eta^{\gamma\delta}\eta^{\kappa\lambda}\eta^{\rho\sigma} + \eta^{\alpha\beta}\eta^{\gamma\lambda}\eta^{\delta\kappa}\eta^{\rho\sigma} + \eta^{\alpha\kappa}\eta^{\beta\lambda}\eta^{\gamma\delta}\eta^{\rho\sigma} - \eta^{\alpha\delta}\eta^{\beta\kappa}\eta^{\gamma\lambda}\eta^{\rho\sigma} \\ & + \eta^{\alpha\gamma}\eta^{\beta\delta}\eta^{\kappa\lambda}\eta^{\rho\sigma}\,. \end{aligned} \tag{6.2.16}$$

Thus, we may consistently neglect gravity when considering galileon forces due to the sun's galileon field $\bar{\pi}$ – for instance in perihelion precession calculations – and when computing the effective potential between the planetary bodies themselves, as long as these phenomena are taking place deep within the Vainshtein radius of the sun.

In the next section we will describe how to calculate the dynamics due to cubic galileon forces in the region where the point masses in question lie well outside the sun's and each other's Vainshtein radii.

6.2.2 Outside the Vainshtein radius

The procedure for calculating the galileon forces perturbatively is straightforward in the case where the two interacting particles are well outside the Vainshtein radius. This is because, as expected, the galileon theory behaves as a simple scalar-tensor theory in this regime, and nonlinear interaction terms can be treated perturbatively.

Thus, using the convention

$$\widetilde{\Box}\langle\phi\phi\rangle = -i\frac{\delta^4(r-r')}{\sqrt{-\tilde{g}}}\,, \tag{6.2.17}$$

the galileon propagator takes the flat-space form

$$\langle\phi(r)\phi(r')\rangle = \frac{i\delta(t-t')}{4\pi\alpha_2|\vec{r}-\vec{r}'|}\,. \tag{6.2.18}$$

We wish to understand how each term of our effective action scales with the physical scales of the solar system. In general relativity the effective action of the solar system arranges into an expansion in v^2 via $S_{\text{eff}} = S_0(1+v^2+\cdots)$. This expansion in only powers of v^2 neglects the large disparity of distances and masses present in the solar system. This subtlety will be important in the galileon case, where we will find that once the planetary bodies in question get too close to each other, for example in the sun-earth-moon configuration, one loses perturbative control over the effective action calculation at hand. The same issue does not present a problem in GR within the solar system, because $G_N m/|\vec{r}_i-\vec{r}_j| \ll 1$ regardless of the planet's mass m and separation distance $|\vec{r}_i-\vec{r}_j|$.

Leaving aside, for the moment, the issue of the disparity of distances and masses, the power counting of diagrams in Table 6.1 is straightforward. As described in [120], the relevant time scale in the dynamics of objects orbiting a central mass is set by their velocity, and so it is sensible to consider all factors of time to scale as $\frac{r}{v}$. An additional subtlety to consider is the virial theorem used to organize potential terms within the expansion, as we have discussed.

These arguments lead to the scaling given in Table 6.1 and to the resulting conclusion that the additional expansion parameter is $\frac{m}{M}\left(\frac{r_v}{r}\right)^3$. Using this, we can then calculate the effective action via Eq. (6.2.3) as discussed above.

At the first few orders, the calculation is relatively simple. At $\mathcal{O}(\widetilde{S}_0)$, only the one-galileon-exchange diagram contributes, giving

$$S_{\text{eff}}^{(0)} = -\frac{m_1 m_2}{4\pi\alpha_2 M_{\text{Pl}}^2}\int \frac{dt}{|\vec{r}_1 - \vec{r}_2|}\,, \tag{6.2.19}$$

while at $\mathcal{O}(\widetilde{S}_0\epsilon)$, only the three-galileon-vertex diagram is relevant, yielding

$$S_{\text{eff}}^{(\epsilon)} = \frac{\alpha_3 m_1 m_2 m_3}{8\pi^2\alpha_2^3 M_{\text{Pl}}^2 M} r_v^3 \int dt \left(\frac{\hat{R}_{13}\cdot\hat{R}_{23}}{R_{13}^2 R_{23}^2} - \frac{\hat{R}_{12}\cdot\hat{R}_{23}}{R_{12}^2 R_{23}^2} + \frac{\hat{R}_{12}\cdot\hat{R}_{13}}{R_{12}^2 R_{13}^2}\right)\,, \tag{6.2.20}$$

with $\vec{R}_{ab} = \vec{r}_a - \vec{r}_b$.

We now see concretely, *e.g.* when object 2=object 3, that the small correction $\mathcal{L}^{(\epsilon)} \sim \frac{m_2}{M}\left(\frac{r_v}{R_{12}}\right)^3 \mathcal{L}^{(0)}$, or, in terms of the Vainshtein radius of object 2, $\mathcal{L}^{(\epsilon)} \sim \left(\frac{r_{v,2}}{R_{12}}\right)^3 \mathcal{L}^{(0)}$. The expansion does not depend at all on the existence of the large central mass, but now it becomes clear that the relevant distance scale is the Vainshtein radius of the small masses whose dynamics we are considering. Thus, to remain within the regime for which perturbation theory about the flat galileon background is valid, the small masses must be well-separated from each other as well as from the large central mass.

At $\mathcal{O}(\widetilde{S}_0 v^2)$ things are, in principle, a little more complicated. There are three diagrams that contribute: the v^2 corrections to the point-particle Lagrangian for each mass involved in the one-galileon-exchange diagram, and the exchange of the

$\mathcal{O}(v^2)$ part of the propagator. This last diagram may be equivalently described as the insertion of the two-time-derivative part of the kinetic term. The first approach is simpler calculationally if one knows the full time dependence of the propagator, which we do not in the current case. However, even though we have not solved the time dependent propagator here, the diagram in question turns out to be proportional to the analogous diagram in GR, for which we know the full time-dependent propagator. Thus, the relevant contribution is

$$\begin{aligned} S_{\text{eff}}^{(v^2)} = &- \frac{m_1 m_2}{4\pi\alpha_2 M_{\text{Pl}}^2} \int dt \frac{v_1^2 + v_2^2}{R_{12}} \\ &- \frac{m_1 m_2}{8\pi\alpha_2^2 M_{\text{Pl}}^2} \int dt \left(\frac{\vec{v_1} \cdot \vec{v_2}}{R_{12}} + \frac{1}{R_{12}^3} (\vec{R}_{12} \cdot \vec{v}_1)(\vec{R}_{12} \cdot \vec{v}_2) \right). \end{aligned} \tag{6.2.21}$$

6.2.3 Breakdown of the perturbative expansion

As mentioned in Section 6.2.2, the effective action expansion we have outlined proves to be valid when one does not take into account distance hierarchies (*e.g.* the fact that the distance from the earth to the sun is much larger than the distance from the earth to the moon). Let us now reconsider the expansion, taking this into consideration. We will keep track of two separate distance scales: r, the distance of a dynamical object from the large central mass, and R, the separation between two arbitrary dynamical objects.

Well within the Vainshtein radius, the propagator in Eq. (6.1.38) now scales as

$$\langle \phi\phi \rangle \sim \frac{v}{r_v^{3/2}\sqrt{r}} \left(1 + \frac{r}{R}\right), \tag{6.2.22}$$

where the first term originates from the solution sourced by the δ function and the second term from the homogeneous solutions. Thus, we must correct each appearance of ϕ by the addition of a factor $\sim \left(1 + \frac{r}{R}\right)$. Note that this is a conservative estimate in the situation where $R \ll r$, since we have treated time and space derivatives as scaling like $\frac{v}{r}$ and $\frac{1}{r}$, respectively. When acting on the propagator given in Eq. (6.1.38), derivatives will also produce terms which scale as $\frac{1}{R}$. Such terms would introduce even larger corrections to instances of ϕ with derivatives acting on them.

These considerations correct the zeroth- and first-order (in either small parameter) diagrams as in Table 6.2. The new effective action amplitude is therefore $\hat{S}_0 = \widetilde{S}_0 \left(1 + \frac{r}{R}\right)$ and the new expansion parameters are

$$v^2 \left(1 + \frac{r}{R}\right) \qquad \text{and} \qquad \hat{\epsilon} = \epsilon \left(1 + \frac{r}{R}\right)^2 . \tag{6.2.23}$$

This effect produces an enhancement in the overall strength of galileon interactions as seen in $\hat{S}_0$, as well as a breakdown of the expansion for sufficiently small separations between astrophysical objects. As an example, consider the earth-moon system: the sun is about 1000 times more distant from the earth than the moon, and the earth is about 10^6 times less massive than the sun. Thus for the dynamics of the earth-moon system, the "small" expansion parameter

$$\hat{\epsilon} = \frac{m_{\text{earth}}}{M_{\text{sun}}} \left(1 + \frac{r_{\text{sun-earth}}}{R_{\text{earth-moon}}}\right)^2 \sim \mathcal{O}(1) . \tag{6.2.24}$$

In particular, this means that this formalism – approximating the galileon force by the first-order force obtained from the one-galileon-exchange diagram – cannot

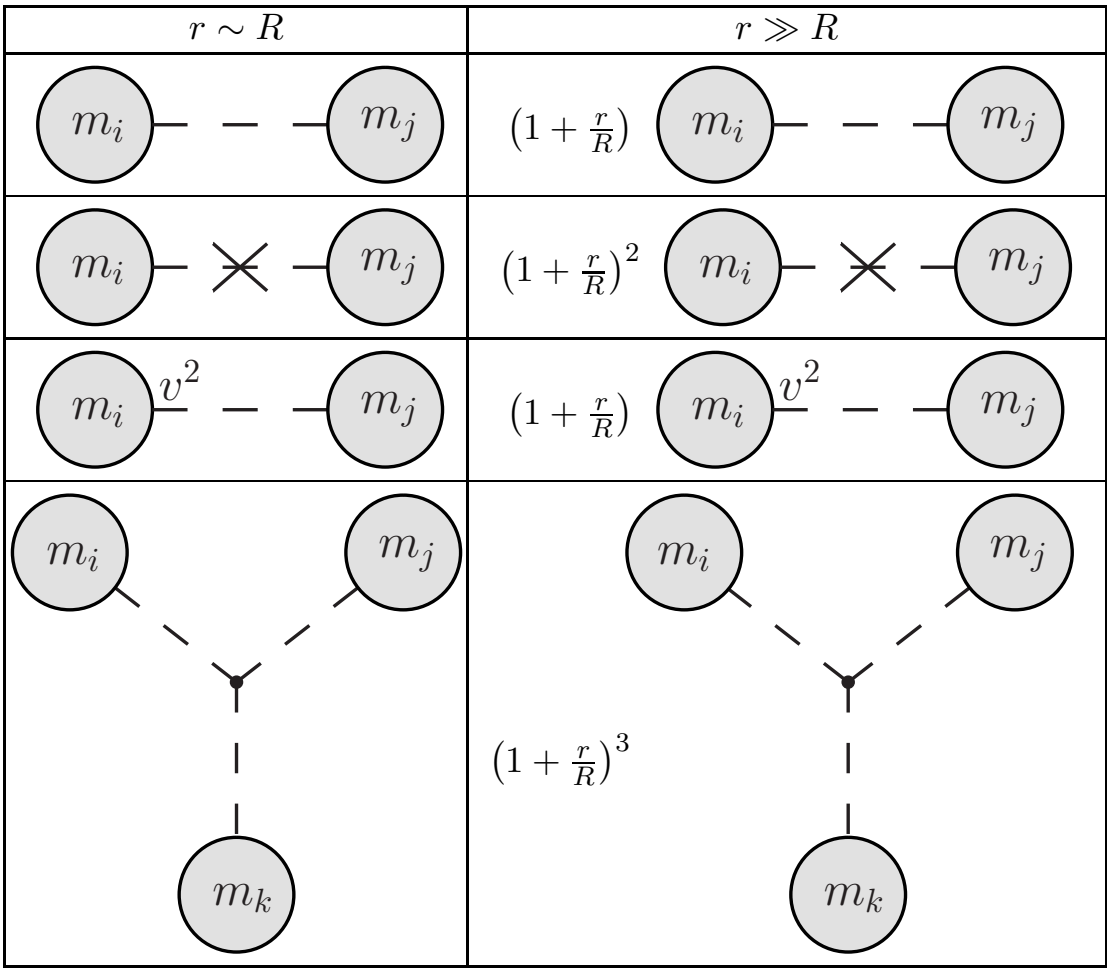

Table 6.2: A conservative estimate of corrections introduced by the consideration of object separations much smaller than the distance from either object to the large central mass.

be used to constrain Λ using lunar laser ranging experimental data, since the corrections to this force are large. In the case of the force acting between the earth and the moon, diagrams with no velocity corrections but any number of galileon vertices all enter at the same order and hence any truncation of the expansion at finite order yields an error in the force of order the result calculated.

This conclusion is qualitatively similar to that reached in [174], which led to an even larger region in which the perturbative expansion is not valid. In that view, the earth's Vainshtein radius renormalized by the presence of the sun is $\tilde{r}^3_{v,\oplus} = (1\ AU)^3 \frac{M_\oplus}{M_\odot}$. Thus the quantity $\frac{m}{M}\left(\frac{r}{R}\right)^3 \sim \left(\frac{\tilde{r}_v}{R}\right)^3$ and the perturbative expansion about the background sourced by the sun breaks down at a distance from the earth of order the earth's Vainshtein radius in the presence of the sun.

Note that there is no analogous breakdown of the PPN expansion in GR, since $\left(\frac{v_{\rm earth}}{c}\right)^2 \sim 10^{-8}$ is smaller than the mass ratio. Nor is there a problem for a system similar to the earth and the moon located outside the sun's Vainshtein radius, as ϵ in this region has an additional small multiplicative factor $\left(\frac{r_v}{r}\right)^3$.

The importance of galileon self-interactions in determining astrophysical dynamics may mean that finite size effects, such as tidal forces acting on planetary bodies or the influence of their intrinsic multipole moments, could play a more significant role than their gravitational counterparts, relative to the lowest order forces between structureless test masses. We may take account of such effects through the addition of non-minimal terms to the world line action $\int dt(m/M_{\rm Pl})\pi$. Of course, whenever we encounter an ultraviolet (UV) divergence when computing one of the relevant diagrams, the introduction of such counterterms is unavoidable. For comparison, in the case of GR, tidal effects first appear at $\mathcal{O}(v^{10})$ and are highly subdominant [120].

6.3 Implications

In this chapter we have studied a number of topics crucial to a complete understanding of the effects of galileons on the dynamics of the solar system. We have obtained for the first time the first-order effects of the full quintic galileon theory. This includes the contribution to the precession of planetary perihelion due to the galileon field $\bar{\pi}$ of the sun, as well as the static propagator for galileon fluctuations about $\bar{\pi}$. The inclusion of the higher interaction terms leads to a qualitatively different force law which yields a parametrically smaller perihelion precession than the cubic case. (The cubic case could potentially be observable with next-generation observations [112].) However, the presence of higher interaction terms exacerbates the superluminal propagation of radial perturbations as well as the very subluminal propagation of angular perturbations deep within the Vainshtein radius of the sun.

To understand the effects of the cubic galileon theory on solar system dynamics, we have constructed a perturbative framework to calculate its effective action in the nonrelativistic limit, about the background $\bar{\pi}$ sourced by the sun. Apart from the typical speed v, there is an additional expansion parameter ϵ introduced by nonlinear galileon interactions. As a concrete example of the framework, we have calculated the first-order corrections in v^2 and in ϵ for the case where the objects whose galileon force we are interested in are outside the Vainshtein radius of the large central mass. Unfortunately, for the earth-moon system, we have shown that the additional expansion parameter ϵ becomes $\mathcal{O}(1)$, and thus that nonlinearities

render the perturbative framework inadequate.

Even for well separated masses, where the perturbative expansion is valid, a concrete calculation of the corrections due to the nonlinear galileon interactions presents a technical challenge. If this could be done, it would yield a quantitative answer to the question of what the Vainshtein radius of the earth is in the presence of the sun. The closed-form propagator obtained in (6.1.38) is only valid in the region deep within the Vainshtein radius; the full propagator in (6.1.39) involves a spherical harmonic expansion. Corrections at $\mathcal{O}(\epsilon)$ involve an integral over *all space* of the propagator and hence require the full infinite sum form of the propagator. The integrals necessary to perform this calculation are not known, nor is there reason to believe it would yield a result that can be then summed into a closed-form solution.

Chapter 7

Doppelgänger defects: noncanonical theories masquerading as canonical

In this chapter, we abandon the requirement of Vainshtein screening to investigate new features of topological defects in scalar field theories with generic noncanonical kinetic terms. In particular, we study kinetic terms with more than two derivatives, but which lead to second-order equations of motion. These scalar field theories are similar to those employed in k-essence models which have been studied in the context of cosmic acceleration and were introduced in [22, 21, 19]. Kinetic terms of this general type also play an important role in other interesting models, such as those of ghost condensation [17] or galileon [175] fields. The topological defects

present in this general class of theories are often termed "k-defects," and some aspects of these objects have been studied in earlier works [23, 24, 190, 5, 151, 38, 25, 34, 2, 114].

In this chapter, based on work done in collaboration with Matt Lewandowski, Mark Trodden, and Daniel Wesley [16], we report on some surprising aspects of k–defects, especially k-domain walls and their associated instantons. We find that there are very reasonable choices for the k-defect kinetic term – such as the Dirac-Born-Infeld (DBI) form – for which there are no static defect solutions in a range of parameters, despite the fact that the potential may have multiple minima. Thus, unlike canonical scalar field theories, knowledge of the homotopy groups of the vacuum manifold is sometimes insufficient to classify the spectrum of topological defects. Due to the close connection between domain walls and instantons, this result also constrains certain instanton solutions to noncanonical 4-dimensional effective theories.

Perhaps more surprisingly, it is also possible for k-defects to masquerade as canonical scalar field domain walls. By this, we mean the following: given a scalar field ϕ with canonical kinetic term and potential $V(\phi)$, then, up to rigid translations $x \to x + c$, the field profile $\phi(x)$ and energy density $E(x)$ are uniquely determined for a solution containing a single wall. We show that there always exists a class of k-defect Lagrangians which generate precisely the same field profile and energy density profile as the unique canonical defect. To an observer who measures the field profile

and energy density of the configuration, any k-defect in this class precisely mimics the canonical domain wall. Nevertheless, despite having identical defect solutions, we show that these two theories are not reparameterizations of each other, since the fluctuation spectra about the walls are different.

Most of our analytical work is carried out for scalar field theories with domain wall solutions. In order to study the generalization to other topological defects, we carry out a numerical investigation of global cosmic string k-defect solutions. For the natural generalization of the DBI kinetic term, we show it is possible to match either the field profile or energy density of the canonical global string, but not both simultaneously. Thus while we are unable to find an analogue of the doppelgänger domain walls in this case, we cannot conclusively show they do not exist.

This chapter is organized as follows. In Section 7.1 we describe the general theory of k-defects and use the specific example of the Dirac-Born-Infeld (DBI) action to illustrate how the question of existence of defects is more complicated than the canonical case. We also discuss instanton solutions to the DBI action and compare our conclusions to existing discussions in the literature. Section 7.2 introduces the idea of doppelgänger domain walls, which can precisely mimic the field profile and energy density of a canonical domain wall. We establish conditions for the existence of doppelgängers, and discuss the fluctuation spectra about doppelgänger and canonical walls. In Section 7.3 we employ numerical methods to search for doppelgänger cosmic strings, but are unsuccessful. We conclude in Section 7.4.

7.1 Existence and properties of k-defects and instantons

Our discussion focuses on two families of models involving a scalar field. The first family consists of canonical scalar field theories of the form

$$S = \int \left[-\frac{1}{2}(\partial\phi)^2 - V(\phi) \right] \, \mathrm{d}^4x \ , \tag{7.1.1}$$

where we use the $(-+++)$ metric signature, set $\hbar = c = 1$, and define $(\partial\phi)^2 \equiv \eta^{\mu\nu}(\partial_\mu\phi)\partial_\nu\phi$. Although we focus our discussion on four spacetime dimensions, essentially all of our conclusions regarding domain walls apply in any spacetime dimension > 2, since all but one of the spatial dimensions are spectators.

The second family of models generalizes the canonical scalar field theory by including additional derivatives of ϕ. This family is described by actions of the form

$$S = \int \left[P(X) - V(\phi) \right] \, \mathrm{d}^4x \ , \tag{7.1.2}$$

where we define

$$X = (\partial\phi)^2 = -\dot{\phi}^2 + (\nabla\phi)^2 \ . \tag{7.1.3}$$

We refer to a Lagrangian of the form (7.1.2) as a "$P(X)$ Lagrangian." (Note that there are multiple conventions for the definition of X in the literature). The canonical scalar field theory corresponds to $P(X) = -X/2$. While there are more than two derivatives of ϕ in the Lagrangian, by assuming that the Lagrangian depends

only on X and ϕ as in (7.1.2) we guarantee that the resulting equations of motion are second order.

In this section, we show that static domain walls need not exist for all parameter ranges of a wide variety of $P(X)$ theories, even when the potential in (7.1.2) possesses multiple disconnected minima. We demonstrate this result using a specific form of $P(X)$, corresponding to the Dirac-Born-Infeld (DBI) kinetic term. We then adapt these results to study the properties of Coleman-de Luccia-type instantons in 4-dimensional effective theories with DBI kinetic terms.

7.1.1 Domain walls in naïve DBI

A simple and well-motivated form of $P(X)$ is contained in the DBI action, given by

$$P(X) = M^4 - M^2\sqrt{M^4 + (\partial\phi)^2}\ , \tag{7.1.4}$$

where M is a mass scale associated with the kinetic term, which we will refer to as the "DBI mass scale." When $(\partial\phi)^2 \ll M^4$, this kinetic term reduces to the canonical one. In what follows, we set $M = 1$, and hence normalize all mass scales to the DBI mass scale. A kinetic term of the form (7.1.4) can arise naturally in various ways: for example, it is the 4-dimensional effective theory describing the motion of a brane with position ϕ in an extra dimension. Often these kinetic terms appear along with additional functions of ϕ, known as "warp factors." These do not influence our conclusions in an essential way and so, for now, we will use the simple form (7.1.4) to illustrate our conclusions, and return to the case with warp factors

in Section 7.1.2.

We refer to the $P(X)$ Lagrangian defined by Eq. (7.1.4) as the "naïve" DBI theory since one is merely adding a potential function $V(\phi)$ to the DBI kinetic term (7.1.4). There are other, and in some respects better, ways to generalize a pure DBI term and include interactions. We will discuss one such extension extensively in Section 7.2. Nonetheless, the $P(X)$ Lagrangian defined by Eq. (7.1.4) is commonly employed in the literature, and will provide an instructive example of k-defects possessing a number of interesting properties, as we now discuss.

The canonical wall

As a warm-up, we first study the canonical domain wall profile. We assume that all fields depend on only one spatial coordinate z, and are independent of time. With these assumptions, there exists a conserved quantity J with $\mathrm{d}J/\mathrm{d}z = 0$, defined by

$$J = \phi' \frac{\partial L}{\partial \phi'} - L = -\frac{1}{2}\phi'^2 + V(\phi) \ , \tag{7.1.5}$$

where L is the Lagrangian density. We assume that the potential is positive semidefinite and has discrete zero-energy minima at $\phi = \phi_\pm$, such that $V(\phi_\pm) = 0$, with $\phi_- < \phi_+$. Assuming boundary conditions where $\phi = \phi_\pm$ at $z = \pm\infty$, we have that $V = \phi' = 0$ at $z = \pm\infty$. Therefore $J = 0$ at infinity, and since it is conserved, it vanishes everywhere. This implies that Eq. (7.1.5) can be rewritten as

$$\phi'^2 = 2V(\phi) \ , \tag{7.1.6}$$

which can be straightforwardly integrated to yield the usual domain wall solution.

To compute the energy density of the solution, we use the fact that

$$H = \dot{\phi}\frac{\partial L}{\partial \dot{\phi}} - L = -L \ , \tag{7.1.7}$$

where H is the Hamiltonian density and the second equality follows from our assumption that the configuration is static. Using Eq. (7.1.6) we have that the energy density $E(\phi)$ is given by

$$H = E(\phi) = 2V(\phi) \ . \tag{7.1.8}$$

In general, the energy density cannot be expressed as a function of the field only, but must include the gradient. A relation like (7.1.8) is only true because we have a conserved quantity for static configurations, which relates the field value and its gradient. Thus, all of the physics of the static canonical domain wall is encoded in the conserved quantity J.

The naïve DBI wall

We can carry out a similar derivation for the DBI wall in a $P(X)$ theory defined by Equations (7.1.2) and (7.1.4). Recalling we have set $M = 1$, the conserved quantity J is given by

$$J = \frac{1}{\sqrt{1+\phi'^2}} - 1 + V(\phi) \ . \tag{7.1.9}$$

As in the canonical case described in Section 7.1.1, we assume that the potential is positive semidefinite and has discrete zero-energy minima at $\phi = \phi_\pm$, such that $V(\phi_\pm) = 0$, with $\phi_- < \phi_+$. We also assume the same boundary conditions, so that

$\phi = \phi_\pm$ at $z = \pm\infty$. Since $V = \phi' = 0$ at $z = \pm\infty$, J must vanish everywhere. Hence, inverting (7.1.9) yields

$$\phi'^2 = \frac{1}{[1 - V(\phi)]^2} - 1 \ . \tag{7.1.10}$$

This expression is the analogue of Eq. (7.1.6), and can be integrated to give the field profile once $V(\phi)$ is specified. Given a static configuration, the energy density is then given by

$$E(\phi) = \frac{V(\phi)\,[2 - V(\phi)]}{1 - V(\phi)} \ , \tag{7.1.11}$$

where we have used Eq. (7.1.9) and the fact that $J = 0$ everywhere.

Unlike the canonical case, it is apparent that problems may arise when integrating Eq. (7.1.10). In the canonical case, so long as $V(\phi)$ is bounded for $\phi \in [\phi_-, \phi_+]$, we have ϕ' finite everywhere. This is no longer the case with Eq. (7.1.10). If there is any $\phi_1 \in [\phi_-, \phi_+]$ such that $V(\phi_1) > 1$, then Eq. (7.1.10) implies that ϕ' is undefined. The problem can be traced back to Eq. (7.1.9), in which the first two terms on the right-hand side can sum to any number between zero (when ϕ' vanishes) and -1 (when $|\phi'|$ is infinite). Thus, at any point where $V(\phi) > 1$, there is simply no value of ϕ' which will allow the requirement that $J = 0$ everywhere to be satisfied. We conclude that there are no nontrivial static solutions to the theory defined by Eq. (7.1.4) if $V(\phi) > 1$ at any $\phi \in [\phi_-, \phi_+]$.

To study the nature of the singularity, suppose we have integrated Eq. (7.1.10) from $\phi = \phi_-$ at $z = -\infty$ and have encountered a value $\phi = \phi_1$ at which $V(\phi_1) = 1$.

Assume that this value is reached at $z = z_1$. For a generic function $V(\phi)$ we have

$$V(\phi_1 + \Delta\phi) = 1 + v'\Delta\phi + \mathcal{O}(\Delta\phi^2) \ , \tag{7.1.12}$$

where $v' = V'(\phi)|_{\phi=\phi_1}$. Retaining only terms up to first order in $\Delta\phi$ and using Eq. (7.1.10) leads to

$$\phi' = -\frac{1}{v'\Delta\phi} \ , \tag{7.1.13}$$

which has the solution

$$\phi(z) = \phi_1 + \sqrt{-\frac{2(z - z_1)}{v'}} \ . \tag{7.1.14}$$

Hence, ϕ is well-defined when $z < z_1$, before the singularity is reached. It is not defined for $z > z_1$, and at $z = z_1$ there is cusp-type singularity in the field, at which the field value is finite but the gradient and all higher derivatives become infinite.

It is natural to ask whether this singularity is integrable; that is, whether the solution can be continued past the singular point at $z = z_1$. We now show that the solution cannot be continued, and hence there are no global solutions to Eq. (7.1.4) with the desired boundary conditions. We prove this claim for the simple case in which there is only one connected interval of field space between the minima for which $V(\phi) > 1$ (the generalization to the case where there are multiple disconnected regions where $V(\phi) > 1$ is straightforward).

The relevant region of field space is naturally divided into three intervals

$$\begin{aligned} I_- &\equiv [\phi_-, \phi_1) \ , \\ I_0 &\equiv (\phi_1, \phi_2) \ , \\ I_+ &\equiv (\phi_2, \phi_+] \ . \end{aligned}$$

The intervals $I_\pm$ include the minima of $V(\phi)$ and all field values for which $V(\phi) < 1$. The interval I_0 includes the field values for which $V(\phi) > 1$. At the boundary points ϕ_1 and ϕ_2 of I_0, $V(\phi) = 1$ and ϕ' reaches $\pm\infty$. We have shown that solutions of Eq. (7.1.4) with the desired boundary conditions can be constructed which take values in $I_\pm$, but now claim that these solutions cannot be continued into I_0.

The key to proving our claim is to employ the quantity J, which must be conserved by the equations of motion, and is well-defined for any value of ϕ' (even $\phi' = \pm\infty$). First, suppose that we have a candidate continuation of the solution on I_- into I_0. Using this continuation, we choose any point z_* for which $\phi(z_*) \in I_0$, and use $\phi(z_*)$ and $\phi'(z_*)$ to evaluate J. Since $V(\phi) > 1$ at z_*, then by inspection of Eq. (7.1.9), we conclude that $J > 0$ at z_*. Since J is conserved by the equations of motion, then J must assume this same positive definite value for all points in I_0. Inspection of Eq. (7.1.9) reveals that, when $J > 0$, ϕ' is finite when $V(\phi) = 1$. Hence, if we approach ϕ_1 while remaining in I_0, then the limiting value of ϕ' at ϕ_1 is finite. On the other hand, we have already shown that $J = 0$ in I_-, and when $J = 0$ we have that $\phi' = \pm\infty$ when $V(\phi) = 1$. Thus if we approach ϕ_1 while remaining in I_- we have $\phi' = \pm\infty$ at $\phi = \phi_1$.

Thus, if there were a global solution, then ϕ' would approach a finite value from one side of ϕ_1, and an infinite value from the other side. This means that the purported global solution would not match smoothly across the singularity at ϕ_1; a contradiction. Hence we conclude that global solutions do not exist.

While the above statements are strictly correct within the context of the specific Lagrangian we have used, there are potential problems in treating the DBI Lagrangian as an effective field theory near the singularity at ϕ_1. Expanding the Lagrangian L about a static background solution $\phi(z)$ gives terms of the form

$$\delta_2 L \supset -\frac{\delta\phi'(z)^2}{2\left(1+\phi'(z)^2\right)^{3/2}} \tag{7.1.15}$$

at quadratic order in the fluctuation $\delta\phi(z)$. Hence the kinetic term for fluctuations vanishes as we approach the point z_1 where $\phi = \phi_1$ and $\phi'(z) \to \infty$. Near the singularity, the effective theory is strongly coupled, quantum corrections to Eq. (7.1.4) are large, and the precise functional form of Eq. (7.1.4) is not trustworthy. Whether these corrections invalidate our conclusions is an open question. Nonetheless, our analysis shows that the topological structure of the vacuum is not enough to guarantee the existence of topological defects in models with extra derivatives.

7.1.2 Application to instantons

Domain wall solutions are closely related to the solutions to Euclidean field theories employed in constructing instantons. This is because the lowest-energy Euclidean configurations typically depend on a single coordinate, and thus have essentially

the same structure as domain wall solutions. Although there are some differences, the correspondence becomes exact in the thin-wall limit. For example, to study the Coleman-de Luccia instanton occurring in a canonical field theory one considers the Euclidean action

$$S_E = 2\pi^2 \int \left[\frac{1}{2}\phi'^2 + V(\phi)\right] \rho^3 \, \mathrm{d}\rho \ , \tag{7.1.16}$$

where ρ is the Euclidean radial coordinate, and in this subsection only we take $\phi' \equiv \partial\phi/\partial\rho$. Instantons are solutions of the equations of motion of this action. The main difference between the action (7.1.16) and the canonical domain wall action is the presence of the ρ^3 factor in the integration measure. When the thickness of the wall is much smaller than ρ – the "thin wall limit" – the measure factor can be neglected, and the instanton problem reduces to the domain wall problem. Thanks to this correspondence, we can apply some of our domain wall techniques to the study of instantons in higher derivative theories.

The properties of instanton solutions for DBI actions of the form (7.1.4) have been studied previously. In particular, in [52] a generalization of Eq. (7.1.4) was considered, of the form

$$S = \int \left[f(\phi)^{-1}\left(1 - \sqrt{1 + f(\phi)(\partial\phi)^2}\right) - V(\phi)\right] \, \mathrm{d}^4x \ , \tag{7.1.17}$$

where the function $f(\phi)$ is the "warp factor." The corresponding Euclidean action is

$$S_E = 2\pi^2 \int \left[f(\phi)^{-1}\left(-1 + \sqrt{1 + f(\phi)\phi'^2}\right) + V(\phi)\right] \rho^3 \, \mathrm{d}\rho \ . \tag{7.1.18}$$

The authors of [52] pointed out that solutions for ϕ develop cusp-like behavior once $V(\phi)$ became large. It was argued that this corresponded to instantons where the field profile is multi-valued, and the graph of $(z, \phi(z))$ traces out an S-curve, as illustrated in Figure 2 of [52] and Figure 4 of [51]. Geometrically, if ϕ is interpreted as the position of a brane in an extra dimension, this would correspond to the brane doubling back upon itself. However, if we treat the action (7.1.18) as a 4-dimensional effective theory, then, as we shall explain below, these solutions only exist for special choices of the functions $f(\phi)$ and $V(\phi)$.

To apply our previous results, we must generalize them to include the measure factor and the warp factor. Since we are concerned entirely with the Euclidean equations of motion arising from Eq. (7.1.18), which are not affected by constants multiplying the Lagrangian, it is convenient to absorb a factor of $-2\pi^2$ into S_E, and thus consider the Euclidean Lagrangian

$$L_E = \left[f(\phi)^{-1} \left(1 - \sqrt{1 + f(\phi)\phi'^2} \right) - V(\phi) \right] \rho^3 \equiv \hat{L}_E \rho^3 \ . \tag{7.1.19}$$

The Lagrangian L_E incorporates the effects of the warp factor and the measure factor, while $\hat{L}_E$ incorporates warp factor effects alone. For static solutions, the conserved quantity corresponding to $\hat{L}_E$ is

$$\hat{J} = f(\phi)^{-1} \left[\frac{1}{\sqrt{1 + \phi'^2 f(\phi)}} - 1 + V(\phi) \right] \ , \tag{7.1.20}$$

which may be compared to Eq. (7.1.9). It is important to stress that Eq. (7.1.20) is not a precise conservation law: $\hat{J}$ arises from $\hat{L}_E$, whereas the full equations of

motion arise from L_E, which contains the measure factor ρ^3. The full equations of motion imply that

$$\frac{\partial \hat{J}}{\partial z} = \left(\frac{3}{\rho}\right) \frac{\phi'^2}{\sqrt{1 + f(\phi)\phi'^2}} \ , \tag{7.1.21}$$

and this non-conservation of $\hat{J}$ describes important physics. Just as in the canonical instanton, this is what enables tunneling between minima of $V(\phi)$ with different vacuum energies, an essential feature of the Coleman-de Luccia instanton. However, in the thin-wall limit, where the width of the instanton solution is much less than ρ, the total change in $\hat{J}$ will be very small across the instanton wall. Hence, if we focus only on the instanton wall itself, $\hat{J}$ is effectively conserved.

The approximate conservation of $\hat{J}$ enables us to employ some of our domain wall techniques from Section 7.1.1 to the instanton problem, and to show that there is no solution to the Euclidean equations of motion in which ϕ curls back on itself. Suppose such a solution did, in fact, exist. Folding back upon itself would occur when $\phi' = \infty$, and we denote the value of ϕ at which this occurs as ϕ_*, and the corresponding value of ρ by ρ_*. Using (7.1.20) and working backwards, we find this defines a value of $\hat{J}$ given by

$$\hat{J}_* = \frac{V(\phi_*) - 1}{f(\phi_*)} \ . \tag{7.1.22}$$

Approximate conservation of $\hat{J}$ means that we can take $\hat{J} = \hat{J}_*$ when dealing with physics in the vicinity of the wall. Despite the fact that the point $\phi = \phi_*$ is in some sense singular, $\hat{J}$ must be the same on either side of this point. This is because, clearly, $\hat{J}$ is approximately conserved away from singular points (such as ϕ_*). If we

denote $\hat{J}_\pm$ as the value of $\hat{J}$ for $\phi < \phi_*$ and $\phi > \phi_*$, respectively, then the only way to ensure that $\lim_{\phi\to\phi_*^+} = \infty$ and $\lim_{\phi\to\phi_*^-} = \infty$ is to have $\hat{J}_+ = \hat{J}_- = \hat{J}_*$.

We now focus on a closed interval I_ϵ in ϕ, of radius ϵ, and centered on $\phi = \phi_*$, so $I_\epsilon = [\phi_* - \epsilon, \phi_* + \epsilon]$. Assuming $f(\phi)$ is smooth, given any $\delta > 0$ we can choose $\epsilon > 0$ so that

$$\frac{1}{f(\phi)\sqrt{1+\phi'^2 f(\phi)}} \leq \delta \qquad \forall \ \ \phi \in I_\epsilon \ . \tag{7.1.23}$$

Conservation of $\hat{J}$ then implies

$$\left| \frac{V(\phi)-1}{f(\phi)} - \hat{J}_* \right| \leq \delta \qquad \forall \ \ \phi \in I \ . \tag{7.1.24}$$

Using the definition (7.1.22) and taking the $\delta \to 0$ limit, we can rewrite this condition as

$$\frac{f'(\phi_*)}{f(\phi_*)} = \frac{V'(\phi_*)}{V(\phi_*)-1} \ . \tag{7.1.25}$$

If this condition is not satisfied, it is impossible to continue the solution through the singular point. Any deviation from Eq. (7.1.25) leads to a singular solution, and no fold is possible. For generic functions f and V, the condition (7.1.25) is not satisfied, and hence the required instanton solutions do not exist.

To illustrate these results, we can consider the case $f(\phi) = 1$, corresponding to the naïve DBI action studied in Section 7.1.1. The cusp is located at $\phi = \phi_*$ where $V(\phi_*) = 1$, and hence $\hat{J}_* = 0$. In order to fold back upon itself, ϕ must be greater than ϕ_* on one branch of the solution, and less than ϕ_* on the other. Hence $V(\phi) > 1$ on one branch, and $V(\phi) < 1$ on the other, for generic $V(\phi)$. However,

from Eq. (7.1.20) it is clear that there is no solution for ϕ' when $V(\phi) > 1$, and hence the solution cannot be continued through the fold. This ultimately arises because the condition (7.1.25) cannot be satisfied if we take $f(\phi) = 1$.

7.2 Doppelgänger domain walls

In Section 7.1.1, we showed that domain walls in $P(X)$ theories can be very different from those in canonical scalar field theories. However, in this section, we show that in a particular class of higher-derivative theories, the walls can actually be remarkably similar to their canonical counterparts! Indeed, the background solution for these walls is completely indistinguishable from the canonical wall, with the same energy density and field profile. As we shall see, the two solutions differ only in their fluctuation spectra.

7.2.1 An example: masquerading DBI

Motivating the action

Rather than diving immediately into a general analysis, it is instructive to begin with a simple and physically motivated example – the DBI action. One way of deriving the DBI kinetic term is to consider ϕ to be the coordinate of an extended object in an extra-dimensional space. Such objects can be described by the Nambu-Goto action, which is simply their surface area multiplied by the tension. If we take

the higher-dimensional space to have coordinates X^N with $N = 0, ...4$ then the action is

$$S_{NG} = -T \int \sqrt{-\det \left[\eta_{MN} \frac{\partial X^M}{\partial x^\mu} \frac{\partial X^N}{\partial x^\nu} \right]} \, \mathrm{d}^4 x \ , \tag{7.2.1}$$

where T is the tension, and η_{MN} is the metric in the full 5-dimensional space, which we take to be Minkowskian. Taking the embedding defined by

$$X^N = x^N, \quad N = 0, ...3, \qquad X^4 = \phi(x^\mu) \tag{7.2.2}$$

leads precisely to the $P(X)$ in Eq. (7.1.4), modulo a constant which only serves to set the energy of the vacuum to zero.

This extra-dimensional setup provides a useful geometrical picture for the origin of the DBI kinetic term. However, it is not clear how the simple addition of a potential $V(\phi)$, as we have done in Section 7.1.1, can be interpreted in this picture. If we hew to the extra-dimensional picture, it would seem that any new terms we add to the DBI action should correspond to geometrical quantities, such as the surface area of the membrane in the higher dimensional space. Such an approach also ensures that these additional terms will be compatible with the coordinate reparameterization symmetry of the action (7.2.1).

Guided by these considerations, we study actions in which the tension T is promoted to a function of the spacetime coordinates X^M, so that Eq. (7.2.1) becomes

$$S_{NG} = -\int T(X) \sqrt{-\det \left[\eta_{MN} \frac{\partial X^M}{\partial x^\mu} \frac{\partial X^N}{\partial x^\nu} \right]} \, \mathrm{d}^4 x \ . \tag{7.2.3}$$

Descending to the 4-dimensional theory, we find that such a system cannot be

described by a $P(X)$-type Lagrangian (7.1.2) because of the way in which X and ϕ are coupled. The resulting action is

$$S = \int \left[1 - (1 + U(\phi))\sqrt{1 + (\partial\phi)^2}\right] \, \mathrm{d}^4x \ , \tag{7.2.4}$$

where, as in Section 7.1.1, we have set $M = 1$, where M is the mass scale associated with the DBI kinetic term. We have also added a constant to the Lagrangian density in order to ensure that the energy density vanishes when $\phi' = 0$ and $U(\phi) = 0$. When gradients are small and $(\partial\phi)^2 \ll M^4$, the Lagrangian is approximately

$$L = 1 - (1 + U(\phi))\sqrt{1 + (\partial\phi)^2} \sim \frac{1}{2}\dot{\phi}^2 - \frac{1}{2}(\nabla\phi)^2 - U(\phi) \ , \tag{7.2.5}$$

and hence $U(\phi)$ is analogous to the potential in the canonical theory. However, as we shall see below, it plays a somewhat different role in the full theory.

Dirac-Born-Infeld doppelgängers

We are now ready to study defect solutions corresponding to the action (7.2.4). For this action, the conserved quantity J is

$$J = \frac{1 + U(\phi)}{\sqrt{1 + \phi'^2}} - 1 \ . \tag{7.2.6}$$

As before, we assume that $U(\phi)$ has two discrete minima $\phi_\pm$ where $U(\phi_\pm) = 0$ and take boundary conditions where $\phi = \phi_\pm$ at $z = \pm\infty$. Thanks to the boundary conditions, $J = 0$ at infinity, and therefore J vanishes everywhere because it is conserved. Inverting Eq. (7.2.6) gives

$$\phi'^2 = U(\phi)\left[U(\phi) + 2\right] \ , \tag{7.2.7}$$

which can be integrated to find the field profile for the defect. The Hamiltonian energy density of the defect is given by

$$E(\phi) = -1 + [1 + U(\phi)]\sqrt{1 + \phi'^2} = U(\phi)\,[U(\phi) + 2] \ , \tag{7.2.8}$$

where in the second equality we have used the expression (7.2.6) and the fact that J vanishes.

The curious properties of the doppelgänger walls arise from the fact that the right-hand sides of (7.2.7) and (7.2.8) are identical: the energy density is equal to ϕ'^2. The only other case we have seen thus far with this property was the canonical domain wall, as seen in Equations (7.1.6) and (7.1.8). This property was not shared by the naïve DBI domain wall, as can be seen from Equations (7.1.10) and (7.1.11). This means that, for static solutions arising from the action (7.2.4), we can define an effective potential function $\hat{V}(\phi)$ for the DBI wall by

$$\hat{V}(\phi) \equiv \frac{1}{2}U(\phi)\,[U(\phi) + 2] \ . \tag{7.2.9}$$

Note that minima of $U(\phi)$ where $U(\phi) = 0$ are also minima of $\hat{V}(\phi)$ where $\hat{V}(\phi) = 0$. With the identification (7.2.9), Equations (7.2.7) and (7.2.8) are precisely the same as the analogous equations for the canonical domain wall (7.1.6) and (7.1.8), but with the substitution $V \to \hat{V}$. By inverting (7.2.9), we find

$$U(\phi) = -1 + \sqrt{1 + 2\hat{V}(\phi)} \ . \tag{7.2.10}$$

So, we conclude with the somewhat surprising result that:

Given a canonical scalar field theory with a positive semi-definite potential $V(\phi) \geq 0$ which supports domain wall solutions, there exists a choice for $U(\phi)$ in the DBI theory (7.2.4), given by setting $\hat{V} = V$ in (7.2.10), which guarantees domain walls with precisely the same field profile and energy density.

In the next two subsections, we present two pieces of evidence which support the idea that our claim is somewhat surprising. First, we show that a claim of this nature cannot be made for arbitrary theories with extra derivatives: generically, there is no way to choose a potential function so that the higher-derivative wall mimics the canonical one. We reinforce this argument by deriving an explicit condition for the existence of doppelgänger defects. Second, we numerically compute the fluctuation spectra about the background domain wall solution, and find they are very different for the canonical wall and the DBI one. This shows that the DBI theory (7.2.4) is not a rewriting of the canonical scalar field theory, despite having solutions with identical field profiles and energy density.

7.2.2 When do doppelgänger defects exist?

A counterexample - other $P(X)$ theories

While we have shown that the action (7.2.4) possesses doppelgänger solutions, this is not a generic property of theories with higher derivatives. The $P(X)$ theory with a DBI kinetic term studied in Section 7.1.1 already provides one example where

a $P(X)$-type theory always leads to domain wall solutions which differ from those of a canonical field theory, with either a different field profile or a different energy density (or both). The DBI wall with a $P(X)$ action of the type (7.1.4) can never mimic a canonical domain wall because, for a canonical wall, we always have that

$$\phi'^2 = E(\phi) \ . \tag{7.2.11}$$

In the $P(X)$ DBI case, this would require the expressions on the right-hand side of Equations (7.1.10) and (7.1.11) to be equal. A quick calculation shows that this can only happen if $V(\phi) = 0$, and hence the $P(X)$ DBI wall can never mimic a canonical wall.

As another example, we consider a different $P(X)$ theory defined by

$$P(X) = -\frac{1}{2}X + \alpha X^2 \ , \tag{7.2.12}$$

where α is a real parameter with dimensions of $[\text{mass}]^{-4}$. When $X \ll \alpha$, this reduces to the canonical scalar field theory. Following the techniques used previously, we find that this theory possesses a conserved quantity J given by

$$J = -\frac{1}{2}\phi'^2 + 3\alpha\phi'^4 + V(\phi) \ , \tag{7.2.13}$$

where $V(\phi)$ is the potential associated with the theory. One might suppose that, since this theory is a deformation of the canonical one, a deformation of the potential would suffice to mimic the canonical wall. Again assuming that the potential is positive semidefinite and has discrete zero-energy minima at $\phi = \phi_\pm$, with $\phi_- < \phi_+$,

so that $V(\phi_\pm) = 0$, and assuming boundary conditions where $\phi = \phi_\pm$ at $\pm\infty$, we find the first integral

$$\phi'^2 = \frac{1 - \sqrt{1 - 48\alpha V(\phi)}}{12\alpha} \ , \tag{7.2.14}$$

whereas

$$E(\phi) = \phi'^2 - 4\alpha\phi'^4 \ . \tag{7.2.15}$$

Since $E(\phi) \neq \phi'^2$, we see that there is no choice of the potential for which the theory defined by Eq. (7.2.12) mimics a canonical wall, so long as $\alpha \neq 0$.

Conditions for doppelgänger defects in more general actions

The discussion in the previous section does not imply the absence of other doppelgänger actions. As we now show, there are infinitely many higher-derivative actions which can mimic canonical domain walls. However, these other actions are "rare" in the sense that they are technically non-generic in the space of all scalar field actions. We make this statement more precise below.

Consider the family of scalar field actions which have second-order equations of motion. Such an action is defined by a Lagrangian which is a function of both $X = (\partial\phi)^2$ and ϕ,

$$L = L(X, \phi) \ , \tag{7.2.16}$$

containing the much smaller family of $P(X)$ actions as a special case. We denote the canonical action by L_0, so that

$$L_0(X, \phi) = -\frac{1}{2}X - V(\phi) \ . \tag{7.2.17}$$

The conserved quantity for the general Lagrangian (7.2.16) is given by

$$J = 2X\frac{\partial L}{\partial X} - L \ , \tag{7.2.18}$$

whereas for the canonical action $J_0 = -X + V(\phi)$. Without loss of generality we assume that the domain wall boundary conditions are such that $J = 0$ everywhere. This can always be enforced by shifting L by a constant $L(X, \phi) \to L(X, \phi) + c$, which does not affect the equations of motion and only shifts the zero point of the energy density. For the canonical action, this implies that we can impose $V(\phi_{\min}) = 0$ for the global minima $\phi_{\min}$ of V.

What is required of a higher-derivative action so that it can mimic a canonical scalar field action? The first requirement is that both actions must have the same field profile $\phi_0(z)$ as a solution to their respective equations of motion. The second requirement is that the energy density of this field profile be the same when evaluated using the Hamiltonians associated with their respective actions.

We employ a geometrical construction to investigate these requirements. Instead of viewing L and L_0 as functions, it is helpful to think of them as surfaces hovering over the (X, ϕ) plane, with a height given by $L(X, \phi)$ or $L_0(X, \phi)$, respectively. These surfaces are referred to as the "graphs" of the functions L and L_0.

We first consider the second requirement, that the field profile $\phi_0(z)$ has the same Hamiltonian energy densities in the two theories. Suppose we have already established that the same field profile $\phi_0(z)$ is a solution to both actions. We denote by ϕ_- the value of ϕ at $z = -\infty$ and by ϕ_+ the value at $z = +\infty$ for this solution.

The specified solution traces out a curve C on the (X, ϕ) plane given in parametric form by

$$C : z \mapsto (X_0(z), \phi_0(z)) \ . \tag{7.2.19}$$

Since the configurations are static, the energy density is simply $-L$. Hence we can satisfy the first requirement if and only if

$$L(X, \phi) = L_0(X, \phi) \text{ on } C \ . \tag{7.2.20}$$

L and L_0 need not agree everywhere, but they must agree when evaluated on points on C. Geometrically, Eq. (7.2.20) means that the graphs of L and L_0 must intersect, and the projection of this intersection on to the (X, ϕ) plane must contain C.

We next consider the first requirement, that the equations of motion for either action admit the specified field profile $\phi_0(z)$ as a solution. We assume that $\phi_0(z)$ is a solution to the canonical theory, and derive the requirement that it also be a solution to L. Recall that, for static configurations, actions of the form (7.2.16) always admit a first integral obtained by solving the equation $J = 0$ for ϕ'^2. Hence, J must vanish when evaluated on the solution to the canonical theory. That is, $\phi_0(z)$ will be a solution to the higher-derivative scalar field theory if and only if

$$2X\frac{\partial L}{\partial X} - L = 2X\frac{\partial L_0}{\partial X} - L_0 \quad \text{ on } C \tag{7.2.21}$$

which, using Eq. (7.2.20), yields

$$\frac{\partial L}{\partial X} = \frac{\partial L_0}{\partial X} \quad \text{ on } C \ . \tag{7.2.22}$$

Hence, we require that the derivatives of L and L_0 with respect to X agree on C. Note that we never need to match derivatives with respect to ϕ – while $\partial L/\partial\phi$ does enter the equations of motion, it does not enter our conserved quantity and hence is not required to find a solution.

We conclude that:

> *An action $L(X,\phi)$ mimics a domain wall $\phi_0(z)$ of the canonical scalar field theory L_0 (that is, has the same field profile and energy density) if and only if the graphs of L and L_0 intersect above the curve $C : z \mapsto (X_0(z), \phi_0(z))$ in the (X,ϕ) plane, and if $\partial L/\partial X = \partial L_0/\partial X$ along the intersection.*

This geometrical picture, when combined with the two constraints (7.2.20) and (7.2.22), allows us to make a powerful statement about how "rare" doppelgänger actions are. The graphs of L and L_0 are codimension-one surfaces in the same three-dimensional space. Hence, they will generically intersect along a one-dimensional curve. Thus, we should not be surprised if two actions satisfy the constraint (7.2.20), which is essentially the statement that the graphs intersect along a one-dimensional curve. However, two codimension-one manifolds will generically intersect "transversely" – the span of their tangent spaces will equal the tangent space of the manifold at the intersection ($\mathbf{R}^3$ in this case). The condition (7.2.22) implies that the graphs of L and L_0 do not intersect trasversely. Thus, the existence of doppelgänger walls depends on constructing graphs in $\mathbf{R}^3$ which intersect non-generically. This

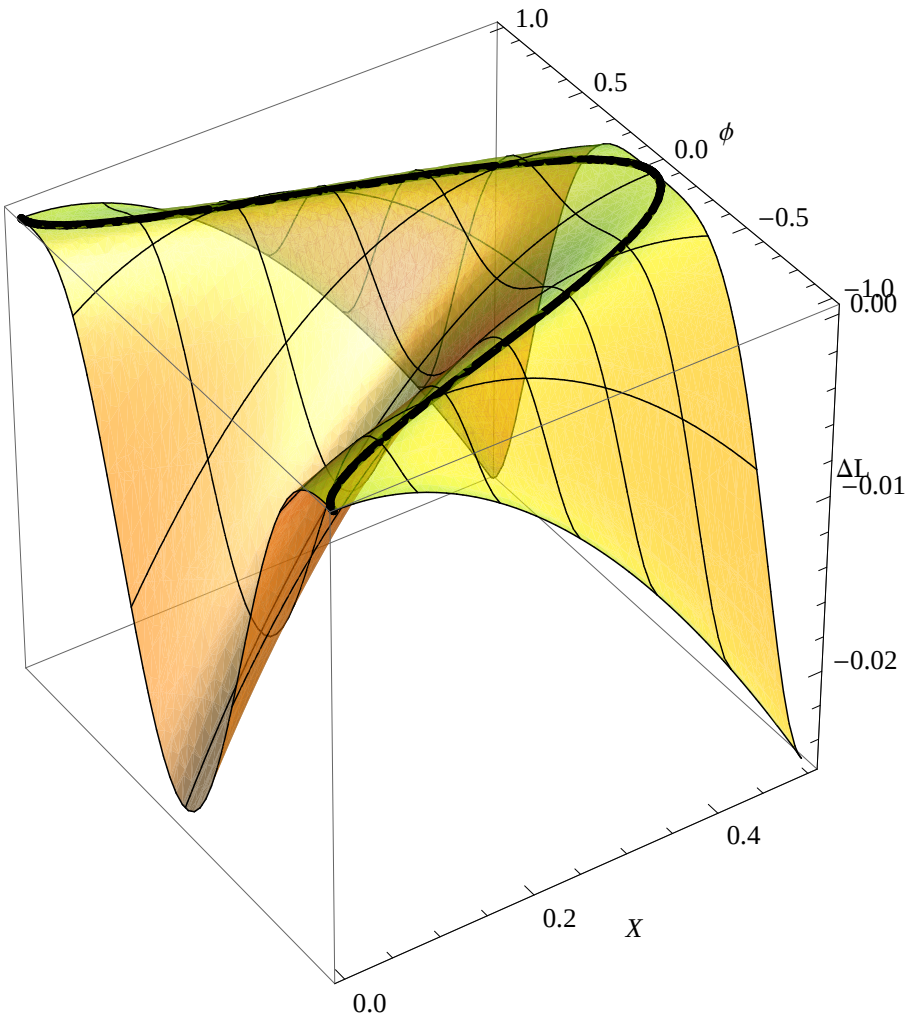

Figure 7.1: An illustration of the geometrical interpretation of doppelgänger actions. The graphs of $L(X, \phi)$ and $L_0(X, \phi)$ intersect along a single curve, whose projection on to the (X, ϕ) plane is the curve C discussed in the text. Here we plot the graph of $L_0 - L$ for the DBI action and the curve C (in black). The intersection of the graphs of L and L_0 is non-generic, since the first derivatives of the $L - L_0$ surface vanish along C.

geometrical interpretation is illustrated in Figure 7.1, where we have compared a canonical action with $V(\phi) = (1/4)(\phi^2 - 1)^2$ and its doppelgänger Lagrangian.

Another way of putting this result is that, given any function $\Delta L(X, \phi)$, such that

$$\Delta L(X, \phi) = 0 \quad \text{on } C \quad \text{and} \quad \frac{\partial \Delta L}{\partial X} = 0 \quad \text{on } C \ , \tag{7.2.23}$$

then we can construct another action

$$L(X, \phi) = L_0(X, \phi) + \Delta L(X, \phi) \ , \tag{7.2.24}$$

which will have the same domain wall solution as L_0. Clearly there are infinitely many functions ΔL satisfying (7.2.23), though they are non-generic in the same sense as non-transversely intersecting pairs of surfaces are non-generic.

7.2.3 DNA tests for defects: fluctuation spectra for doppelgängers

The existence of doppelgänger defects raises the question of whether such objects are merely a reparameterization of the original, canonical scalar field wall. As we shall demonstrate here, the fluctuation spectra of the doppelgänger walls are distinctly different from those of canonical walls. Among other differences, when the doppelgänger walls are deeply in the DBI regime (V_0/M^4 large), they have far more bound states than the canonical wall. Since the fluctuation spectra are different, the two theories cannot be reparameterizations of each other.

We find the action and equation of motion for the fluctuations by taking

$$\phi(t,z) = \phi_0(z) + \delta\phi(t,z) \ , \tag{7.2.25}$$

where $\phi_0(z)$ is a static background solution to the equations of motion and $\delta\phi(t,z)$ the fluctuation. We then expand the Lagrangian to quadratic order in $\delta\phi$. The term linear in $\delta\phi$ vanishes since $\phi_0(z)$ satisfies the equations of motion, and the purely quadratic piece is of the form

$$\delta_2 L = A(z)\delta\dot{\phi}^2 + B(z)\delta\phi^2 + C(z)\delta\phi'^2 + D(z)\delta\phi\delta\phi' \ . \tag{7.2.26}$$

For the canonical action, $A = 1/2$, $B = -V''(\phi_0(z))/2$, $C = -1/2$, and $D = 0$. For other cases, these coefficients depend on the particular background solution $\phi_0(z)$ and on the specific action used.

Since the action is independent of t, different frequencies do not mix and we can study an individual mode with frequency ω by taking

$$\delta\phi(t,z) = e^{-i\omega t}\delta\phi(z) \ . \tag{7.2.27}$$

This leads to the quadratic action

$$\delta_2 L = (\omega^2 A(z) + B(z))\delta\phi^2 + C(z)\delta\phi'^2 + D(z)\delta\phi\delta\phi' \ , \tag{7.2.28}$$

yielding the equation of motion

$$\frac{C}{A}\delta\phi'' + \frac{C'}{A}\delta\phi' + \left[\frac{D' - 2B}{2A}\right]\delta\phi = \omega^2\delta\phi \ . \tag{7.2.29}$$

Finding the energies of the flutuation modes amounts to finding values of ω so that Eq. (7.2.29) is satisfied by a normalizable function $\delta\phi$.

The problem (7.2.29) is an eigenvalue problem of the Sturm-Liouville type. Ideally, it would be in the form of a Schrödinger equation, which would allow us to readily identify free and bound states by analogy to the corresponding quantum mechanical system. Unfortunately, in general Eq. (7.2.29) is not of Schrödinger type, thanks to the presence of the $\delta\phi'$ term. However, in many interesting cases the quantity

$$E_0 \equiv \frac{D' - 2B}{2A} \tag{7.2.30}$$

tends to a constant far away from the wall. Hence, evaluating (7.2.30) far away from the wall defines an analogue to the "binding energy" of various fluctuation modes. We call modes with $\omega^2 < E_0$ the "bound states," and modes with $\omega^2 > E_0$ "free states." This definition gives reasonable agreement with our expectations for bound and free states, as we discuss below.

The eigenvalue problem (7.2.29) can be solved numerically using a simple finite element approach. We have computed the lowest-lying eigenmodes for a canonical wall with potential

$$V(\phi) = \frac{V_0}{4}\left(\phi^2 - \phi_0^2\right)^2 \tag{7.2.31}$$

and some of its doppelgänger walls, assuming periodic boundary conditions with periodicity much larger than the wall width. Some of these solutions are shown in Figure 7.2. These figures show the energies ω^2 of these fluctuation modes, normalized to the binding energy E_0 defined in Eq. (7.2.30), which is itself shown by the black horizontal line in the figure. As can be seen, our definition of bound states is

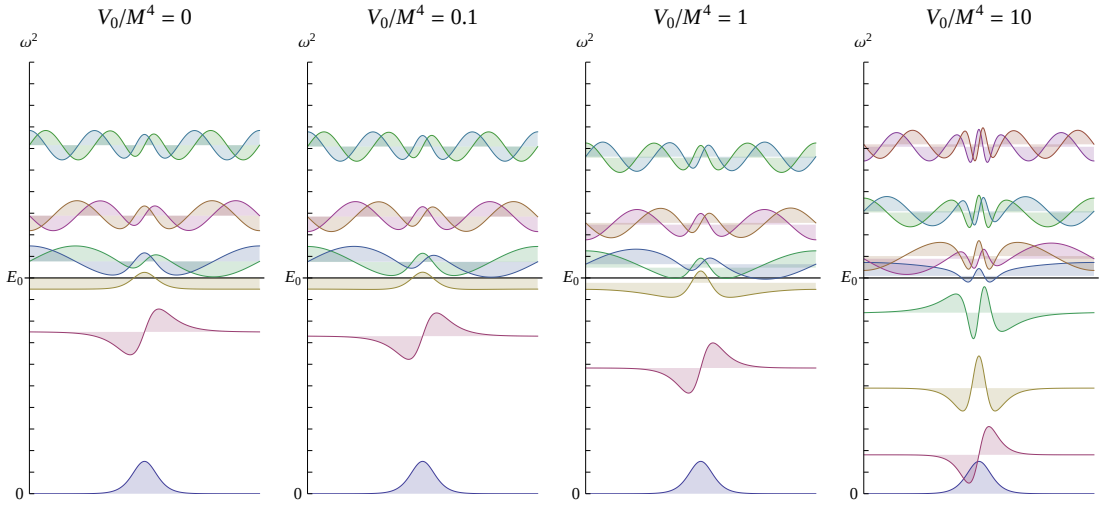

Figure 7.2: The lowest-lying fluctuation eigenmodes for various domain walls. The vertical position of each eigenmode is the eigenvalue ω^2 normalized by the binding energy E_0. Shown are the spectra for a canonical scalar field wall with $V_0/M^4 = 0$ (leftmost panel) and then some of its doppelgängers with $V_0/M^4 = 0.1$, 1, and 10 respectively. As the ratio V_0/M^4 increases, the wall possesses more bound states. The lowest-lying state is identical for each wall, reflecting the fact that these walls share a background field profile.

reasonable, since the eigenmodes possess the properties one would expect of bound states (such as compact support) when their energies are below E_0, and the properties of free states (such as oscillatory behavior) when their energies are above E_0. Since the eigenspectra are different, we can conclude that the two theories, while possessing an identical background solution, are in fact distinct theories.

The figures also show that there are many more bound states for the doppelgänger wall when we increase the mass scale of the potential relative to the DBI scale. These bound states are possible because the DBI action "weights" gradient energy much less in the interior of the domain wall, and hence even highly oscillatory fluctuation modes can remain as bound states. Physically, the presence of these bound states means that the doppelgänger wall possesses additional oscillation modes which the canonical wall does not.

7.3 k-strings

It is natural to ask whether it is also possible to find doppelgängers of other defect solutions, such as global strings or monopoles. This question is somewhat difficult to answer since higher codimension defects are generally less analytically tractable than the domain wall. In particular, the existence of the conserved quantity J in the codimension-one (domain wall) case allowed us to find the field profile and energy density and construct a doppelgänger existence proof. No analogous quantity is available for higher codimension defects, such as global strings or monopoles.

In this section, we generalize the one-field DBI action to a two-field system, and investigate some properties of the correponding global string solutions. Since we have no conserved quantity, we take a numerical approach and directly integrate the equations of motion. Using our two-field DBI model, we find no doppelgänger global string solutions. Nevertheless, since we cannot treat the two-field system analytically, we cannot prove a 'no-go' theorem and hence the existence of higher codimension doppelgänger defects remains an open question.

The canonical global string solution can be found by starting from the action with two real scalar fields

$$S = \int \left[-\frac{1}{2}(\partial\phi_1)^2 - \frac{1}{2}(\partial\phi_2)^2 - V(\phi_1, \phi_2) \right] \mathrm{d}^4x \ , \tag{7.3.1}$$

where the potential $V(\phi_1, \phi_2)$ respects a global $O(2)$ symmetry, corresponding to rotations in the (ϕ_1, ϕ_2) plane. To study string solutions, we assume the field configuration is static and cylindrically symmetric, employ polar coordinates (r, θ) in real space, and use the rotational symmetry to decompose the fields in terms of new functions ϕ and Θ as

$$\phi_1(r, \theta) = \phi(r) \cos\Theta(N\theta), \quad \phi_2(r, \theta) = \phi(r) \sin\Theta(N\theta) \ , \tag{7.3.2}$$

where $N \in \mathbf{Z}$ is the winding number of the string. Restricting ourselves to strings of unit winding number $N = 1$, the entire action may then be written in terms of the single function $\phi(r)$. The equation of motion for this field is

$$\phi'' + \frac{\phi'}{r} - \frac{\phi}{r^2} - \frac{\partial V}{\partial \phi} = 0 \ , \tag{7.3.3}$$

where $\phi' = \partial\phi/\partial r$. Given a potential $V(\phi)$ which admits a defect solution, that is, $V(0) \neq 0$ and there exists $\phi_0 > 0$ such that $V(\phi_0) = 0$ is a minimum, the string solution is subject to the boundary conditions that $\phi(0) = 0$ and $\phi \to \phi_0$ as $r \to \infty$. It is then straightforward to solve for the string field profile using the relaxation method.

There are many multi-field generalizations of the basic DBI kinetic term (7.1.4) which appear in the literature. Typically these generalizations reduce to the usual DBI kinetic term when there is only a single field. Based on our experience with the doppelgänger solutions, the best-motivated generalization is analogous to (7.2.3), based on a generalization of the Nambu-Goto action with two extra dimensions given by

$$S_{NG} = -\int T(X)\sqrt{-\det\left[\eta_{MN}\frac{\partial X^M}{\partial x^\mu}\frac{\partial X^N}{\partial x^\nu}\right]}\,\mathrm{d}^4x\ , \tag{7.3.4}$$

where, as before, the tension T is a function of the embedding coordinates. We depart from (7.2.3) by taking six-dimensional embedding coordinates X^N, with $N = 0...5$ and

$$X^N = x^N\ :\ N = 0, ...3, \qquad X^4 = \phi_1(x^\mu)\ ,\ \ X^5 = \phi_2(x^\mu)\ . \tag{7.3.5}$$

Hence, the 4-dimensional theory contains two real scalar fields $\phi_{1,2}$ with an $O(2)$ global symmetry. With a suitable choice of tension $T(X)$, we can construct DBI generalizations of the usual global string.

At this point, we can follow a similar procedure to that carried out in the case of the canonical global string. The reduction of the fields in the case of the unit

winding number string proceeds exactly as before, with the same decomposition defined by Eq. (7.3.2). If we use this decomposition in (7.3.4) we find

$$S_{NG} = 2\pi \int \left[r - (1 + U(\phi)) \sqrt{(r^2 + \phi^2)(1 + \phi'^2)} \right] \, \mathrm{d}r \ , \tag{7.3.6}$$

where, as before, we have rewritten $T = 1 + U(\phi)$ and added a constant to the Lagrangian so that the energy is zero when $\phi' = 0$ and $U(\phi) = 0$. Note that there is no factor of r next to the differential, since the action (7.3.4) already correctly accounts for the volume measure in four dimensions.

To investigate whether doppelgänger strings can be constructed, we assume a symmetry-breaking potential $U(\phi) = U_0(\phi^2 - 1)^2$ in the DBI theory and solve via the relaxation method for the DBI field profile. Given the field profile $\phi(r)$ of the DBI string, we solve numerically for the potential in the canonical scalar field theory which gives the same field profile. With this potential function, we compute the energy density in the canonical theory. In the examples we study, we find that the energy densities are different in the two theories. Analogous results hold if we match energy densities between the DBI and canonical theory – we find the field profile does not match. Hence we do not find any doppelgänger defects.

When taking the field profiles to be equal, we can construct a potential such that the DBI field profile is a solution to the canonical equations of motion by integrating the canonical equation of motion for ϕ, setting the potential to be 0 at large r:

$$V(\phi) = \int_{\phi}^{\phi_0} \left(\tilde{\phi}'' + \frac{\tilde{\phi}'}{r} - \frac{\tilde{\phi}}{r^2} \right) \, \mathrm{d}\tilde{\phi} \, . \tag{7.3.7}$$

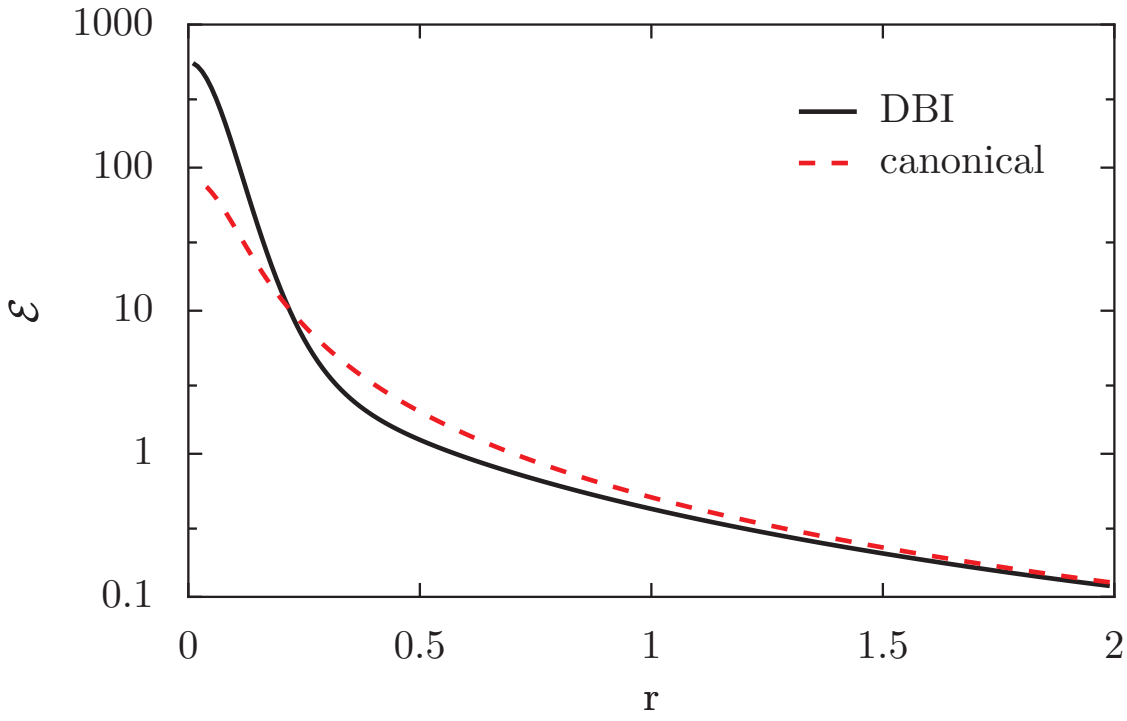

Figure 7.3: Energy density as a function of radius for a DBI string and a canonical string with identical field profiles. The DBI potential is given by $U(\phi) = 10(\phi^2 - 1)^2$.

For the examples we have studied, this leads to a total energy density which differs from the DBI energy density, as shown in Figure 7.3.

We also consider the case where the energy densities are constrained to be equal. In this case, after solving for the field profile and energy density of the DBI string, we then similarly solve for the field profile of the canonical string while maintaining the canonical potential as $V = \mathcal{E}_{\rm DBI} - \frac{1}{2}\left(\phi'^2_{\rm canonical} + \frac{\phi^2_{\rm canonical}}{r^2}\right)$. The results are shown in Figure 7.4.

The two approaches, both constraining the field profiles to be equal and constraining the energy densities to be equal, yield a DBI string which is observably

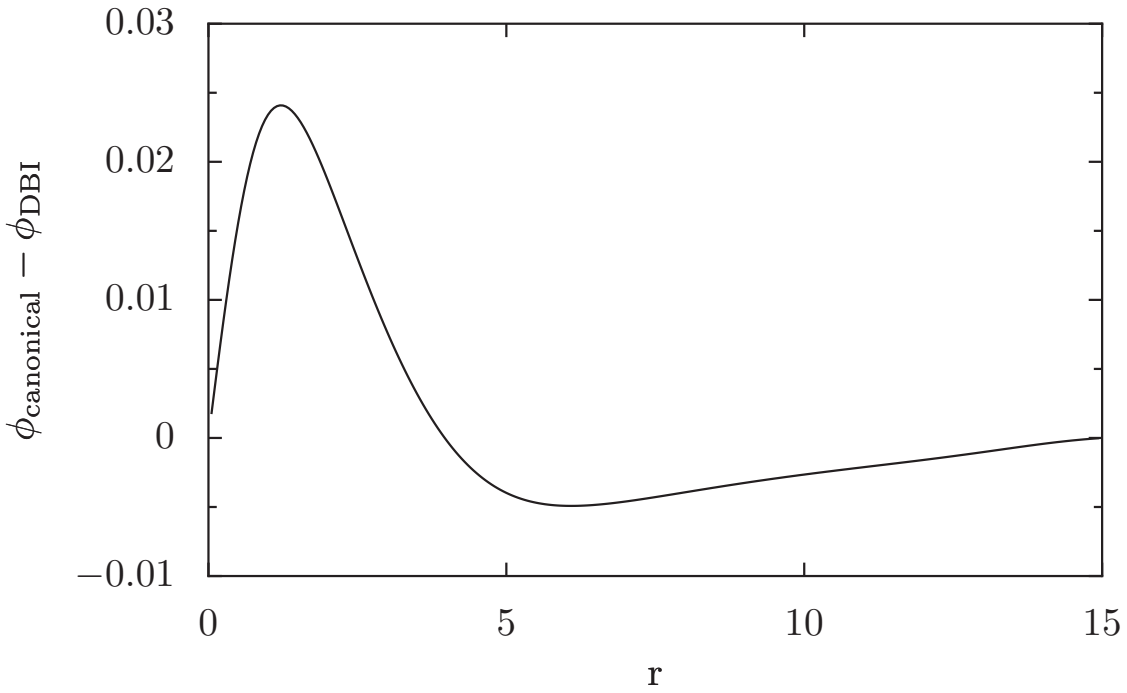

Figure 7.4: The difference in field values for a DBI string and a canonical string with identical energy densities. The DBI potential is given by $U(\phi) = \frac{1}{4}(\phi^2 - 1)^2$.

different from the canonical string for the examples we have studied. Thus we have found no examples of doppelgänger solutions for cosmic strings.

7.4 Implications

Nonperturbative field configurations such as topological defects may be formed during phase transitions in the early universe, and their interactions and dynamics can have significant effects on cosmic evolution. In the case of a scalar field with a canonical kinetic term, the behavior of such configurations has been understood for some time. The resulting constraints on the types and scales of symmetry breaking

are well-understood, and the possibilities for interesting cosmological phenomena have been thoroughly investigated.

However, in recent years, particle physicists and cosmologists have become interested in noncanonical theories, such as those that might drive k-inflation and k-essence. Ghost-free and stable examples of such theories can be constructed, and as such one may take them seriously as microphysical models. Several authors have then studied the extent to which the properties of topological defects are modified by the presence of a more complicated kinetic term.

In this chapter we have studied k-defect solutions to the DBI theory in some detail, discussing walls and strings, and clarifying the existence criteria and the behavior of instantons in these theories. Furthermore, we have addressed the question of whether k-defects, and in particular k-walls and global k-strings, can mimic canonical defects. We have demonstrated that given a classical theory with a canonical kinetic term and a spontaneously broken symmetry with a vacuum manifold admitting domain wall solution, there exists a large family of general Lagrangians of the $P(\phi, X)$ form which admit domain wall solutions with the same field profiles and same energy per unit area. These doppelgänger defects can mimic the field profile and energy density of canonical domain walls. Nevertheless, we have also shown that the fluctuation spectrum of a doppelgänger is different from its canonical counterpart, allowing one in principle to distinguish a canonical defect from its doppelgänger.

In the case of cosmic strings we have been unable to prove a similar result. Despite investigating several examples for the potential function in the DBI theory, we have been unable to find cases where there is a canonical theory which results in a matching energy density and field profile. However, since we have less analytic control in the case of defects of higher codimension, we have not been able to prove a 'no-go' theorem. Hence the existence of doppelgänger defects for strings or monopoles remains an open question.

The subject of doppelgänger or "twinlike" defects has generated interest among the scientific community, leading to studies in the context of kink-antikink collisions [121], multifield models [37, 35], noncanonical theories with defects that mimic those of a different noncanonical theory [36], cosmologies with nonzero curvature [33], doppelgängers that share fluctuation spectra as well as field profiles and energy densities [4], gauge theories [32], and further exploration of the space of twinned models [39, 3].

Chapter 8

Conclusions

In this thesis, we have investigated the theoretical consistency and potential observational testability of several infrared modifications of gravity belonging to the Vainshtein-screened class. This class of theories passes precision tests of gravity by recovering general relativistic behavior near astrophysical objects due to nonlinear derivative self-interactions. Many of the member theories also implement accelerating cosmologies in the absence of any dark energy component, and thus pose a possible solution to the cosmological constant problem. Due to non-renormalization by quantum corrections, the amount of acceleration is a technically natural quantity and thus does not require fine-tuning to match the observed value.

One such theory is that of a scalar subject to a Galilean symmetry coupled to a massive graviton. We have shown in this thesis that this theory propagates the appropriate two tensor, two vector, and two scalar degrees of freedom and thus is

not plagued by instability due to the presence of the Boulware-Deser ghost generic to theories where the graviton gains a mass. The homogeneous and isotropic cosmological solutions of ghost-free massive gravity with no extra scalars suffer from strong coupling of the scalar and vector perturbations, and thus are phenomenologically not viable. We find that the analogous branch of cosmological solutions in the massive gravity theory coupled to a galileon suffers the same strong-coupling problem; however, there remains an unexplored branch of solutions which may be of interest.

We also investigate the theory of N multiple galileons subject to an $SO(N)$ symmetry (as derived from a codimension-N braneworld theory). We find that Schwarzschild-like solutions of this theory are unstable, raising serious concerns about the model's phenomenological viability. Such a result suggests that the derivative coupling arising from such a braneworld construction, which respects both the $SO(N)$ and Galilean symmetries, should be included in the analysis. Additionally, a derivation such as the cascading gravity setup which breaks the $SO(N)$ symmetry by introducing a hierarchy of codimension-one branes may display more stable behavior.

In the interest of deriving precise theoretical predictions of the force mediated by a galileon in the solar system, where observations give the strongest constraints on departures from general relativity, we develop a formalism to perturbatively calculate the n-body galileon-mediated interactions in the presence of a large screened

body. This formalism presents a proof of concept for use in general theories of modified gravity exhibiting a screening mechanism. However, in the case studied we find the form of the galileon propagators derived herein present an obstacle to analytical calculation of corrections to the first-order forces. Additionally, the perturbative scheme breaks down for similar-mass objects separated by a distance small compared to the distance to the screening mass. In particular, one of the small parameters controlling the perturbative expansion is order one for the earth-moon system in the presence of the sun. Thus the first-order force typically used to constrain the theory using lunar laser ranging should in fact recieve sizeable corrections from higher-order galileon interactions.

Vainshtein-screened modified gravity theories remain an interesting alternative to the standard cosmological constant for driving late-time cosmic acceleration. Much work remains to develop precise and unique theoretical predictions of these modifications to gravity in order to distinguish them from the standard paradigm.

Additionally, we found that it is possible to construct theories with nonstandard derivative structure such that certain observations cannot distinguish the theory from a canonical one. In particular, we found a class of $P(\phi, X)$ Lagrangians such that the domain wall solutions have identical field profile and energy density to a canonical domain wall. We investigated numerically the existence of such solutions for the higher-codimension cosmic strings, but found no doppelgänger strings. However, this does not constitute a proof of their nonexistence.

There are a number of observed cosmological phenomena, in particular the late-time cosmic acceleration and inflation, that require the introduction of new fundamental physics. Theories that introduce new scalars with noncanonical kinetic terms have a number of interesting properties such as the Vainshtein screening mechanism, non-renormalization by quantum corrections, non-unit sound speed, and violation of energy positivity conditions (*e.g.* the null energy condition). These theories pose a theoretical challenge due to their nonlinear nature, and thus much more work is required to make predictions of comparable precision to the existing observational constraints. The search for a way to distinguish between these theories and the standard paradigm will continue to produce interesting new observational tests which will either lead to the discovery of new physics or increase the robustness of our understanding of the standard models. Regardless of which of these outcomes is realized, the study of nonstandard explanations for cosmological phenomena will add to our understanding of the fundamental physics describing the universe.

Bibliography

[1] A. Achucarro and T. Vachaspati. Semilocal and electroweak strings. *Phys.Rept.*, 327:347–426, 2000.

[2] C. Adam, P. Klimas, J. Sanchez-Guillen, and A. Wereszczynski. Compact gauge K vortices. *J.Phys.*, A42:135401, 2009.

[3] C. Adam and J. Queiruga. An algebraic construction of twin-like models. *Phys.Rev.*, D84:105028, 2011.

[4] C. Adam and J. Queiruga. Twinlike models with identical linear fluctuation spectra. *Phys.Rev.*, D85:025019, 2012.

[5] C. Adam, J. Sanchez-Guillen, and A. Wereszczynski. k-defects as compactons. *J.Phys.*, A40:13625–13643, 2007.

[6] A. Adams, N. Arkani-Hamed, S. Dubovsky, A. Nicolis, and R. Rattazzi. Causality, analyticity and an IR obstruction to UV completion. *JHEP*, 0610:014, 2006.

[7] P. Ade et al. Planck 2013 results. XVI. Cosmological parameters. 2013.

[8] N. Agarwal, R. Bean, J. Khoury, and M. Trodden. Cascading Cosmology. *Phys.Rev.*, D81:084020, 2010.

[9] A. Aguirre, S. Gratton, and M. C. Johnson. Hurdles for recent measures in eternal inflation. *Phys.Rev.*, D75:123501, 2007.

[10] A. Ali, R. Gannouji, and M. Sami. Modified gravity a la Galileon: Late time cosmic acceleration and observational constraints. *Phys.Rev.*, D82:103015, 2010.

[11] L. Anderson, E. Aubourg, S. Bailey, D. Bizyaev, M. Blanton, et al. The clustering of galaxies in the SDSS-III Baryon Oscillation Spectroscopic Survey: Baryon Acoustic Oscillations in the Data Release 9 Spectroscopic Galaxy Sample. *Mon.Not.Roy.Astron.Soc.*, 427(4):3435–3467, 2013.

[12] M. Andrews, Y.-Z. Chu, and M. Trodden. Galileon forces in the Solar System. *Phys.Rev.*, D88:084028, 2013.

[13] M. Andrews, G. Goon, K. Hinterbichler, J. Stokes, and M. Trodden. Massive Gravity Coupled to Galileons is Ghost-Free. *Phys.Rev.Lett.*, 111(6):061107, 2013.

[14] M. Andrews, K. Hinterbichler, J. Khoury, and M. Trodden. Instabilities of Spherical Solutions with Multiple Galileons and SO(N) Symmetry. *Phys.Rev.*, D83:044042, 2011.

[15] M. Andrews, K. Hinterbichler, J. Stokes, and M. Trodden. Cosmological perturbations of massive gravity coupled to DBI Galileons. *Class.Quant.Grav.*, 30:184006, 2013.

[16] M. Andrews, M. Lewandowski, M. Trodden, and D. Wesley. Distinguishing k-defects from their canonical twins. *Phys.Rev.*, D82:105006, 2010.

[17] N. Arkani-Hamed, H.-C. Cheng, M. A. Luty, and S. Mukohyama. Ghost condensation and a consistent infrared modification of gravity. *JHEP*, 0405:074, 2004.

[18] N. Arkani-Hamed, H. Georgi, and M. D. Schwartz. Effective field theory for massive gravitons and gravity in theory space. *Annals Phys.*, 305:96–118, 2003.

[19] C. Armendariz-Picon, T. Damour, and V. F. Mukhanov. k - inflation. *Phys.Lett.*, B458:209–218, 1999.

[20] C. Armendariz-Picon and E. A. Lim. Haloes of k-essence. *JCAP*, 0508:007, 2005.

[21] C. Armendariz-Picon, V. F. Mukhanov, and P. J. Steinhardt. A Dynamical solution to the problem of a small cosmological constant and late time cosmic acceleration. *Phys.Rev.Lett.*, 85:4438–4441, 2000.

[22] C. Armendariz-Picon, V. F. Mukhanov, and P. J. Steinhardt. Essentials of k essence. *Phys.Rev.*, D63:103510, 2001.

[23] E. Babichev. Global topological k-defects. *Phys.Rev.*, D74:085004, 2006.

[24] E. Babichev. Gauge k-vortices. *Phys.Rev.*, D77:065021, 2008.

[25] E. Babichev, P. Brax, C. Caprini, J. Martin, and D. A. Steer. Dirac Born Infeld (DBI) Cosmic Strings. *JHEP*, 0903:091, 2009.

[26] E. Babichev, C. Deffayet, and R. Ziour. The Recovery of General Relativity in massive gravity via the Vainshtein mechanism. *Phys.Rev.*, D82:104008, 2010.

[27] E. Babichev and G. Esposito-Farse. Time-Dependent Spherically Symmetric Covariant Galileons. *Phys.Rev.*, D87(4):044032, 2013.

[28] E. Babichev, V. Mukhanov, and A. Vikman. k-Essence, superluminal propagation, causality and emergent geometry. *JHEP*, 0802:101, 2008.

[29] A. Barreira, B. Li, C. M. Baugh, and S. Pascoli. Spherical collapse in Galileon gravity: fifth force solutions, halo mass function and halo bias. *JCAP*, 1311:056, 2013.

[30] A. Barreira, B. Li, W. A. Hellwing, C. M. Baugh, and S. Pascoli. Nonlinear structure formation in the Cubic Galileon gravity model. 2013.

[31] A. Barreira, B. Li, A. Sanchez, C. M. Baugh, and S. Pascoli. Parameter space in Galileon gravity models. *Phys.Rev.*, D87(10):103511, 2013.

[32] D. Bazeia, E. da Hora, and R. Menezes. Twinlike Models for Self-Dual Abelian-Higgs Theories. *Phys.Rev.*, D85:045005, 2012.

[33] D. Bazeia and J. Dantas. On the presence of twinlike models in cosmology. *Phys.Rev.*, D85:067303, 2012.

[34] D. Bazeia, A. Gomes, L. Losano, and R. Menezes. Braneworld Models of Scalar Fields with Generalized Dynamics. *Phys.Lett.*, B671:402–410, 2009.

[35] D. Bazeia, A. Lobao, L. Losano, and R. Menezes. First-order formalism for flat branes in generalized N-field models. *Phys.Rev.*, D88:045001, 2013.

[36] D. Bazeia, J. Lobao, A.S., and R. Menezes. Twinlike models for kinks and compactons in flat and warped spacetime. *Phys.Rev.*, D86:125021, 2012.

[37] D. Bazeia, A. Lobo, L. Losano, and R. Menezes. First-order formalism for twinlike models with several real scalar fields. *Eur.Phys.J.*, C74:2755, 2014.

[38] D. Bazeia, L. Losano, R. Menezes, and J. Oliveira. Generalized Global Defect Solutions. *Eur.Phys.J.*, C51:953–962, 2007.

[39] D. Bazeia and R. Menezes. New results on twinlike models. *Phys.Rev.*, D84:125018, 2011.

[40] L. Berezhiani, G. Chkareuli, and G. Gabadadze. Restricted Galileons. *Phys.Rev.*, D88:124020, 2013.

[41] J. Beringer et al. Review of Particle Physics (RPP). *Phys.Rev.*, D86:010001, 2012 and 2013 partial update for the 2014 edition.

[42] F. Beutler, C. Blake, M. Colless, D. H. Jones, L. Staveley-Smith, et al. The 6dF Galaxy Survey: Baryon Acoustic Oscillations and the Local Hubble Constant. *Mon.Not.Roy.Astron.Soc.*, 416:3017–3032, 2011.

[43] C. Blake, E. Kazin, F. Beutler, T. Davis, D. Parkinson, et al. The WiggleZ Dark Energy Survey: mapping the distance-redshift relation with baryon acoustic oscillations. *Mon.Not.Roy.Astron.Soc.*, 418:1707–1724, 2011.

[44] D. Boulware and S. Deser. Can gravitation have a finite range? *Phys.Rev.*, D6:3368–3382, 1972.

[45] R. H. Brandenberger, B. Carter, A.-C. Davis, and M. Trodden. Cosmic vortons and particle physics constraints. *Phys.Rev.*, D54:6059–6071, 1996.

[46] R. H. Brandenberger and A.-C. Davis. Electroweak baryogenesis with electroweak strings. *Phys.Lett.*, B308:79–84, 1993.

[47] R. H. Brandenberger, A.-C. Davis, and M. Hindmarsh. Baryogenesis from collapsing topological defects. *Phys.Lett.*, B263:239–244, 1991.

[48] R. H. Brandenberger, A.-C. Davis, and A. M. Matheson. Cosmic Strings and Baryogenesis. *Phys.Lett.*, B218:304, 1989.

[49] R. H. Brandenberger, A.-C. Davis, and M. Trodden. Cosmic strings and electroweak baryogenesis. *Phys.Lett.*, B335:123–130, 1994.

[50] P. Brax, C. van de Bruck, A.-C. Davis, and D. J. Shaw. f(R) Gravity and Chameleon Theories. *Phys.Rev.*, D78:104021, 2008.

[51] A. R. Brown. Brane tunneling and virtual brane-antibrane pairs. *PoS*, CARGESE2007:022, 2007.

[52] A. R. Brown, S. Sarangi, B. Shlaer, and A. Weltman. A Wrinkle in Coleman-De Luccia. *Phys.Rev.Lett.*, 99:161601, 2007.

[53] J.-P. Bruneton. On causality and superluminal behavior in classical field theories: Applications to k-essence theories and MOND-like theories of gravity. *Phys.Rev.*, D75:085013, 2007.

[54] C. Burrage, C. de Rham, and L. Heisenberg. de Sitter Galileon. *JCAP*, 1105:025, 2011.

[55] C. Burrage, C. de Rham, L. Heisenberg, and A. J. Tolley. Chronology Protection in Galileon Models and Massive Gravity. *JCAP*, 1207:004, 2012.

[56] C. Burrage, C. de Rham, D. Seery, and A. J. Tolley. Galileon inflation. *JCAP*, 1101:014, 2011.

[57] C. Burrage and D. Seery. Revisiting fifth forces in the Galileon model. *JCAP*, 1008:011, 2010.

[58] R. Caldwell, R. Dave, and P. J. Steinhardt. Cosmological imprint of an energy component with general equation of state. *Phys.Rev.Lett.*, 80:1582–1585, 1998.

[59] S. Capozziello, S. Carloni, and A. Troisi. Quintessence without scalar fields. *Recent Res.Dev.Astron.Astrophys.*, 1:625, 2003.

[60] S. M. Carroll. Quintessence and the rest of the world. *Phys.Rev.Lett.*, 81:3067–3070, 1998.

[61] S. M. Carroll, V. Duvvuri, M. Trodden, and M. S. Turner. Is cosmic speed - up due to new gravitational physics? *Phys.Rev.*, D70:043528, 2004.

[62] B. Carter and A.-C. Davis. Chiral vortons and cosmological constraints on particle physics. *Phys.Rev.*, D61:123501, 2000.

[63] N. Chow and J. Khoury. Galileon Cosmology. *Phys.Rev.*, D80:024037, 2009.

[64] Y.-Z. Chu. The n-body problem in General Relativity up to the second post-Newtonian order from perturbative field theory. *Phys.Rev.*, D79:044031, 2009.

[65] Y.-Z. Chu and G. D. Starkman. Retarded Green's Functions In Perturbed Spacetimes For Cosmology and Gravitational Physics. *Phys.Rev.*, D84:124020, 2011.

[66] Y.-Z. Chu and M. Trodden. Retarded Green's Function Of A Vainshtein System And Galileon Waves. *Phys.Rev.*, D87:024011, 2013.

[67] D. Comelli, M. Crisostomi, and L. Pilo. Perturbations in Massive Gravity Cosmology. *JHEP*, 1206:085, 2012.

[68] O. Corradini, K. Koyama, and G. Tasinato. Induced gravity on intersecting brane-worlds. Part I. Maximally symmetric solutions. *Phys.Rev.*, D77:084006, 2008.

[69] O. Corradini, K. Koyama, and G. Tasinato. Induced gravity on intersecting brane-worlds. Part II. Cosmology. *Phys.Rev.*, D78:124002, 2008.

[70] P. Creminelli, A. Nicolis, and E. Trincherini. Galilean Genesis: An Alternative to inflation. *JCAP*, 1011:021, 2010.

[71] P. Creminelli, M. Serone, G. Trevisan, and E. Trincherini. Inequivalence of Coset Constructions for Spacetime Symmetries. 2014.

[72] G. D'Amico, C. de Rham, S. Dubovsky, G. Gabadadze, D. Pirtskhalava, et al. Massive Cosmologies. *Phys.Rev.*, D84:124046, 2011.

[73] G. D'Amico, G. Gabadadze, L. Hui, and D. Pirtskhalava. Quasidilaton: Theory and cosmology. *Phys.Rev.*, D87(6):064037, 2013.

[74] R. Davis and E. Shellard. COSMIC VORTONS. *Nucl.Phys.*, B323:209–224, 1989.

[75] S. C. Davis, A.-C. Davis, and M. Trodden. N=1 supersymmetric cosmic strings. *Phys.Lett.*, B405:257–264, 1997.

[76] A. De Felice, A. E. Gumrukcuoglu, and S. Mukohyama. Massive gravity: nonlinear instability of the homogeneous and isotropic universe. *Phys.Rev.Lett.*, 109:171101, 2012.

[77] A. De Felice, A. E. Gmrkolu, C. Lin, and S. Mukohyama. Nonlinear stability of cosmological solutions in massive gravity. *JCAP*, 1305:035, 2013.

[78] A. De Felice, A. E. Gmrkolu, C. Lin, and S. Mukohyama. On the cosmology of massive gravity. *Class.Quant.Grav.*, 30:184004, 2013.

[79] A. De Felice and S. Tsujikawa. Cosmology of a covariant Galileon field. *Phys.Rev.Lett.*, 105:111301, 2010.

[80] A. De Felice and S. Tsujikawa. f(R) theories. *Living Rev.Rel.*, 13:3, 2010.

[81] A. De Felice and S. Tsujikawa. Generalized Galileon cosmology. *Phys.Rev.*, D84:124029, 2011.

[82] A. De Felice and S. Tsujikawa. Cosmological constraints on extended Galileon models. *JCAP*, 1203:025, 2012.

[83] C. de Rham. Massive Gravity. 2014.

[84] C. de Rham, G. Dvali, S. Hofmann, J. Khoury, O. Pujolas, et al. Cascading gravity: Extending the Dvali-Gabadadze-Porrati model to higher dimension. *Phys.Rev.Lett.*, 100:251603, 2008.

[85] C. de Rham, M. Fasiello, and A. J. Tolley. Galileon Duality. 2013.

[86] C. de Rham and G. Gabadadze. Generalization of the Fierz-Pauli Action. *Phys.Rev.*, D82:044020, 2010.

[87] C. de Rham, G. Gabadadze, L. Heisenberg, and D. Pirtskhalava. Nonrenormalization and naturalness in a class of scalar-tensor theories. *Phys.Rev.*, D87(8):085017, 2013.

[88] C. de Rham, G. Gabadadze, and A. J. Tolley. Helicity Decomposition of Ghost-free Massive Gravity. *JHEP*, 1111:093, 2011.

[89] C. de Rham, G. Gabadadze, and A. J. Tolley. Resummation of Massive Gravity. *Phys.Rev.Lett.*, 106:231101, 2011.

[90] C. de Rham, G. Gabadadze, and A. J. Tolley. Ghost free Massive Gravity in the Stúckelberg language. *Phys.Lett.*, B711:190–195, 2012.

[91] C. de Rham, S. Hofmann, J. Khoury, and A. J. Tolley. Cascading Gravity and Degravitation. *JCAP*, 0802:011, 2008.

[92] C. de Rham, L. Keltner, and A. J. Tolley. Generalized Galileon Duality. 2014.

[93] C. de Rham, J. Khoury, and A. J. Tolley. Flat 3-Brane with Tension in Cascading Gravity. *Phys.Rev.Lett.*, 103:161601, 2009.

[94] C. de Rham, J. Khoury, and A. J. Tolley. Cascading Gravity is Ghost Free. *Phys.Rev.*, D81:124027, 2010.

[95] C. de Rham, A. Matas, and A. J. Tolley. Galileon Radiation from Binary Systems. *Phys.Rev.*, D87(6):064024, 2013.

[96] C. de Rham and A. J. Tolley. DBI and the Galileon reunited. *JCAP*, 1005:015, 2010.

[97] C. de Rham, A. J. Tolley, and D. H. Wesley. Vainshtein Mechanism in Binary Pulsars. *Phys.Rev.*, D87(4):044025, 2013.

[98] C. Deffayet. Cosmology on a brane in Minkowski bulk. *Phys.Lett.*, B502:199–208, 2001.

[99] C. Deffayet, S. Deser, and G. Esposito-Farese. Generalized Galileons: All scalar models whose curved background extensions maintain second-order field equations and stress-tensors. *Phys.Rev.*, D80:064015, 2009.

[100] C. Deffayet, S. Deser, and G. Esposito-Farese. Arbitrary p-form Galileons. *Phys.Rev.*, D82:061501, 2010.

[101] C. Deffayet, G. Dvali, G. Gabadadze, and A. I. Vainshtein. Nonperturbative continuity in graviton mass versus perturbative discontinuity. *Phys.Rev.*, D65:044026, 2002.

[102] C. Deffayet, G. Esposito-Farese, and A. Vikman. Covariant Galileon. *Phys.Rev.*, D79:084003, 2009.

[103] C. Deffayet, X. Gao, D. Steer, and G. Zahariade. From k-essence to generalised Galileons. *Phys.Rev.*, D84:064039, 2011.

[104] C. Deffayet, J. Mourad, and G. Zahariade. A note on 'symmetric' vielbeins in bimetric, massive, perturbative and non perturbative gravities. *JHEP*, 1303:086, 2013.

[105] C. Deffayet, J. Mourad, and G. Zahariade. Covariant constraints in ghost free massive gravity. *JCAP*, 1301:032, 2013.

[106] C. Deffayet, O. Pujolas, I. Sawicki, and A. Vikman. Imperfect Dark Energy from Kinetic Gravity Braiding. *JCAP*, 1010:026, 2010.

[107] S. Deser and C. Isham. Canonical Vierbein Form of General Relativity. *Phys.Rev.*, D14:2505, 1976.

[108] S. Deser and A. Waldron. Acausality of Massive Gravity. *Phys.Rev.Lett.*, 110(11):111101, 2013.

[109] S. Dubovsky and V. Rubakov. Brane induced gravity in more than one extra dimensions: Violation of equivalence principle and ghost. *Phys.Rev.*, D67:104014, 2003.

[110] G. Dvali and G. Gabadadze. Gravity on a brane in infinite volume extra space. *Phys.Rev.*, D63:065007, 2001.

[111] G. Dvali, G. Gabadadze, and M. Porrati. 4-D gravity on a brane in 5-D Minkowski space. *Phys.Lett.*, B485:208–214, 2000.

[112] G. Dvali, A. Gruzinov, and M. Zaldarriaga. The Accelerated universe and the moon. *Phys.Rev.*, D68:024012, 2003.

[113] G. DAmico, G. Gabadadze, L. Hui, and D. Pirtskhalava. On Cosmological Perturbations of Quasidilaton. *Class.Quant.Grav.*, 30:184005, 2013.

[114] S. Endlich, K. Hinterbichler, L. Hui, A. Nicolis, and J. Wang. Derrick's theorem beyond a potential. *JHEP*, 1105:073, 2011.

[115] M. Fairbairn and A. Goobar. Supernova limits on brane world cosmology. *Phys.Lett.*, B642:432–435, 2006.

[116] W. Fang, S. Wang, W. Hu, Z. Haiman, L. Hui, et al. Challenges to the DGP Model from Horizon-Scale Growth and Geometry. *Phys.Rev.*, D78:103509, 2008.

[117] M. Fierz and W. Pauli. On relativistic wave equations for particles of arbitrary spin in an electromagnetic field. *Proc.Roy.Soc.Lond.*, A173:211–232, 1939.

[118] G. Gabadadze, K. Hinterbichler, J. Khoury, D. Pirtskhalava, and M. Trodden. A Covariant Master Theory for Novel Galilean Invariant Models and Massive Gravity. *Phys.Rev.*, D86:124004, 2012.

[119] G. Gabadadze and M. Shifman. Softly massive gravity. *Phys.Rev.*, D69:124032, 2004.

[120] W. D. Goldberger and I. Z. Rothstein. An Effective field theory of gravity for extended objects. *Phys.Rev.*, D73:104029, 2006.

[121] A. Gomes, R. Menezes, K. Nobrega, and F. Simas. Kink-antikink collisions for twin models. 2013.

[122] G. Goon, K. Hinterbichler, A. Joyce, and M. Trodden. Galileons as Wess-Zumino Terms. *JHEP*, 1206:004, 2012.

[123] G. Goon, K. Hinterbichler, A. Joyce, and M. Trodden. Gauged Galileons From Branes. *Phys.Lett.*, B714:115–119, 2012.

[124] G. Goon, K. Hinterbichler, and M. Trodden. A New Class of Effective Field Theories from Embedded Branes. *Phys.Rev.Lett.*, 106:231102, 2011.

[125] G. Goon, K. Hinterbichler, and M. Trodden. Galileons on Cosmological Backgrounds. *JCAP*, 1112:004, 2011.

[126] G. Goon, K. Hinterbichler, and M. Trodden. Symmetries for Galileons and DBI scalars on curved space. *JCAP*, 1107:017, 2011.

[127] G. L. Goon, K. Hinterbichler, and M. Trodden. Stability and superluminality of spherical DBI galileon solutions. *Phys.Rev.*, D83:085015, 2011.

[128] P. Gratia, W. Hu, and M. Wyman. Self-accelerating Massive Gravity: Exact solutions for any isotropic matter distribution. *Phys.Rev.*, D86:061504, 2012.

[129] A. E. Gumrukcuoglu, C. Lin, and S. Mukohyama. Open FRW universes and self-acceleration from nonlinear massive gravity. *JCAP*, 1111:030, 2011.

[130] A. E. Gumrukcuoglu, C. Lin, and S. Mukohyama. Anisotropic Friedmann-Robertson-Walker universe from nonlinear massive gravity. *Phys.Lett.*, B717:295–298, 2012.

[131] A. E. Gumrukcuoglu, C. Lin, and S. Mukohyama. Cosmological perturbations of self-accelerating universe in nonlinear massive gravity. *JCAP*, 1203:006, 2012.

[132] A. E. Gmrkolu, K. Hinterbichler, C. Lin, S. Mukohyama, and M. Trodden. Cosmological Perturbations in Extended Massive Gravity. *Phys.Rev.*, D88(2):024023, 2013.

[133] J. Hadamard. *Lectures on Cauchy's Problem in Linear Partial Differential Equations*. Yale University Press, New Haven, 1923.

[134] Z. Haghani, H. R. Sepangi, and S. Shahidi. Curvature perturbations of quasidilaton nonlinear massive gravity. *Phys.Rev.*, D87(12):124014, 2013.

[135] S. Hassan and R. A. Rosen. Bimetric Gravity from Ghost-free Massive Gravity. *JHEP*, 1202:126, 2012.

[136] S. Hassan and R. A. Rosen. Confirmation of the Secondary Constraint and Absence of Ghost in Massive Gravity and Bimetric Gravity. *JHEP*, 1204:123, 2012.

[137] S. Hassan and R. A. Rosen. Resolving the Ghost Problem in non-Linear Massive Gravity. *Phys.Rev.Lett.*, 108:041101, 2012.

[138] S. Hassan, R. A. Rosen, and A. Schmidt-May. Ghost-free Massive Gravity with a General Reference Metric. *JHEP*, 1202:026, 2012.

[139] S. Hawking. The Chronology protection conjecture. *Phys.Rev.*, D46:603–611, 1992.

[140] K. Hinterbichler. Theoretical Aspects of Massive Gravity. *Rev.Mod.Phys.*, 84:671–710, 2012.

[141] K. Hinterbichler and J. Khoury. Symmetron Fields: Screening Long-Range Forces Through Local Symmetry Restoration. *Phys.Rev.Lett.*, 104:231301, 2010.

[142] K. Hinterbichler, J. Khoury, A. Levy, and A. Matas. Symmetron Cosmology. *Phys.Rev.*, D84:103521, 2011.

[143] K. Hinterbichler and R. A. Rosen. Interacting Spin-2 Fields. *JHEP*, 1207:047, 2012.

[144] K. Hinterbichler, J. Stokes, and M. Trodden. Cosmologies of extended massive gravity. *Phys. Lett.*, B725:, 1–3, 1–5, 2013.

[145] K. Hinterbichler, M. Trodden, and D. Wesley. Multi-field galileons and higher co-dimension branes. *Phys.Rev.*, D82:124018, 2010.

[146] T. Hiramatsu, W. Hu, K. Koyama, and F. Schmidt. Equivalence Principle Violation in Vainshtein Screened Two-Body Systems. *Phys.Rev.*, D87:063525, 2013.

[147] Q.-G. Huang, Y.-S. Piao, and S.-Y. Zhou. Mass-Varying Massive Gravity. *Phys.Rev.*, D86:124014, 2012.

[148] L. Iorio. Constraints on Galileon-induced precessions from solar system orbital motions. *JCAP*, 1207:001, 2012.

[149] R. Jaffe. The Casimir effect and the quantum vacuum. *Phys.Rev.*, D72:021301, 2005.

[150] B. Jain, V. Vikram, and J. Sakstein. Astrophysical Tests of Modified Gravity: Constraints from Distance Indicators in the Nearby Universe. *Astrophys.J.*, 779:39, 2013.

[151] X.-h. Jin, X.-z. Li, and D.-j. Liu. Gravitating global k-monopole. *Class.Quant.Grav.*, 24:2773–2780, 2007.

[152] N. Kaloper and D. Kiley. Charting the landscape of modified gravity. *JHEP*, 0705:045, 2007.

[153] K. Kampf and J. Novotny. Unification of Galileon Dualities. 2014.

[154] J. U. Kang, V. Vanchurin, and S. Winitzki. Attractor scenarios and superluminal signals in k-essence cosmology. *Phys.Rev.*, D76:083511, 2007.

[155] N. Khosravi, G. Niz, K. Koyama, and G. Tasinato. Stability of the Self-accelerating Universe in Massive Gravity. *JCAP*, 1308:044, 2013.

[156] J. Khoury, J.-L. Lehners, and B. A. Ovrut. Supersymmetric Galileons. *Phys.Rev.*, D84:043521, 2011.

[157] J. Khoury and A. Weltman. Chameleon cosmology. *Phys.Rev.*, D69:044026, 2004.

[158] J. Khoury and M. Wyman. N-Body Simulations of DGP and Degravitation Theories. *Phys.Rev.*, D80:064023, 2009.

[159] J. Kluso and J. Kluson. Hamiltonian Analysis of Minimal Massive Gravity Coupled to Galileon Tadpole TermHamiltonian analysis of minimal massive gravity coupled to Galileon tadpole term. *JHEP*, 1308:080, 2013.

[160] T. Kobayashi. Cosmic expansion and growth histories in Galileon scalar-tensor models of dark energy. *Phys.Rev.*, D81:103533, 2010.

[161] T. Kobayashi, H. Tashiro, and D. Suzuki. Evolution of linear cosmological perturbations and its observational implications in Galileon-type modified gravity. *Phys.Rev.*, D81:063513, 2010.

[162] M. Kolanovic, M. Porrati, and J.-W. Rombouts. Regularization of brane induced gravity. *Phys.Rev.*, D68:064018, 2003.

[163] C. F. Kolda and D. H. Lyth. Quintessential difficulties. *Phys.Lett.*, B458:197–201, 1999.

[164] K. Koyama. Ghosts in the self-accelerating universe. *Class.Quant.Grav.*, 24:R231–R253, 2007.

[165] K. Koyama, G. Niz, and G. Tasinato. The Self-Accelerating Universe with Vectors in Massive Gravity. *JHEP*, 1112:065, 2011.

[166] A. Lue, R. Scoccimarro, and G. D. Starkman. Probing Newton's constant on vast scales: DGP gravity, cosmic acceleration and large scale structure. *Phys.Rev.*, D69:124015, 2004.

[167] M. A. Luty, M. Porrati, and R. Rattazzi. Strong interactions and stability in the DGP model. *JHEP*, 0309:029, 2003.

[168] R. Maartens. Is the Universe homogeneous? *Phil.Trans.Roy.Soc.Lond.*, A369:5115–5137, 2011.

[169] C. Marinoni, J. Bel, and A. Buzzi. The Scale of Cosmic Isotropy. *JCAP*, 1210:036, 2012.

[170] M. Mirbabayi. A Proof Of Ghost Freedom In de Rham-Gabadadze-Tolley Massive Gravity. *Phys.Rev.*, D86:084006, 2012.

[171] Y. Nambu. String-Like Configurations in the Weinberg-Salam Theory. *Nucl.Phys.*, B130:505, 1977.

[172] S. Nesseris, A. De Felice, and S. Tsujikawa. Observational constraints on Galileon cosmology. *Phys.Rev.*, D82:124054, 2010.

[173] J. Neveu, V. Ruhlmann-Kleider, A. Conley, N. Palanque-Delabrouille, P. Astier, et al. Experimental constraints on the uncoupled Galileon model

from SNLS3 data and other cosmological probes. *Astron.Astrophys.*, 555:A53, 2013.

[174] A. Nicolis and R. Rattazzi. Classical and quantum consistency of the DGP model. *JHEP*, 0406:059, 2004.

[175] A. Nicolis, R. Rattazzi, and E. Trincherini. The Galileon as a local modification of gravity. *Phys.Rev.*, D79:064036, 2009.

[176] A. Nicolis, R. Rattazzi, and E. Trincherini. Energy's and amplitudes' positivity. *JHEP*, 1005:095, 2010.

[177] S. Nobbenhuis. Categorizing different approaches to the cosmological constant problem. *Found.Phys.*, 36:613–680, 2006.

[178] H. Okada, T. Totani, and S. Tsujikawa. Constraints on f(R) theory and Galileons from the latest data of galaxy redshift surveys. *Phys.Rev.*, D87:103002, 2013.

[179] A. Padilla, P. M. Saffin, and S.-Y. Zhou. Bi-galileon theory I: Motivation and formulation. *JHEP*, 1012:031, 2010.

[180] A. Padilla, P. M. Saffin, and S.-Y. Zhou. Bi-galileon theory II: Phenomenology. *JHEP*, 1101:099, 2011.

[181] A. Padilla, P. M. Saffin, and S.-Y. Zhou. Multi-galileons, solitons and Derrick's theorem. *Phys.Rev.*, D83:045009, 2011.

[182] N. Padmanabhan, X. Xu, D. J. Eisenstein, R. Scalzo, A. J. Cuesta, et al. A 2 per cent distance to z=0.35 by reconstructing baryon acoustic oscillations - I. Methods and application to the Sloan Digital Sky Survey. *Mon.Not.Roy.Astron.Soc.*, 427(3):2132–2145, 2012.

[183] R. Peccei. Light scalars in cosmology. pages 98–104, 2000.

[184] S. Perlmutter et al. Measurements of Omega and Lambda from 42 high redshift supernovae. *Astrophys.J.*, 517:565–586, 1999.

[185] E. Poisson. The Motion of point particles in curved space-time. *Living Rev.Rel.*, 7:6, 2004.

[186] E. Poisson, A. Pound, and I. Vega. The Motion of point particles in curved spacetime. *Living Rev.Rel.*, 14:7, 2011.

[187] M. Porrati. Fully covariant van Dam-Veltman-Zakharov discontinuity, and absence thereof. *Phys.Lett.*, B534:209–215, 2002.

[188] B. Ratra and P. Peebles. Cosmological Consequences of a Rolling Homogeneous Scalar Field. *Phys.Rev.*, D37:3406, 1988.

[189] A. G. Riess et al. Observational evidence from supernovae for an accelerating universe and a cosmological constant. *Astron.J.*, 116:1009–1038, 1998.

[190] S. Sarangi. DBI global strings. *JHEP*, 0807:018, 2008.

[191] M. Scrimgeour, T. Davis, C. Blake, J. B. James, G. Poole, et al. The WiggleZ Dark Energy Survey: the transition to large-scale cosmic homogeneity. *Mon.Not.Roy.Astron.Soc.*, 425:116–134, 2012.

[192] F. P. Silva and K. Koyama. Self-Accelerating Universe in Galileon Cosmology. *Phys.Rev.*, D80:121301, 2009.

[193] V. Sivanesan. Hamiltonian of galileon field theory. *Phys.Rev.*, D85:084018, 2012.

[194] Y.-S. Song, I. Sawicki, and W. Hu. Large-Scale Tests of the DGP Model. *Phys.Rev.*, D75:064003, 2007.

[195] M. Sullivan et al. SNLS3: Constraints on Dark Energy Combining the Supernova Legacy Survey Three Year Data with Other Probes. *Astrophys.J.*, 737:102, 2011.

[196] N. Suzuki, D. Rubin, C. Lidman, G. Aldering, R. Amanullah, et al. The Hubble Space Telescope Cluster Supernova Survey: V. Improving the Dark Energy Constraints Above $z > 1$ and Building an Early-Type-Hosted Supernova Sample. *Astrophys.J.*, 746:85, 2012.

[197] M. Trodden and K. Hinterbichler. Generalizing Galileons. *Class.Quant.Grav.*, 28:204003, 2011.

[198] A. Vainshtein. To the problem of nonvanishing gravitation mass. *Phys.Lett.*, B39:393–394, 1972.

[199] H. van Dam and M. Veltman. Massive and massless Yang-Mills and gravitational fields. *Nucl.Phys.*, B22:397–411, 1970.

[200] A. Vilenkin and E. P. S. Shellard. *Cosmic strings and other topological defects*. Cambridge monographs on mathematical physics. Cambridge Univ. Press, Cambridge, 1994.

[201] M. S. Volkov. Self-accelerating cosmologies and hairy black holes in ghost-free bigravity and massive gravity. *Class.Quant.Grav.*, 30:184009, 2013.

[202] M. von Strauss, A. Schmidt-May, J. Enander, E. Mortsell, and S. Hassan. Cosmological Solutions in Bimetric Gravity and their Observational Tests. *JCAP*, 1203:042, 2012.

[203] J. Wang, L. Hui, and J. Khoury. No-Go Theorems for Generalized Chameleon Field Theories. *Phys.Rev.Lett.*, 109:241301, 2012.

[204] S. Wang, L. Hui, M. May, and Z. Haiman. Is Modified Gravity Required by Observations? An Empirical Consistency Test of Dark Energy Models. *Phys.Rev.*, D76:063503, 2007.

[205] S. Weinberg. The Cosmological Constant Problem. *Rev.Mod.Phys.*, 61:1–23, 1989.

[206] C. Wetterich. Modified gravity and coupled quintessence. 2014.

[207] C. M. Will. The Confrontation between general relativity and experiment. *Living Rev.Rel.*, 9:3, 2006.

[208] S. Winitzki. Predictions in eternal inflation. *Lect.Notes Phys.*, 738:157–191, 2008.

[209] E. Witten. Superconducting Strings. *Nucl.Phys.*, B249:557–592, 1985.

[210] M. Wyman. Galilean-invariant scalar fields can strengthen gravitational lensing. *Phys.Rev.Lett.*, 106:201102, 2011.

[211] M. Wyman, W. Hu, and P. Gratia. Self-accelerating Massive Gravity: Time for Field Fluctuations. *Phys.Rev.*, D87(8):084046, 2013.

[212] M. Wyman and J. Khoury. Enhanced Peculiar Velocities in Brane-Induced Gravity. *Phys.Rev.*, D82:044032, 2010.

[213] L. Xu. Confronting DGP braneworld gravity with cosmico observations after Planck data. *JCAP*, 1402:048, 2014.

[214] V. Zakharov. Linearized gravitation theory and the graviton mass. *JETP Lett.*, 12:312, 1970.

[215] S.-Y. Zhou. Goldstone's Theorem and Hamiltonian of Multi-galileon Modified Gravity. *Phys.Rev.*, D83:064005, 2011.

[216] S.-Y. Zhou and E. J. Copeland. Galileons with Gauge Symmetries. *Phys.Rev.*, D85:065002, 2012.

[217] I. Zlatev, L.-M. Wang, and P. J. Steinhardt. Quintessence, cosmic coincidence, and the cosmological constant. *Phys.Rev.Lett.*, 82:896–899, 1999.